ENERGY CONSTRAINED LINK ADAPTATION FOR MULTI-HOP RELAY NETWORKS

by

Xiao Zhao

A thesis submitted to the Department of Electrical and Computer Engineering

In conformity with the requirements for

the degree of Master of Applied Science

Queen's University

Kingston, Ontario, Canada

(January, 2011)

Abstract

Wireless Sensor Network (WSN) is a widely researched technology that has applications in a broad variety of fields ranging from medical, industrial, automotive and pharmaceutical to even office and home environments. It is composed of a network of self-organizing sensor nodes that operate in complex environments without human intervention for long periods of time. The energy available to these nodes, usually in the form of a battery, is very limited. Consequently, energy saving algorithms that maximize the network lifetime are sought-after. Link adaptation polices can significantly increase the data rate and effectively reduce energy consumption. In this sense, they have been studied for power optimization in WSNs in recent research proposals.

In this thesis, we first examine the Adaptive Modulation (AM) schemes for flat-fading channels, with data rate and transmit power varied to achieve minimum energy consumption. Its variant, Adaptive Modulation with Idle mode (AMI), is also investigated. An Adaptive Sleep with Adaptive Modulation (ASAM) algorithm is then proposed to dynamically adjust the operating durations of both the transmission and sleep stages based on channel conditions in order to minimize energy consumption. Furthermore, adaptive power allocation schemes are developed to improve energy efficiency for multi-hop relay networks.

Experiments indicate that a notable reduction in energy consumption can be achieved by jointly considering the data rate and the transmit power in WSNs. The proposed ASAM algorithm considerably improves node lifetime relative to AM and AMI. Channel conditions play an important role in energy consumption for both AM and ASAM protocols. In addition, the number of modulation stages is also found to substantially affect energy consumption for ASAM. Node lifetime under different profiles of traffic intensity is also investigated. The optimal power control values and optimal power allocation factors are further derived for single-hop networks and

multi-hop relay networks, respectively. Results suggest that both policies are more suitable for ASAM than for AM. Finally, the link adaptation techniques are evaluated based on the power levels of commercial IEEE 802.15.4-compliant transceivers, and ASAM consistently outperforms AM and AMI in terms of energy saving, resulting in substantially longer node lifetime.

Acknowledgements

I would like to express my sincere gratitude to my supervisor, Prof. Mohamed Ibnkahla, for this opportunity to pursue research under his tutelage. His support, guidance and encouragement were of great help in completing this thesis. I thank Prof. Elyes Bdira for his precious time and valuable discussions on my research. His great passion has always been an inspiration for me.

I am also grateful to my colleagues and friends in the Wireless Sensor Network and Communication Laboratory, Amr El-Mougy, Basel Nabulsi, Gayathri Vijay, Peng Hu, Ala Abu Alkheir, Zouheir El-Jabi, and Chun Tang, for their insights, valuable suggestions and comments, and friendship. I would also like to thank all the professors that have taught me during my study at Queen's, all ECE staff members for their kindness and patience. I also wish to thank all my friends for making my life enjoyable.

To my wonderful parents, for the happiness and care they give me. I am extremely fortunate to have their endless love and support.

Table of Contents

List of Figures

List of Tables

List of Acronyms

AM – Adaptive Modulation

AMI – Adaptive Modulation with Idle Mode

AS – Adaptive Sleep

ASAM – Adaptive Sleep combined with Adaptive Modulation

AWGN – Additive White Gaussian Noise

BER – Bits Error Rate

CPU – Control Processing Unit

CSI – Channel State Information

LAN – Local Area Network

LOS – Line of Sight

PAP – Power Adaptation Policy

PDF – Probability Density Function

PSD – Power Spectral Density

QAM – Quadrature Amplitude Modulation

QoS – Quality of Service

SNR - Signal to Noise Ratio

WSN - Wireless Sensor Network

Chapter 1

Introduction

1.1 Background and Motivation

Wireless Sensor Networks (WSNs) enable monitoring, controlling, and analyzing complex phenomena over a large region for a long period of time [1]. Recent advances in research have led to the development of network infrastructure and hardware platform that allow small, cheap and long-lasting sensor nodes. These sensor nodes can collect a large amount of information about the surrounding environment such as temperature, humidity, pressure, noise level, air quality, position, direction and so on [2]. The WSN technology, therefore, engenders a wide range of applications in habitat and environment monitoring, health care, military surveillance, industrial machinery, home automation and smart interaction [1].

The inherent requirements for WSNs to work under complex conditions introduce a substantial number of constraints. A few essential issues that still challenge the research community include:

- **Realistic Protocol Design** – Many of the current WSN platforms are developed with assumptions that simplify the wireless communication process and the operation environments [3]. The lack of realistic models for system design often makes the solutions work well in simulation but not robust enough for actual networks. Research is needed to focus on developing better models and new network protocols for the realistic sensing environments.
- **Power Management –** Due to the very limited capacity of the battery powering the sensor nodes, energy is a precious resource in the network. The fact that most sensor

network applications require a long operating lifetime emphasizes the importance of research to improve energy efficiency in WSNs [4].

- **Real-Time Operation –** WSNs are highly time constrained. In many of the applications, sensing information needs to be collected within a short time frame in order to make the data acquisition valid and accurate. However, most current protocols do not meet the real-time operation requirement satisfactorily. This leads to the need for designing real-time operation protocols that can sufficiently reduce the delay [5].
- **Security and Privacy Issues –** Sensor nodes are normally deployed over large and accessible areas. Unencrypted information may be intercepted during transmission. To ensure privacy in the system, security issues must be considered and properly addressed in every component.

Notwithstanding, WSNs are gaining increasing popularity due to many attractive features in flexibility, cost-efficiency, high resolution, cooperative effort and self-organizing capabilities [1], [4], [6]. Although each node is only capable of a limited amount of processing, the coordination of a large group of sensor nodes can form a WSN able to sense the environment in great detail [7].

1.2 Thesis Contribution

This thesis mainly focuses on the power management issue mentioned above. The primary contributions of this work are summarized as follows:

1. Different link adaptation policies are evaluated for energy saving. The goal of this analysis is to achieve optimal spectral efficiency while minimizing energy consumption in the network, thus extending the network operating lifetime while simultaneously meeting the Quality of

Service (QoS) requirements. We extend the work of Goldsmith et al. [8], to compute the energy performance in the network where the total available energy constraints are imposed on all nodes in the communication path. Data rate and transmit power, the two key factors determining energy consumption in the network, are studied.

2. We propose an Adaptive Sleep with Adaptive Modulation (ASAM) algorithm to adaptively adjust the durations of the node operating stages in the wireless channels for minimizing energy expenditure and enhancing the network lifetime. Relevant formulas for calculating energy consumption are derived for different Medium Access Control (MAC) layer protocols. The energy consumption of Adaptive Modulation (AM), Adaptive Modulation with Idle mode (AMI) and the proposed ASAM algorithm is evaluated and compared.
3. Adaptive power control and allocation algorithms are introduced to analyze the overall achievable rate and power level in single-hop and multi-hop communications, respectively. Optimal power control and allocation factors are also derived. An example of a two-link multi-hop network is explored using different link adaptive transmission protocols.

1.3 Thesis Outline

This thesis is organized as follows:

- Chapter 2 provides the necessary background and analytical framework for this work. Relevant parameters and system models are described. Functions of the system components are given in detail and fading models are explained.
- Chapter 3 presents the literature review of link adaptation and feedback communication systems. The system model of the adaptive feedback network is built. Based on the feedback system, link adaptation for energy optimization is discussed. Recent research and

designs for energy saving protocols are reviewed. The fundamentals of different adaptive techniques are also explained.

- Chapter 4 proposes the ASAM algorithm and adaptive power allocation policy. It first describes the composition of energy consumption in WSNs. Link adaptation techniques for single-hop and multi-hop networks are explained. In particular, power allocation factors are introduced to find optimal network energy consumption. The formulas for calculating energy consumption are derived using ASAM, AMI, and AM with respect to MAC layer protocols.
- Chapter 5 presents the simulation results. The simulation parameters, assumptions procedures and methodologies are described. We calculate the overall achievable data transmission rates, optimal power allocation factors, and AM switching threshold levels over Lognormal shadowing and Rician fading channels. The effects of channel conditions, traffic intensity and number of modulation stages are investigated. The per-node operating lifetime for point-to-point communication and multi-hop networks using the link adaptation polices and ASAM is evaluated and discussed. The performance of AM, AMI, and ASAM algorithms on commercial transceivers is further examined, with the node lifetime comparison.
- Finally, Chapter 6 gives concluding remarks and suggests possible future work.

Chapter 2

System Models

2.1 Introduction

This chapter presents the system models for wireless communication networks and discusses the conceptual framework for analysis. The system architecture and Physical Layer (PHY) components of a wireless communication system are introduced. In general, wireless communication systems are operated in complex environments. Therefore, the channel may be easily influenced by reflection, diffraction, scattering and multi-path effects. In this thesis, we investigate the network performance in flat-fading phenomena. The channel fading models are explained here with the communication strategy.

2.2 System Architecture

In this work, we are particularly interested in PHY layer channel characteristics. Figure 2.1 displays the architecture of a typical wireless communication system and the main components of interests.

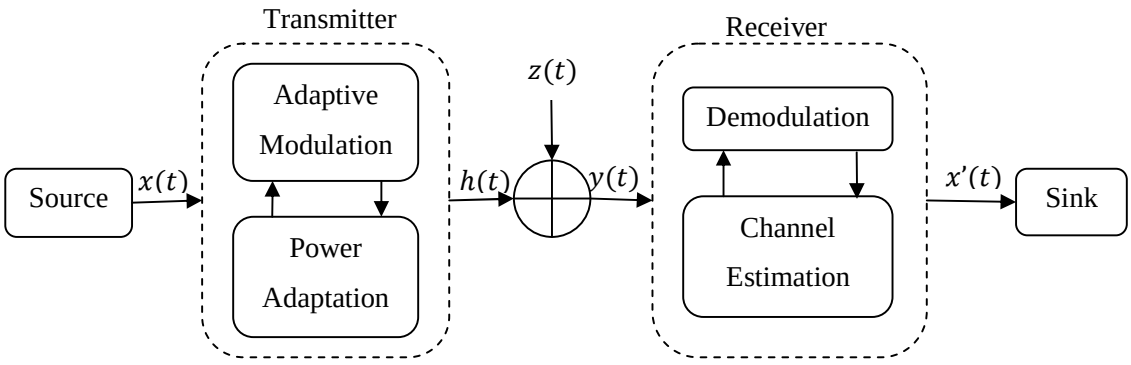

Figure 2.1: System architecture for a typical wireless communication system

2.2.1 Information Source and Sink

The communication information data $x(t)$ are generated by the source unit. In order to reduce the implementation complexity in practice, it is assumed that the data is uniformly distributed and is generated at a fixed symbol rate (see Section 3.6 for details). The communication system bandwidth is denoted as B, which in the case of ideal Nyquist pulse is given by: $B \approx 1/T_s = R_s$, where R_s is the fixed symbol rate. The data are transmitted through a flat-fading wireless channel where Additive White Gaussian Noise (AWGN) is added during the process.

2.2.2 Transmitter

One of the most important components in the system is the transmitter. Instead of being responsible only for sending information, the transmitter in this model has three main tasks:

- Transmission: The transmitter sends the data through a wireless channel to a receiver base on the selected modulation schemes and power levels.
- Adaptive Modulation: Unlike in a traditional modulator, the modulation scheme here is not fixed but varied based on QoS criteria. In this thesis an instantaneous Bit-Error-Rate (BER) requirement is further imposed. Therefore, the data rates and the transmission durations are determined by different modulation schemes, which in turn, are selected according to the performance requirements.
- Power adaptation: The most appropriate Power Adaptation Policy (PAP) is selected to optimize power levels according to the Channel State Information (CSI) feedback from the receiver. Two techniques of power adaptation are considered in this work, namely power allocation and adaptive sleep, both discussed in detail in Chapter 4.

2.2.3 Receiver

The Receiver is responsible for receiving data, demodulating the received information, and estimating the CSI after the wireless channel. Hence a feedback channel is further required so that the estimated CSI can be fed back to the transmitter. Normally there might be estimation errors and delays involved in this feedback process, which negatively affects the transmitter decisions. In this case, however, we assume that the channel estimation is perfect for the receiver and the delay from the feedback channel is negligible.

2.2.4 Wireless Channel

During the processes of transmission, reception and signal propagation, the additive noise is formed and should be considered in the analysis. Considering the channel gain and additive noise, the output signal can be expressed as:

$$y = h \cdot x + z \qquad (2.1)$$

where x is the input signal, h is the channel gain, and z is the AWGN here formed by taking a zero-mean Gaussian random variable with Power Spectral Density (PSD) of $N_0/2$.

2.3 Lognormal shadowing Channel Model

Wireless links experience shadowing and fading effects. In this thesis, the shadowing effect of the channel is modeled as a lognormal distribution. The Probability Density Function (PDF) of a lognormal distribution is represented as [9]:

$$f(x;\mu,\sigma) = \frac{1}{x\sigma\sqrt{2\pi}} exp\left(-\frac{(lnx-\mu)^2}{2\sigma^2}\right) \qquad (2.2)$$

where μ and σ are the mean and standard deviation of the natural logarithm. The lognormal distribution has a mean and a variance which are given by:

$$Mean: = e^{\mu+\sigma^2/2} \tag{2.3}$$

$$Variance: = (e^{\sigma^2} - 1)e^{2\mu+\sigma^2} \tag{2.4}$$

The lognromal distribution therefore can be used to describe the random shadowing effects in the link burget calcuation. The received power level is formulated by considering the lognormal distribted path loss. Use this approximation, a simple path-loss model can be expressed as [9]:

$$P_r = P_t + 20\,log_{10}\left(\frac{\lambda}{4\pi d_0}\right) + 10n\,log_{10}\left(\frac{d_0}{d}\right) + X_\sigma \tag{2.5}$$

where P_r and P_t are the receive power and transmit power, respectively; λ is the signal wavelength; d_0 is a reference point distance; d is the distance between the transmitter and the receiver; X_σ is a zero-mean Gaussian distributed random variable with standard deviation σ; and n is the path-loss exponent which is highly dependent on the propagation channel. The typical values of n in the range of [2, 5] for common wireless sensor environments [10].

2.4 Rician Fading Channel Model

The multi-path fading effects are modeled by Rician distribution. The PDF of Rician or Rice distribution can be denoted as [11]:

$$f(x|v,\sigma) = \frac{x}{\sigma^2}\,exp\left(\frac{-(x^2+v^2)}{2\sigma^2}\right) I_0\left(\frac{xv}{\sigma^2}\right) \tag{2.6}$$

where σ is the standard deviation; v is the distance between the reference point and the center of the bi-variant distribution; and I_0 is the modified Bessel function of the first kind with order zero.

When analyzing the fading probability distribution of the wireless channel, Rician PDF is normally represented as a distribution of the received SNRs (γ) [10]:

$$P_r(\gamma) = \frac{(1+K)}{\bar{\gamma}} e^{\left(-K-\frac{(1+K)\gamma}{\bar{\gamma}}\right)} I_0\left(2\sqrt{\frac{K(1+K)\gamma}{\bar{\gamma}}}\right), \gamma \geq 0. \quad (2.7)$$

where $K = \frac{v^2}{2\sigma^2}$ is the Rician K-factor defined as the ratio of dominant component signal power over the local mean scattered power. In other words, the K-factor shows the strength of the Line-of-Sight (LOS) signal in the channel. By varying the K-factor, the mean and variance of the distribution is changed [11]. In this thesis, links are uncorrelated so that the shadowing and fading effect on one link has no impact on others. Thus, the channel Rician K-factors can be varied independently for each link.

The Rician distribution can also be modeled as $R = \sqrt{X^2 + Y^2}$ where $X \sim N(v\cos\theta, \sigma^2)$ and $Y \sim N(v\sin\theta, \sigma^2)$ are two independent normal distributions, and θ is any real number. The mean and variance of the distribution is given by:

$$Mean: = \sigma\sqrt{\frac{\pi}{2}} L_{1/2}\left(-\frac{v^2}{2\sigma^2}\right) = \sigma\sqrt{\frac{\pi}{2}} L_{1/2}(-K) \quad (2.8)$$

$$Variance: = 2\sigma^2 + v^2 - \frac{\pi\sigma^2}{2} L_{1/2}^2\left(-\frac{v^2}{2\sigma^2}\right) = 2\sigma^2 + v^2 - \frac{\pi\sigma^2}{2} L_{1/2}^2(-K) \quad (2.9)$$

where $Lv(x)$ denotes a Laguerre polynomial. For a given K-factor and mean value, N values are drawn from the Rician distribution as the instantaneous SNRs γ_i in each link. The instantaneous SNRs are used to obtain the received SNRs at the sink nodes after power allocation.

2.5 Summary

This chapter has presented the analytical framework and channel fading models used in the following chapters. The system architecture and the network components are explained. In this thesis, channel fading condition is an important parameter for analyzing the energy consumption in the communication process. Two fading models, namely Lognormal propagation and Rician distribution, have been examined. Relations between channel fading and node lifetime will be investigated in Chapter 5.

Chapter 3

Adaptive Transmission and Feedback Communication System

3.1 Introduction

With the rapidly increasing demand for the radio spectrum in wireless communication systems, there arises a keen need for developing spectral efficient networks. In order to use the spectrum efficiently, the transmission schemes should be able to adapt to channel characteristics through estimation and feedback. But traditional non-adaptive protocols fix the transmission parameters regardless of channel conditions. Such systems need to maintain an acceptable performance for the worst case scenario, which often results in insufficient utilization of the full channel capacity.

Adaptive modulation (AM) or link adaptation, on the other hand, allows for dynamic adjustment of the communication systems (e.g., by changing modulation [12] and coding [13] schemes and other parameters [14]), according to characteristics of the time-varying channel [15]. This effectively improves spectral efficiency by adapting transmission parameters to specific communication conditions.

The basic concept behind the adaptive transmission is to maintain a stable level of E_b/N_0 by varying the transmit power, data rate, coding rate, coding scheme, or a combination of them. It takes advantage of favorable channel conditions by transmitting data at high speed. In this way, spectral efficiency is improved with BER requirement maintained simultaneously. For wireless communication applications with emphasis on high quality-of-service (QoS) or minimal distortions, such as high-speed modems and satellite links, adaptive techniques are of particular importance [15].

3.2 Adaptive System Design

In adaptive transmission, both transmitter and receiver in the system will have multiple functionalities. Figure 3.1 illustrates the system model for a typical adaptive transmission system. Unlike in traditional communication systems, modulation level and transmit power in adaptive systems are not fixed but dynamically controlled by transmitter. Through the feedback channel, transmitter exchanges information with the receiver and collects the current CSI data. The transmitter can then make decisions on the proper transmission parameters to use. During the process, both adaptive modulation control and power adaptation units are functioning simultaneously to ensure modulation schemes and transmit power are selected accurately.

The Receiver also has two functionalities: demodulation and estimation. It cooperates with transmitter to determine the transmitted information and to estimate the CSI. During the estimation and feedback process, delay and error can occur, impairing the accuracy of the estimates.

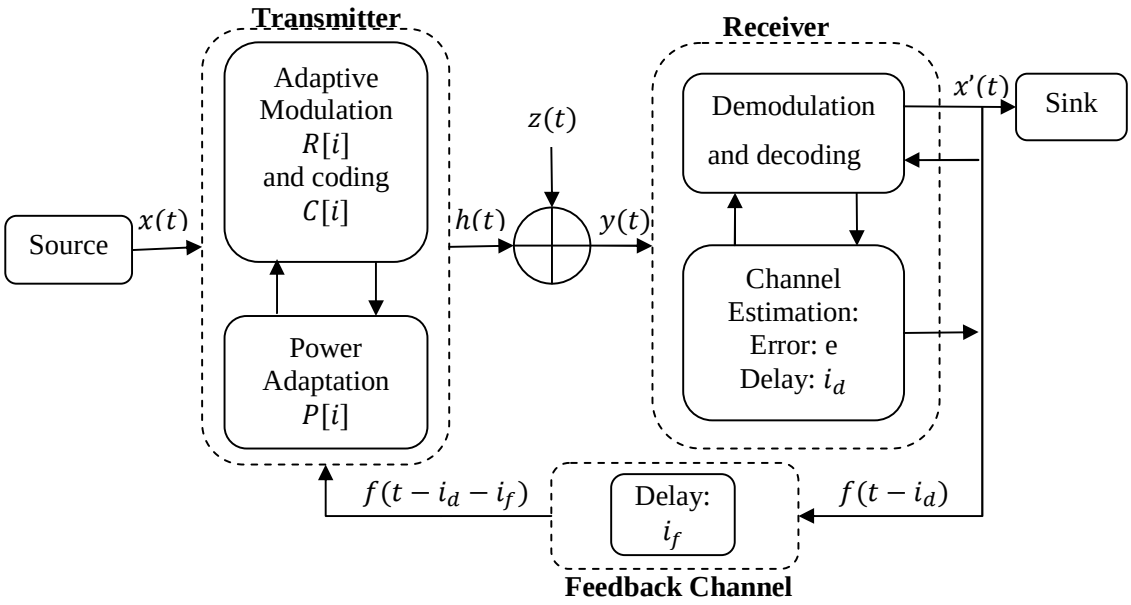

Figure 3.1: Adaptive Feedback System Model

3.3 Link Adaptations

Link adaptation, also known as adaptive modulation and coding, is an innovative technology in wireless communications. The goal of the technique is to adapt the system parameters to radio link conditions such as available power level, channel path-loss, signal interference and sensitivity of the receiver [12]. The parameters for adjustment can include: symbol rate [16], modulation schemes or constellation size, transmit power [17], data transmission rate [12], [18], [19], [20], and coding parameters [21], [22], [23], [24]. These parameters can be varied either individually or jointly according to application and performance requirements. Recent researches focus on adapting one or two parameters, specifically, power and/or rate [15], [16], [20], [19], [25], rate and coding [13], [21], and BER in [21].

However, the work by Goldsmith et al. [20] indicates that the Shannon capacity of a flat-fading channel can be best achieved by jointly varying the data rate and transmit power. In addition, since the data rate and the transmit power are two parameters for calculating the network energy, variable-rate variable-power adaptation techniques become the most interesting link adaptation policy in research when analyzing the network energy consumption. In this thesis, the link adaptation system performance is evaluated using variable rate and variable power both individually and jointly. The objective is to solve the energy optimization problem so that the maximum node lifetime is achieved under network constraints.

Early studies on adaptation techniques were done by Cavers [16] and Hayes [17] in the 1960's. The results showed promising results for adaptive techniques to improve the system efficiency and throughput by supporting various communication profiles and multiple transmission rates according to the link quality. However, due to the hardware limitations and difficulties in accurate estimation of the CSI, link adaptation was considered unfeasible at that time [8]. With advances

in technology, especially in hardware, the original concerns of link adaptation become less prohibitive. Technologies that incorporate AM into wireless LANs [26], [27], [28], [29], MIMO communications [30], and 3G/4G cellular networks have revived [25], [31], [32], [33], [34].

It has to be noted that the adaptive systems must be designed to ensure that consistent communication requirements are met under the worst case scenarios. Link adaptation protocols can avoid the poor utilization of the channel even with deep fading. Therefore, it increases the spectral efficiency by transmitting at desirable speed based on channel conditions. Particularly, for multi-hop relay networks, communication links can transmit at different data rates and power levels to achieve optimal spectral efficiency and minimum energy consumption.

Having that said, link adaptation still suffers from a few practical limitations [35]. First, it is highly dependent on reliable receivers and feedback channels to estimate and relay accurate CSI to transmitters. In addition, the communication process requires real-time estimation and error-free transmission in order to ensure the accuracy of the transmitter decisions. If the time varying CSI cannot be received correctly or timely, link adaptation is not possible. Furthermore, most link adaptation techniques are evaluated mainly in terms of simulations. Actual experiments in realistic networks are desperately needed.

3.4 Energy Constrained Networks

A network with finite fixed energy budget is defined as energy constrained network. WSN is one example of energy constrained networks. Sensor nodes in the network are usually battery driven devices. The amount of energy available to each node is finite and the operating lifetime is limited. With advances in research and design, more functionalities have been integrated into one single chip, yet the size and the weight of sensor nodes are effectively reduced [2]. In many

applications, sensor nodes are designed to have powerful transceivers and central controllers to sense, process data, and transmit and receive information at the same time. However, this also makes the devices more important and difficult to be replaced.

Therefore, nodes must be able to operate for a long period of time without replacing the battery. Consequently, energy optimization for the communication processes becomes more crucial. It is necessary to understand the tradeoff between the system performance and the amount of energy that can be used for each process. Investigations of recent researches indicate that to ensure a long period of network lifetime, the amount of energy used to deliver each packet has to be minimized [36], [37]. Energy efficiency is the key in this energy saving problem.

3.5 Link Adaptation in Energy Optimization

Applying link adaptation to energy constrained sensor network has received a significant amount of interests in research [38], [39], [40]. Many designs offer optimal energy performance by using extra low-power components in sensor nodes [37], [41], [42]. However, additional hardware can introduce noise and errors to the network and influence the system performance [35]. Some works also consider using dynamic routing protocols for delivering the information from source to destination [43], [44], [45]. The design often focuses on balancing battery power for all nodes along the transmission routes.

Recent research in the field of energy constrained sensor network also proposes the concept of energy-aware protocols to control the power levels during transmission [46], [47]. Instead of being fixed beforehand, the transmit power is dynamically allotted. Energy-aware protocols balance the link budget through adaptive variation, so that each transmission can spend different amount of energy given the channel conditions [17]. Thus, without wasting the power or

sacrificing BER, the protocol provides high average link energy efficiency by taking advantage of flat-fading through adaptation. No energy will be wasted during the process, hence maximizing the node lifetime.

One of the essential ideas in these energy-aware protocols is to power down the nodes when they are not performing any tasks. This is due to the fact that in WSNs, nodes normally need to be communicating for a short period of time only; thus a high degree of redundancy usually exists in network topology [30]. It is possible to design wireless communication protocols to minimize energy consumption by letting the nodes sleep for the maximum amount of time. Adaptive sleep (AS) technique, therefore, has been proposed so that nodes sleep time can be adjusted based on current fading conditions. Most of the time when there are no communication occurring, nodes are powered down and operated at the minimum power level. This stand-by power can be orders of magnitude lower than the active power. Energy efficiency is thereby improved as maximum sleep time is used in the network.

3.6 Adaptive Techniques

Dynamically adjusting the transmission parameters leads to various adaptive techniques in research. This thesis investigates the network energy consumption issues by considering the data rate and the transmit power. For a given BER constraint, the spectral efficiency has to be optimized, which applies to all adaptive techniques. The approximations and formulas for different link adaptation polices are presented in the following sections.

3.6.1 BER Approximation for MQAM

The spectral efficiency is the main advantage to be gained from AM analysis. It is defined as the average data rate per unit bandwidth (R/B). The transmission rates are determined by modulation schemes, i.e. $r(\gamma) = \log_2[M(\gamma)]$ (bits/symbol) [8]. Therefore, the spectral efficiency for continuous rate adaptation (3.1) and the discrete rate adaptation (3.2), respectively, is given by [8]:

$$\frac{R}{B} = \int_0^{\infty} r(\gamma)p(\gamma)d\gamma \tag{3.1}$$

$$\frac{R}{B} = \sum_{i=0}^{N-1} r_i \int_{\gamma_i}^{\gamma_{i+1}} p(\gamma)d\gamma \tag{3.2}$$

The adaptive rate $r(\gamma)$ is determined by the modulation schemes typically restricted by an average transmit power $\bar{P}$. The transmit power constraint in this assumption is given by:

$$\int_0^{\infty} P(\gamma)p(\gamma)d\gamma \leq \bar{P} \tag{3.3}$$

Average BERs in the channel is usually defined as the number of error bits per transmission over the total number of bits per transmission. i.e.:

$$\overline{BER} = E\left[\frac{error\ bits\ per\ transmission}{total\ bits\ per\ transmission}\right] \tag{3.4}$$

With Gray bit mapping, the expression for the BER of MQAM can be approximated as a function of the receiver SNR $\gamma\left(\frac{P(\gamma)}{\bar{P}}\right)$ and the constellation size M [8]:

$$BER_{MQAM}(\gamma) \approx \frac{2}{log_2 M}\left(1 - \frac{1}{\sqrt{M}}\right) \times erfc\left(\sqrt{1.5\frac{\gamma\frac{P(\gamma)}{\bar{P}}}{M-1}}\right) \tag{3.5}$$

As this expression cannot be easily solved for its power $P(\gamma)$ and its rate $R = \log_2 M$, it can be considered as a tight approximation of the following equation for constellation size $M \geq 2$ and BER less than 10^{-3} [8]:

$$BER_{MQAM}(\gamma) \leq 0.2exp\left(\frac{-1.5\gamma\frac{P(\gamma)}{\bar{P}}}{M-1}\right) \tag{3.6}$$

This tight approximation for rate variation and power adaptation is used in this these for network lifetime analysis. The constellation sizes are taken as 2 or above and the BER constraint value is set to 10^{-4}.

3.6.2 Variable Rate

Considering the data transmission rate varied with channel gain, the network can achieve its optimal transmission rate by two means: 1) fixing the symbol rate and using multiple modulation schemes or constellation sizes, or 2) fixing the modulation scheme and changing the symbol rates. Usually, the second method is difficult to implement because varying symbol rate requires varying signal bandwidth which is complicated in practice [23]. In contrast, changing the modulation types or the constellation sizes is more feasible. For this reason, it is employed in this thesis, i.e., the modulation schemes are varied to achieve the optimal rate during transmission.

To formulate the variable-rate modulation problem, we consider a family of MQAM modulation signals with a fixed symbol rate T_s , with M denoting the constellation size of the modulation scheme, $\bar{P}$ denoting the average transmit power, and N_0 and B being the noise and

bandwidth, respectively. Assuming ideal Nyquist pulses for each constellation, the average received SNR $\bar{\gamma}$ is expressed as [8]:

$$\bar{\gamma} = \frac{\bar{P}T_s}{N_0} = \frac{\bar{P}}{N_0 B} = \frac{E_s}{N_0} \tag{3.7}$$

Recall that the spectral efficiency is defined as data rate per unit bandwidth R/B. For a fixed M, it becomes $R/\mathrm{B} = (\log_2 M)/\mathrm{B}$ bits/symbol. In this case, we are only considering the variable rate. The spectral efficiency is therefore parameterized by the average transmit power and the BER. Rearrange equation (3.6) in terms of M, the expression for the constellation size is obtained as a function of the received SNR γ:

$$M(\gamma) = 1 + \frac{-1.5\gamma}{ln\,(5BER)} \frac{P(\gamma)}{\bar{P}} \tag{3.8}$$

where $\bar{P}$ is the average power and $\frac{P(\gamma)}{\bar{P}}$ is the normalized transmit power. In rate adaptation, the sensor node always communicate using the transmit power so that $\frac{P(\gamma)}{\bar{P}} = 1$.

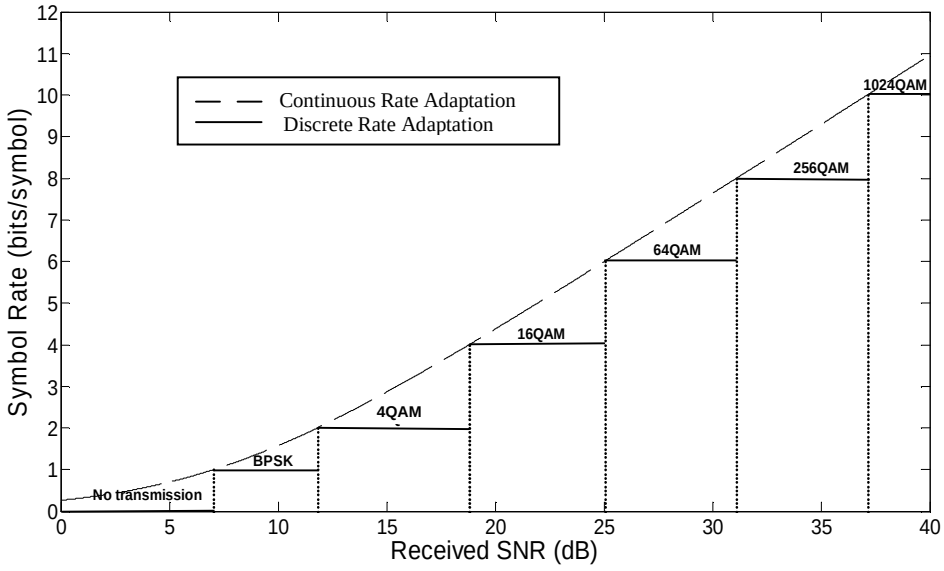

Figure 3.2: Symbol rate verification using adaptive modulation when Pe = 10^{-4}

The relation between symbol rates and received SNRs for continuous and discrete rate adaptation is depicted in Figure 3.2. The spectral efficiency can then be optimized by maximizing:

$$E[r(\gamma)] = E\left[log_2\left(M(\gamma)\right)\right] = \int log_2\left(1 + \frac{-1.5\gamma}{ln\,(5BER)}\frac{P(\gamma)}{\bar{P}}\right)p(\gamma)d\gamma \tag{3.9}$$

with respect to the power constraint in equation (3.3).

3.6.3 Variable Power

The transmit power can be adapted to compensate for SNRs. The goal is to maintain a fixed BER and equivalently, a constant received SNR. In [8], two techniques are proposed for fixed-rate variable-power adaptation: channel inversion adaptation and truncated channel inversion. Although both techniques are aiming to maintain a constant received SNR, the former suffers from a larger power penalty since most of the average signal power is used to compensate for deep fading channel condition, while the latter provides a cutoff level below which no signal is transmitted. The power adaptation formula for channel inversion is given by [8]:

$$\frac{P(\gamma)}{\bar{P}} = \frac{\sigma}{\gamma} \tag{3.10}$$

where σ is the constant received SNR, and γ is the channel gain.

Using this power adaptation policy, the spectral efficiency is obtained by substituting equation (3.10) into (3.8):

$$\frac{R}{B} = log_2\left(1 + \frac{-1.5\gamma}{ln(5BER)E[1/\gamma]}\right) \tag{3.11}$$

When using the truncated channel inversion for power adaptation, the fading can be inverted above a given cutoff γ_0. The power adaptation is [8]:

$$\frac{P(\gamma)}{\bar{P}} = \begin{cases} \frac{\sigma}{\gamma} & \gamma \geq \gamma_0 \\ 0 & \gamma \leq \gamma_0 \end{cases} \tag{3.12}$$

Similarly, the spectral efficiency for truncated channel inversion is given by:

$$\frac{R}{B} = max_{\gamma_0}\, log_2\left(1 + \frac{-1.5\gamma}{ln(5BER)E_{\gamma_0}[1/\gamma]}\right) \tag{3.13}$$

By introducing a power control technique to determine the power level needed for a successful transmission, power control values are formulated by rearranging equation (3.6) in terms of $\frac{P(\gamma)}{\bar{P}}$. We then obtain the expression of the normalized power control factor as:

$$\frac{P(\gamma)}{\bar{P}} = \frac{ln(5BER)\times(M-1)}{-1.5\cdot\gamma} \tag{3.14}$$

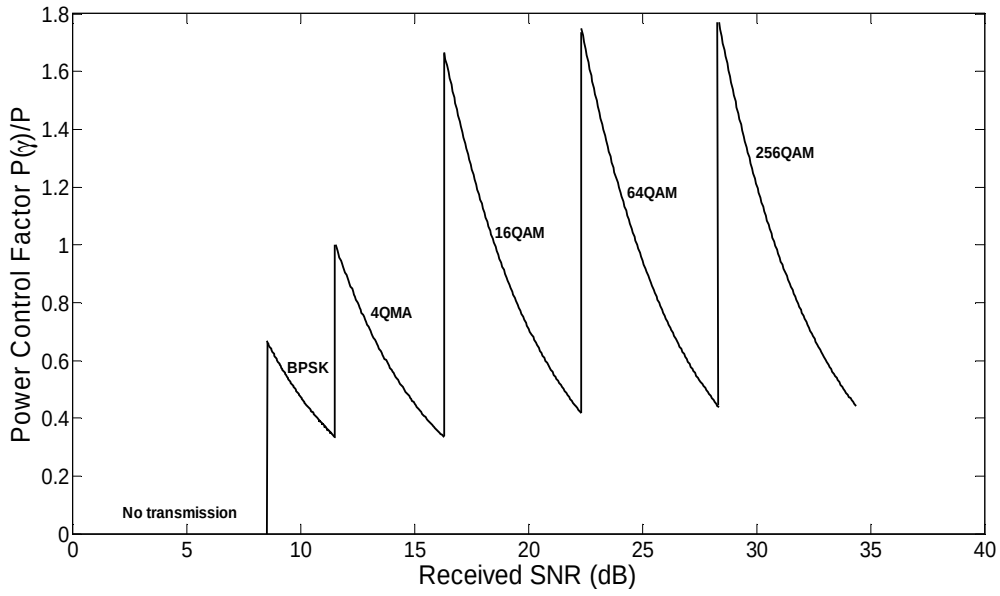

Figure 3.3: Normalized power allocation for MQAM

For each received SNR value, the instantaneous power value $P(\gamma)$ can be calculated as the product of the power control factor $\frac{P(\gamma)}{\bar{P}}$ and the average power $\bar{P}$. Thus, instead of using a fixed average power for transmission at all time, the instantaneous power level can be varied according to the channel conditions. The power control factors relative to the received SNRs are displayed in Figure 3.3. As shown in the figure, the power level is reduced with increased SNR for the same modulation scheme. Significant power increase occurs only when the transmitter is switching from the lower modulation levels to the higher ones.

3.6.4 Adaptive Rate and Power for MQAM modulation scheme

By combining rate adaptation and variable-power technique, the spectral efficiency can be further improved. Optimal spectral efficiency can be determined for four cases: continuous rate adaptation with an average BER constraint (C-Rate A-BER), continuous rate adaptation with an instantaneous BER constraint (C-Rate I-BER), discrete rate adaptation with an average BER constraint (D-Rate A-BER), and discrete rate adaptation with an instantaneous BER constraint (D-Rate I-BER). Obviously the instantaneous BER constraints are special cases of the average BER constraints; therefore, it has lower spectral efficiency under the same conditions [18].

In this thesis, the discrete rate continuous power adaptation (c.f. Section 4.3 for details) is used to maximize the spectral efficiency with the constraints of average power and average BER. This then becomes a constrained optimization problem, which can be solved using the Lagrange method. The general Lagrange equation for this optimization problem subject to the power and BER constraints is given by:

$$f_{opt} = f_r(\gamma) + \lambda_1 \sum_{i=1}^{n} BER_i(\gamma) + \lambda_2 \sum_{i=1}^{m} P_i(\gamma) \tag{3.15}$$

where f_r is the energy optimization problem; BER_i is the instantaneous BER constraints; and P_i is the average transmit power constrains subject to each SNR values. The optimal rate and power can be satisfied by solving the following equation:

$$\frac{\partial f_{opt}}{\partial r(\gamma)} = 0 \; and \; \frac{\partial f_{opt}}{\partial P(\gamma)} = 0 \tag{3.16}$$

where $r(\gamma)$ and $P(\gamma)$ are the rate and power respectively with additional constraints. Both of them are non-negative for all SNR γ.

3.7 Summary

This chapter has reviewed the adaptive modulation and link adaptation techniques in energy constrained networks. Adaptive modulation relies on a feedback channel to deliver the estimated CSI from receiver to transmitter so as to make decisions on appropriate modulation schemes and transmit power levels to use. Benefited from such adaptive process, the network resources, especially energy, can be used more wisely. A variety of energy saving techniques have been discussed. The fundamental concept of energy-aware adaptation protocols for energy constrained network is also explained. In addition, by considering the BER approximation, the optimization formulas for variable-rate and variable-power link adaptation are explained.

Chapter 4

Multi-hop Relay Network and Energy Constrained Network Analysis

4.1 Introduction

Advances in the WSN technology have given rise to the deployment of small and cheap sensor nodes in a multitude of environmental monitoring and control applications [48], [49]. Due to the small-size, light-weight design and extreme energy constraints imposed on sensor nodes, energy-aware protocol design is desirable given its ability to extend network lifetime for WSNs.

In this chapter, we discuss the energy consumption issues in energy constrained networks for WSN design. Single-hop discrete rate continuous power adaptation policy is first considered. Link adaptation in multi-hop relay networks is then examined, and adaptive power allocation algorithms are developed. We proposed an ASAM algorithm that optimizes nodes sleep time to reduce energy consumption. The algorithm is formulated with respect to MAC layer protocols.

4.2 Energy Consumption with Adaptation Techniques

In energy constrained networks, the total amount of energy available is fixed and finite. In order to avoid frequent battery replacement for the sensor nodes, reducing energy expenditure during transmission is crucial. The general formula of energy consumption can be expressed as power level and transmission time:

$$E = P \times T \tag{4.1}$$

where P is the power level and T is the transmission time determined as the reciprocal of the data rate: $T = 1/R$. Therefore, energy consumption is also dependent on the communication data rate.

In this thesis, we define four operation stages with different power levels for the sensor nodes:

- Transmission stage: The packet is transmitted from one node to another. Both radio transmission and the Central Processing Unit (CPU) are active in transmission mode. The device is able to activate the processor, listen to the channel, wait for receptions, and transmit the data. This stage has the highest power level since the transmission requires a large amount of energy for delivering the packets and for overcoming the channel noise to achieve an acceptable SNR.
- Active stage: The node is awake and waiting for the packets to be transmitted. In this stage, the transmission is off while the CPU is still active. The current consumption now is referred to as "run current", which supports the high volume of CPU activities. This stage spends less energy than the transmission stage. However, since the node is still active, it will still be operating at a much higher power level relative to the idle stage.
- Idle stage: This is also known as the "idle mode". It is different from the sleep stage (or hibernation stage) in which all the functionalities of the device are dormant. In this stage, the CPU can still maintain low activities. The radio transmission is off and the data is retained. Therefore, the current consumption in this mode is lower than in both the transmission and the active stage, but higher than the sleep stage.
- Sleep stage: After the data is successfully delivered, the node is hibernating or deep sleeping. All the components are powered down and placed on stand-by to save energy. To wake up the transmitter and CPU again, it only needs a clock signal. The current consumption in this stage is the lowest among the four stages.

The energy consumed at each stage is determined by its power level and operating duration. This work studies the pre-node lifetime during communication by considering the energy

consumption of the four different operating stages. Link adaptation technique is analyzed in point-to-point communication for single-hop networks. In addition, adaptive power allocation factors for the multi-hop relay networks are also derived.

4.3 Single-hop Discrete Rate Continuous Power Adaptation

We first investigate the single-hop network case where the source directly transmits to its destination. Here, we consider the discrete rate continuous power adaptation with instantaneous BER adaptation, since it has been proven that this protocol is a superior candidate to other protocols [35]. For a given set of discrete rates $\{r_i\}_{i=1}^{N-1} = log_2(M_i)$, each rate remains a constant in the region $[\gamma_i, \gamma_{i+1})$, where $i = 1,2, \dots, N-1$. According to equations (3.15) and (3.16), the optimal power adaptation is expressed as [8]:

$$\frac{P(\gamma)}{\bar{P}} = \frac{h(r_i)}{\gamma} \tag{4.2}$$

where $h(r_i) = \frac{ln\,(5BER)}{-1.5} \times (M_i - 1)$ and $BER(\gamma) = \overline{BER}$ in this case.

The optimal rate region boundaries can be found via the Lagrange optimization method. The Lagrange equation for a discrete rate continuous power protocol is given by [18]:

$$J(\gamma_1, \gamma_2, \dots, \gamma_N) = \sum_{0 \le i \le N-1} r_i \int_{\gamma_i}^{\gamma_{i+1}} p(\gamma) d\gamma + \lambda \left[\sum_{0 \le i \le N-1} \int_{\gamma_i}^{\gamma_{i+1}} \frac{h(r_i)}{\gamma} p(\gamma) d\gamma - 1 \right] \tag{4.3}$$

Solve the equations:

$$\frac{\partial J}{\partial \gamma_i} = 0, \;\; 0 \le i \le N-1 \tag{4.4}$$

Therefore, the SNR thresholds of the optimal power can be found as:

$$\gamma_0 = \frac{h(r_0)}{r_0} \rho \tag{4.5}$$

and

$$\gamma_i = \frac{h(r_i) - h(r_{i-1})}{r_i - r_{i-1}} \rho, \;\; 0 \le i \le N-1 \tag{4.6}$$

where ρ a constant determined by the average power constraints in equation (3.3).

Interpreting this equation in a discrete rate manner, the average power can be determined by:

$$\sum_{0\le i\le N-1} \int_{\gamma_i}^{\gamma_{i+1}} \frac{h(r_i)}{\gamma} p(\gamma) d\gamma = 1 \tag{4.7}$$

Since source nodes directly transmit to the destination, energy consumption in the network can be quantified by the node lifetime. The node lifetime, in turn, is defined as the period of time during which the node has sufficient energy for transmitting information to its destination. The objective of single-hop discrete rate continuous power adaptation is then to achieve maximum node lifetime, by adaptively changing the transmission rate and power level according to the channel conditions, based on the discrete rate threshold values derived via equations (4.5)-(4.7).

4.4 Multi-hop Relay Networks

In the previous section, the node lifetime in single-hop WSNs has been discussed. However, a typical WSN system usually consists of several nodes. These nodes communicate with each other and form a multi-hop network. In this scenario, we will need to focus on the lifetime of the overall network instead of the lifetime of a single node.

In particular, this work concerns in two types of multi-hop networks: 1) relay networks in which source data is transmitted to the destination via relay nodes, and 2) multiple-link networks in which multiple wireless communication links are formed by several independent sources and destinations. In both cases, wireless channels can be easily influenced by each other. As a result, the shadowing effects between links are normally correlated. This phenomenon will lead to new research direction in multi-hop correlated shadowing. Recent research considers such correlation effects and proposes more realistic channel models [50], [51]. In this thesis, however, we consider a simplified model in which the links are independent with no correlated shadowing effects.

4.4.1 Link Adaptation in Multi-hop Relay Networks

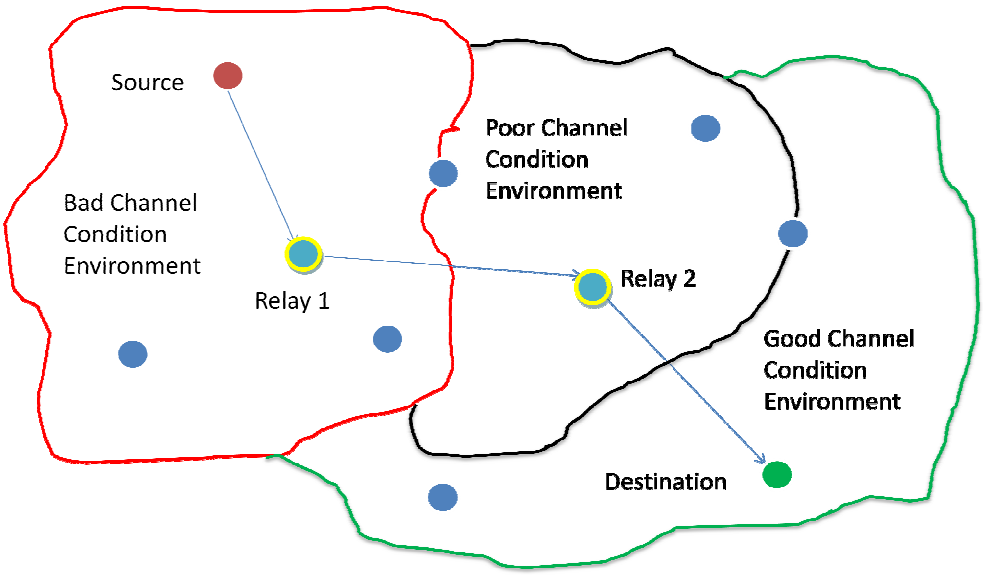

Figure 4.1: An example of multi-hop relay network

In the same WSN, communication links are usually subject to different channel conditions [52]. This is because wireless links are formed by sensor nodes randomly distributed in the environment, and channel fading is often varying with time, geographical position and radio frequency. Figure 4.1 illustrates an example of a multi-hop relay network model. In the figure, the source node and destination node are located in bad and good channel conditions, respectively, with several relay nodes distributed under different channel conditions. Information will be forwarded to a destination through the chosen relays by taking the energy saving routing protocol into consideration [53]. In this scenario, we are interested in analyzing the behavior of link adaptation in two-link relay networks. A simplified model for this two-link relay network is shown in Figure 4.2.

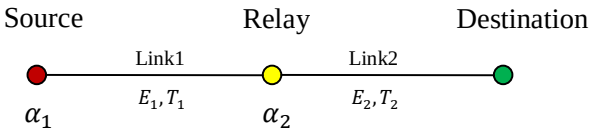

Figure 4.2: Two-link Relay Network Model

In this model, source, relay and destination nodes form two wireless channels. The same packet will be delivered through both communication links. However, transmitters in source node and relay node make independent decisions on which modulation type and power level to employ. The network is constrained by the total available energy. Although the amount of energy is fixed, the necessary transmit power allotted to each node is adaptively adjusted to achieve minimum network energy consumption.

We introduce the power allocation factor α. It is defined as the percentage of the total average power allocated to the node; hence α must satisfy $0 < \alpha < 1$. Extending equation (4.3) and considering the scenario of discrete rate continuous power adaptation, the optimal problem can be interpreted as:

$$J(\gamma_1, \gamma_2, \dots, \gamma_N) = \sum_{0 \le i \le N-1} r_i \int_{\gamma_i}^{\gamma_{i+1}} p(\gamma) d\gamma + \lambda \left[\sum_{0 \le i \le N-1} \int_{\gamma_i}^{\gamma_{i+1}} \frac{h(r_i)}{\gamma} p(\gamma) d\gamma - \alpha \right] \tag{4.8}$$

The optimal rate and power region boundaries can be obtained using essentially the same procedure described by equations (4.4)-(4.6). Inserting the new parameter α to equation (4.7), the transmit power constraint become:

$$\sum_{0 \le i \le N-1} \int_{\gamma_i}^{\gamma_{i+1}} \frac{h(r_i)}{\gamma} p(\gamma) d\gamma = \alpha \tag{4.9}$$

In this two link relay network shown in Figure 4.2, the total energy is divided between the source node and the relay node. Denote their power allocation factors as α_1 and α_2, respectively. Both α_1 and α_1 satisfy the energy constraints in the network. i.e.:

$$0 < \alpha_1 < 1\ ,\ 0 < \alpha_2 < 1 \tag{4.10}$$

$$\alpha_1 + \alpha_2 = 1 \tag{4.11}$$

Denote the energy consumption in link 1 and link 2 as E_1 and E_2, and the link lifetimes as T_1 and T_2, respectively. In addition, it is assumed that when the energy allocated to either node has been exhausted, the whole network is considered as "dead" and reaches the limit of its lifetime. Define the network lifetime as the period of time that both nodes are alive and able to transmit data, i.e. $Network\ Lifetime = min\ (Link1\ lifetime, Link2\ lifetime)$. The optimal network lifetime T^* is expressed as:

$$T^* = T(\alpha^*) \tag{4.12}$$

where $\alpha^* = arg\,max_{\alpha^*}\big(min\big(T_1(\alpha), T_2(\alpha)\big)\big)$ is the optimal power allocation vector that contains the power allocation factors for both links when the network lifetime is maximized. Considering the energy consumption, we can also formulate the problem by calculating the minimum energy consumption in the entire network subject to optimal power allocation:

$$E^* = E(\alpha^*) \tag{4.13}$$

Thus, by solving the optimal network energy consumption problem, the optimal power allocation factors are determined.

4.4.2 Link Adaptation Multiple-Link Networks

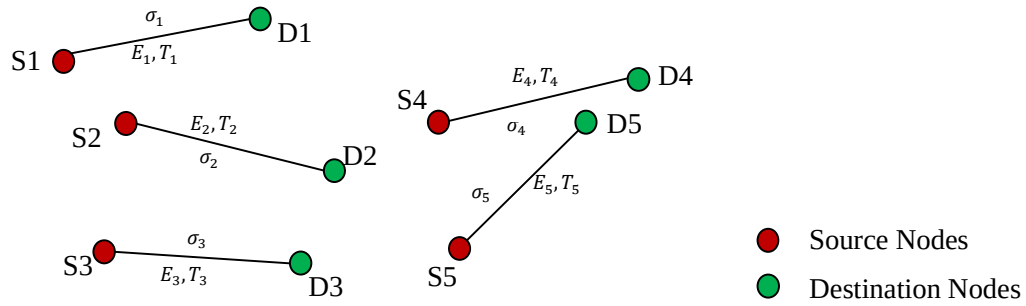

Figure 4.3: An Example of Multiple Sources and Destinations Network Model

When there are several source nodes and destination nodes in the network, data transmission between nodes establish multiple communication links. This is known as the multiple-link network. Figure 4.3 depicts a five-link example where five source nodes and five destination nodes are randomly distributed in the network. Each source node can only communicate with its own destination node and all the links operate individually. Therefore, energy consumption of each link could be considered independently. For different channel fading conditions, the nodes consume different amounts of energy for delivering packets successfully. When a source node exhausts its battery energy, it is no longer able to transmit information and the connectivity of this particular path is lost. The network lifetime is related to the number of nodes still alive.

4.5 MAC Layer Adaptive Modulation and Adaptive Sleep

The MAC layer is a sub-layer of the Data Link Layer specified in the seven-layer OSI model [54]. It sits directly on top of the PHY layer and acts as an interface between the Logical Link Control (LLC) sub-layer and the PHY layer in order to manage access to the shared wireless medium [55]. At the network level, it provides addressing and channel access control for nodes or

terminals to communicate within a multi-hop network [56]. In wireless standards, MAC layer protocols deal with collision through contention resolution algorithms. These algorithms provide sufficient time intervals between packets which effectively avoid message overlapping [57]. As shown in Figure 4.4, the total frame duration can be split into the actual data transmission time (labeled as Tx in the figure) and active/idle time when the transmission process has been completed and no further actions are required. Between two subsequent transmissions, the nodes can be put to sleep.

It needs to be noticed that the active/idle stage is the MAC layer pre-allocated contention period which ensures that the previous transmission is completed before the next one happens. During this contention period, the node can operate either in the active stage with high CPU activities or in the idle stage with low CPU activities depends on different CPU functionalities. Obviously, the active stage requires higher power level than the idle stage. But since the radio transmission is off, the power levels are much smaller compared to the transmission stage. In WSNs, nodes send acknowledgement (ACK) packets such as idle channel information, clear to send (CTS), and request to send (RTS), to indicate their channel status. Based on different ACKs, the node responds with corresponding actions. These actions themselves, however, also take time to be processed, thus incurring delays and sometimes collisions. In this sense, the contention period gives extra room for the channel to deliver the pervious packet and prepare the channel for the next one. After the fixed contention period, node enters the sleep stage to wait for the next transmission.

Sleep stage, on the other hand, is the time interval between transmissions. It is also known as the “hibernation stage”, during which all the components in the node are not processing to effectively reduce energy consumption. Since nodes in WSNs do not need to operate at all time,

they can be powered down right after completing the contention period. The energy consumption is minimized in this way because the nodes are operating with a much lower power level. Depending on how frequently the data is transmitted, the sleep time might account for a substantial portion of the overall communication duration. Consequently, the energy saving can be very considerable in such cases, as also demonstrated in Chapter 5.

The basic MAC layer protocol fixes the time of channel occupation for one transmission. It also pre-allocates the durations of the node transmission, active, and idle stages, giving no freedom for energy adaptation. As illustrated in Figure 4.4, every time the node detects a packet waiting to be transmitted, the protocol wakes up the node and sets the fixed durations for the transmission, active and sleep stages. Adaptive modulation techniques, on the other hand, dynamically change the data rates according to the channel conditions. This normally varies the transmission duration to be less than the pre-allocated transmission, hence reducing the amount of energy consumed by the transmission stage. For further optimization in energy consumption, the network can consider employing energy-aware protocol for inter-communication between sensor nodes, also known as MAC layer adaptive sleep [58]. Adaptive sleep techniques have been studied recently to ameliorate energy efficiency in WSNs. It uses MAC layer protocols to set the duty cycle for the contention period and meanwhile adaptively adjusts the sleep time according to current CSI. Therefore, instead of remaining in the active and idle stage, it can stay in the sleep stage after the contention period until the next packet is ready to be transmitted.

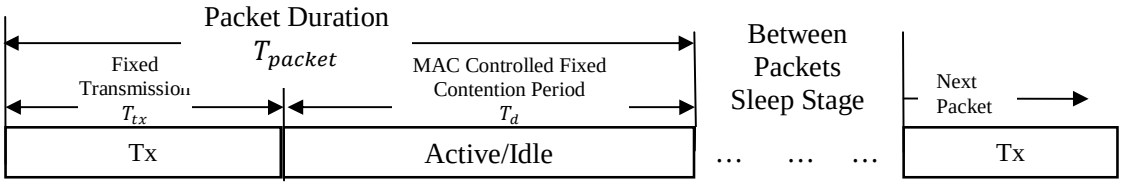

Figure 4.4: Packet duration in MAC layer protocol

In the following sections, we explain the operating stages for Adaptive Modulation (AM), Adaptive Modulation with Idle mode (AMI) and Adaptive Sleep with Adaptive Modulation mode (ASAM). The total energy (E_t) is defined as the available battery energy pre-node. The communication processes consume energy and due to different operation stages the total consumed energy (E_c) is consists of: 1) Transmission energy (E_{tx}), 2) Active energy (E_{active}), and 3) Idle energy (E_{idle}). The sleep energy (E_{sleep}) is also considered in the process. In order to conduct a fair comparison of the energy consumption among the three algorithms, the sleep energy level and the time intervals between packets are considered the same. However, the sleep duration is dependent on the traffic intensity in the network (explained in Chapter 5). The time dedicated to one packet (T_{packet}) and duty cycle of the contention period (T_d) is pre-determined by the MAC layer protocols. The energy consumption formulas for calculating E_c formed based on equation (4.1).

4.5.1 Energy Consumption in Adaptive Modulation Mode (AM)

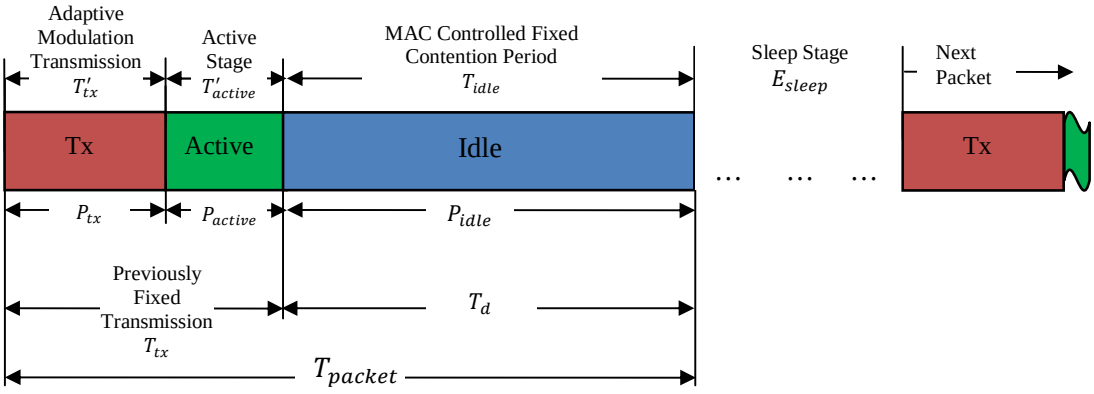

Figure 4.5: Energy consumption in adaptive modulation mode

Combining AM techniques with the MAC layer protocol, the transmission time can be dynamically adjusted via adapting modulation schemes. As mentioned in Section 4.2, energy consumption is the product of the power level and transmission time. Hence, the less time for the transmission, the less energy is used during the process. AM allows the data to be transmitted at different rates according to the channel conditions. It adaptively changes the modulation constellation size, therefore varying the rate and transmission time. Thus, the duration for the actual transmission process does not necessarily cover the entire transmission time (T_{tx} as shown in Figure 4.4).

As illustrated in Figure 4.5, the node firstly switches to the active stage with a lower power level after the transmission. It then enters the idle stage which has further reduced the power level compare to the other two stages. Note that the time for the transmission stage is controlled by AM while the node idle durations is still controlled by MAC layer protocols. The overall energy consumption is calculated by considering the three types of energy expenditure in the network:

$$\begin{aligned} E_c^{AM} &= E'_{tx} + E'_{active} + E_{idle} \\ &= P_{tx} \times T'_{tx} + P_{active} \times T'_{active} + P_{idle} \times T_{idle} \\ &= P_{tx} \times \frac{l}{R} + P_{active} \times (T_{packet} - \frac{l}{R} - T_d) + P_{idle} \times T_d \end{aligned} \tag{4.14}$$

where P_{tx} is the transmit power; $T'_{tx} = \frac{l}{R}$ is the adaptive transmission time with l is the packet length and R being the AM rate; $E'_{tx} = P_{tx} \times T'_{tx}$ is the transmission energy. P_{active} is the active power; T'_{active} is the time for the node operates in active stage, which varies in line with T'_{tx}; $E'_{active} = P_{active} \times T'_{active}$ is the active energy. P_{idle} is the idle power; $T_{idle}$is the fixed idle time determined by MAC layer protocol; $E_{idle} = P_{idle} \times T_{idle}$ is the idle energy. Also note that $T'_{tx} = \frac{l}{R}$, $T_{idle} = T_d$ and $T'_{tx} + T'_{active} + T_{idle} = T_{packet}$

4.5.2 Energy Consumption in Adaptive Modulation with Idle Mode (AMI)

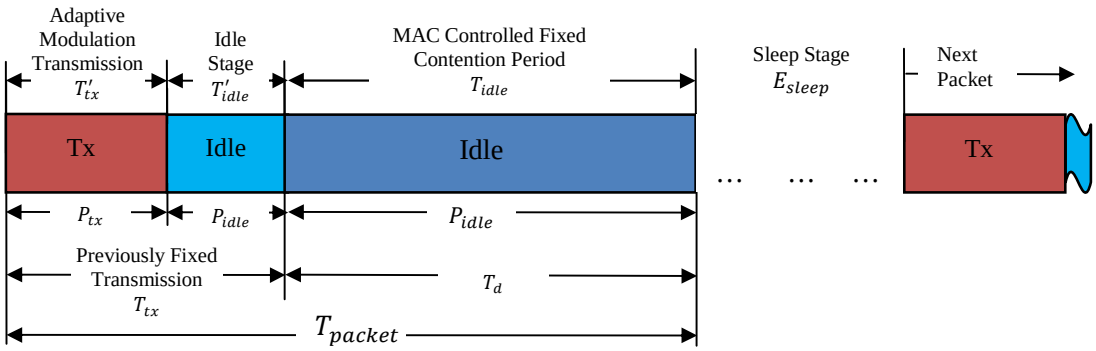

Figure 4.6: Energy consumption for adaptive modulation with idle mode

In AM, node operates in the active mode after the transmission when the CPU still has high activities, which might include executing back-stage programs and/or storing information to the memory. However, in WSNs, there is no need for the node to maintain a high volume of activities after each transmission. Instead, it can operate in idle mode immediately after the transmission to with minimum CPU activities (see Figure 4.6). This offers additional improvement in energy efficiency. This process is so-called adaptive modulation with idle mode. Its total energy consumption is determined as:

$$\begin{aligned} E_c^{AMI} &= E'_{tx} + E'_{idle} \\ &= P_{tx} \times T'_{tx} + P_{idle} \times T'_{idle} + P_{idle} \times T_{idle} \\ &= P_{tx} \times \frac{l}{R} + P_{idle} \times (T_{packet} - \frac{l}{R} - T_d) + P_{idle} \times T_d \\ &= P_{tx} \times \frac{l}{R} + P_{idle} \times (T_{packet} - \frac{l}{R}) \end{aligned} \tag{4.15}$$

Similarly, P_{tx} is the transmit power; $T'_{tx} = \frac{l}{R}$ is the adaptive transmission time, l is the packet length and R is the AM rate; $E'_{tx} = P_{tx} \times T'_{tx}$ is the transmission energy. P_{idle} is the idle power; T'_{idle} is the adaptive idle time; $T_{idle} = T_d$ is the fixed node idle time; $E'_{idle} = P_{idle} \times T'_{idle} + P_{idle} \times T_{idle}$ is the idle energy. In this case, $T'_{tx} + T'_{idle} + T_{idle} = T_{packet}$

4.5.3 Energy Consumption in Adaptive Sleep with Adaptive Modulation Mode (ASAM)

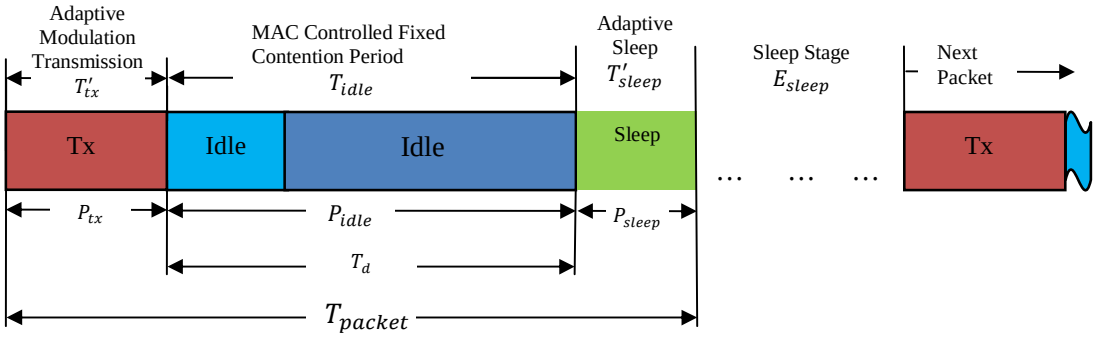

Figure 4.7: Energy consumption for adaptive sleep with adaptive modulation mode

In order to further minimize energy consumption, an ASAM algorithm is proposed, which combines the adaptive sleep with adaptive modulation based on the MAC layer protocol. As shown in Figure 4.7, the MAC layer still allocates the same amount of idle period to ensure the pervious packet is successfully delivered. However, instead of staying in the active or idle stage for a while, node is put into the sleep stage right after the pre-allocated contention period T_d. In other words, the additional active or idle stage is not necessary for this algorithm. The total time for completing one packet is adaptively reduced. Therefore, not only the transmission time is adapted by AM, but also the sleep time is varied by AS. The energy consumption formula in this case becomes:

$$\begin{aligned} E_c^{ASAM} &= E'_{tx} + E_{idle} + E'_{sleep} \\ &= P_{tx} \times T'_{tx} + P_{idle} \times T_{idle} + P_{sleep} \times T'_{sleep} \\ &= P_{tx} \times \frac{l}{R} + P_{idle} \times T_d + P_{sleep} \times (T_{packet} - \frac{l}{R} - T_d) \end{aligned} \tag{4.16}$$

Notes that in this case, P_{sleep} is the sleep power; T'_{sleep} is the adaptive sleep duration; $E'_{sleep} = P_{sleep} \times T'_{sleep}$ is the sleep energy dynamically controlled by AS protocol.

4.6 Summary

Energy consumption issues have been discussed in this chapter. Network energy consumption using discrete rate continuous power adaptation polices in single-hop networks as well as power allocation algorithm in multi-hop relay networks has been examined. Formulas of energy consumption in various networks are presented, and link adaptation techniques are analyzed. Moreover, an ASAM algorithm is proposed based on the concept of link adaptation policies and MAC layer protocols. It can further reduce the energy consumption in the network by forcing the nodes into the sleep stage immediately after the pre-allocated contention period. Simulations and comparison results of AM, AMI, and ASAM for energy saving will be presented in Chapter 5.

Chapter 5

Simulation Results

5.1 Introduction

This chapter first explains the simulation steps and methodology and then presents the simulation results. The experimental parameters and assumptions are discussed. Based on the framework established in Chapter 2, we investigate the energy consumption in the network under different degrees of Lognormal shadowing and Rician fading channel conditions. Different link adaptation policies are studied and used to evaluate the network lifetime. Comparisons are drawn among the AM method, the AMI scheme and the proposed ASAM algorithm. The impact of different transmission parameters on node lifetime is analyzed. Furthermore, we calculate the optimal power allocation vectors for a two-link relay network and investigate its effects on the network lifetime.

5.2 Simulation Objective

The objective of this work is to evaluate the performance of adaptive modulation polices under energy constraints for WSNs. By considering the network constraints, various link adaptation protocols are evaluated based on energy optimization methods. The joint optimization of rate and power is performed for point-to-point communication. The adaptive power allocation algorithm is further examined for reducing energy cost in multi-hop networks. The second goal is to investigate the ability of the ASAM algorithms to improve energy saving. The system's operating lifetime is compared by assessing the energy efficiency using different algorithms. Finally, the performance of AM, AMI, and ASAM on commercial transceivers is compared.

5.2.1 Simulation Parameters

The simulation parameters are selected such that the QoS requirements for the worst case scenario are met [59], [60]. Relevant parameters are listed in Table 5.1.

Table 5.1: Simulation Parameters

Parameter	Description	Value
K	Rician K-factor	{0, 5, 10, 15, 20}dB
σ	Lognormal shadowing Variance	{0, 2, 4, 6, 8}dB
$\bar{\gamma}$	Average SNR	10-36 dB
P_b	BER requirement for QoS	10^{-4}
M	MQAM modulation constellation size	{2, 4, 16, 64, 256}
B	Channel Bandwidth	200 kHz
n	Path-loss Exponent	3
E_t	Total Battery Capacity	1200mAhr
V	Operating Voltage	3.6V
I_{Tx}	Transmit Current	120 mA
I_{active}	Active Current	100 mA
I_{idle}	Idle Current	1 mA
I_{sleep}	Sleep Current	0.1mA
T_d	Duty Cycle for Contention Period	75%
T_{packet}	Packet Duration	1 unit of time

5.2.2 Simulation Assumptions

Trading off the simulation accuracy with complexity, the following assumptions are made:

- Both transmitter and receiver have perfect knowledge of CSI
- The transmission parameters remain constant over one frame period
- Channel conditions stay the same during transmission
- No errors are introduced by the feedback channel, and the delay is negligible
- The transmission process is reliable and all packets arrive independently
- Perfect routing nodes are selected and all nodes are aware of their position to others

5.3 Simulation Procedures and Methodologies

In this thesis, all the simulations are conducted in MATLAB. In this section, the simulation model and procedures are explained, which are used to evaluate the performance of the network link adaptation behaviors. The evaluation system responds to communication and considers two system layers: PHY layer and MAC layer.

- PHY Layer is responsible for:
    1. Generating source data;
    2. Adaptively controlling the modulation schemes and power levels;
    3. Transmitting data over the fading channel;
    4. Demodulating the received data;
    5. Estimating and feeding back the current CSI.
- MAC Layer is responsible for:
    1. Coordinating the access to the medium;
    2. Allocating time for different stages under MAC layer protocols for AM policies;
    3. Synchronizing the transmission time.

The simulation analyzes the results for energy consumption in point-to-point communication and multi-hop relay networks. Various link adaptation policies are used for minimizing energy consumption and enhancing spectral efficiency, while still maintaining the required QoS during the communication.

For systematic organization of the results, all of the link adaptation policies analyzed in this chapter are listed here. We analyzed the energy consumption for the following protocols:

- AM, AMI, and ASAM Comparison (Sections 3.6.4, 4.3, and 4.5)
    1. Channel Conditions : Lognormal shadowing and Rician Fading
    2. Average SNR
    3. Modulation Stages
    4. Traffic Intensity
- Single-hop Power Control Adaptation Policies (Section 3.6.3)
- Multi-hop Link Adaptation (Section 4.4)

5.4 Energy Optimization Methods

The energy efficiency in the network is highly dependent on the transmission parameters and channel conditions. The focus of the simulation is to evaluate different energy optimization algorithms by adjusting the network parameters. For a given BER constraint, the optimal energy in the network is obtained by jointly considering the data rate and the transmit power. Formulas for calculating the energy consumption using link adaptation techniques have been explained in Chapter 4. Since nodes in a network can be distributed among different channel condition environments, the channel conditions are modeled by considering different fading effects for each link. Specifically, Lognormal shadowing and Rician fading effects are considered in this study. Moreover, sensor nodes in the network normally do not communicate continuously. It is assumed that on average each packet is sent at a 10-second interval. The impact of different traffic intensity on energy consumption is also analyzed.

As described in Sections 3.6.4 and 4.3, optimizing the data rate and the transmit power jointly contributes to energy cost reduction in transmission under fading channel conditions. With link adaptation, a transmitter dynamically makes decisions on the appropriate modulation schemes and power levels to use, based on the current CSI. Given the set of MQAM constellations and BER constraints listed in Table 5.1, the switching levels for the discrete rate adaptation can be calculated using equation (3.8). The transmitter is designed to automatically switch to the next level modulation scheme once the average SNR exceeds the threshold. However, within the same modulation scheme, the transmission rate stays as a constant. Using equations (4.5) and (4.6), the optimal transmission rates are obtained. Packets are then delivered at the optimal rate to decrease the transmission time.

5.4.1 Energy Consumption in AM, AMI, and ASAM

This section investigates the energy consumption in AM, AMI, and ASAM. Recalling the energy consumption formulas discussed in Section 4.5, the node lifetime of AM, AMI, and ASAM is calculated based on the different operating stages required by each algorithm. We analyze the source nodes lifetime for successfully delivering a certain number of packets using the adaptive discrete rate continuous power policy. The source node sends one packet every 10 seconds and is powered down to the according stage after transmission. In each experiment, the same channel conditions are used in AM, AMI, and ASAM for a fair comparison.

The node lifetime achieved by the three algorithms under different degrees of channel fading conditions are shown in Figure 5.1-Figure 5.5 for Lognormal shadowing and in Figure 5.6-Figure 5.10 for Rician fading, respectively. As can be seen from the figures, the proposed ASAM algorithm consistently outperforms the AM technique. Nodes can operate up to 221 days using

ASAM while the longest node lifetime using AM is only 42 days. This translates into an approximately 80% improvement. In addition, the AMI also slightly improves the node lifetime compare to AM. At the high SNR region, AMI extends the node lifetime by approximately 10 days.

In AM, the node is first active after the transmission stage, then switches to the idle stage, and finally enters the sleep stage. In AMI, the active stage is replaced by the idle stage since the processor only requires minimum functionality. Therefore, this portion of the energy is reduced from active energy to idle energy. However, since the power level at the sleep stage is the least, it would be desirable to have the node stay in this stage for the maximum period of time. The ASAM algorithm provides an optimal adjustment of nodes sleep duration according to the CSI, and therefore further enhances the energy efficiency. The main difference between ASAM and AM is that the former enters the sleep stage right after the contention period that is pre-allocated by the MAC layer protocol, while the latter still stays active for a certain period of time before entering the contention period. The significant difference between the sleep power and active power can considerably affect node lifetime, as verified in the figures.

Furthermore, the results also indicate that there are a number of factors that can affect the node lifetime. The factors investigated in this thesis include the following: channel fading conditions, average SNR levels, traffic intensity, and modulation stages. They will be discussed in detail in the following sections.

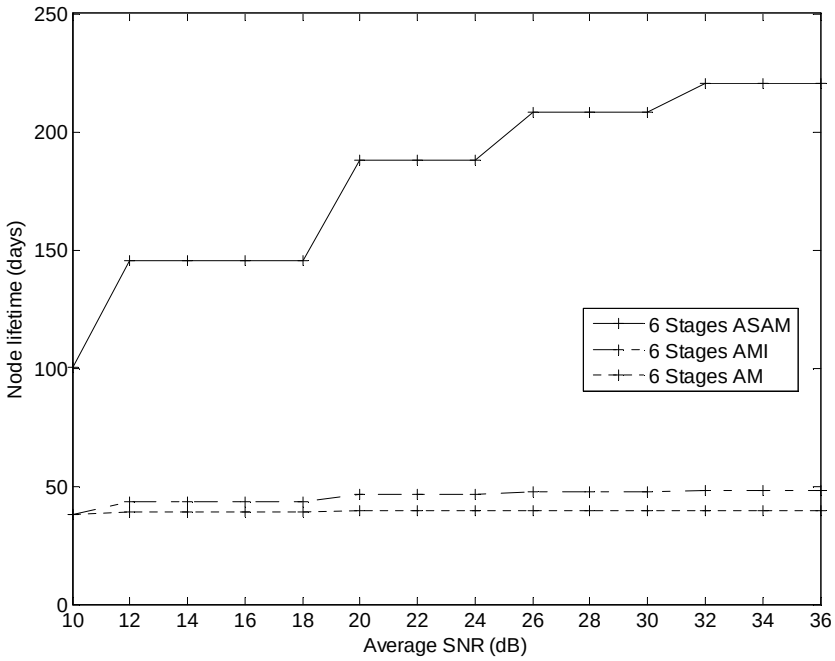

Figure 5.1: Node lifetime simulation: comparison of 6 stages ASAM, AMI, and AM when Lognormal shadowing $\sigma = 0$

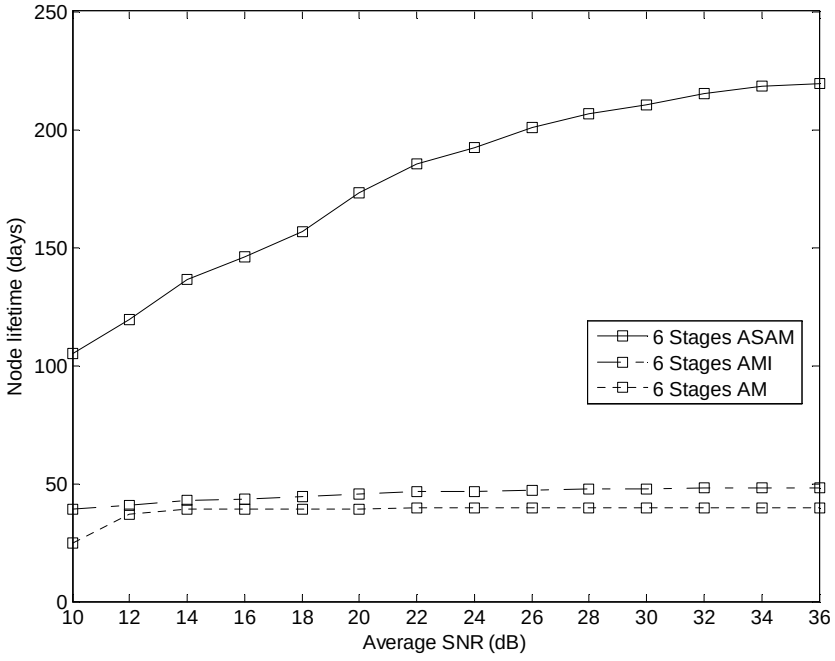

Figure 5.2: Node lifetime simulation: comparison of 6 stages ASAM, AMI, and AM when Lognormal shadowing $\sigma = 2$dB

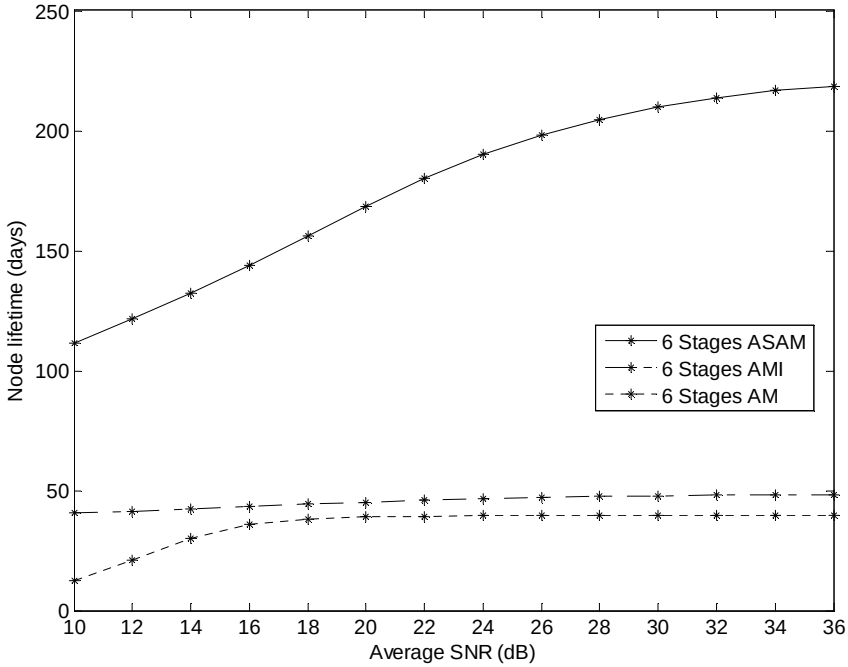

Figure 5.3: Node lifetime simulation: comparison of 6 stages ASAM, AMI, and AM when Lognormal shadowing σ = 4dB

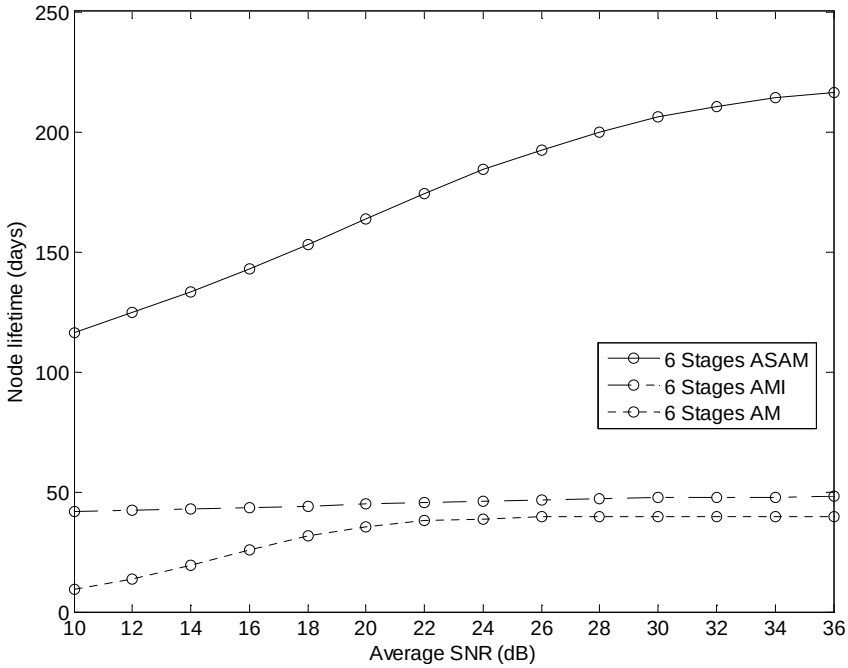

Figure 5.4: Node lifetime simulation: comparison of 6 stages ASAM, AMI, and AM when Lognormal shadowing σ = 6dB

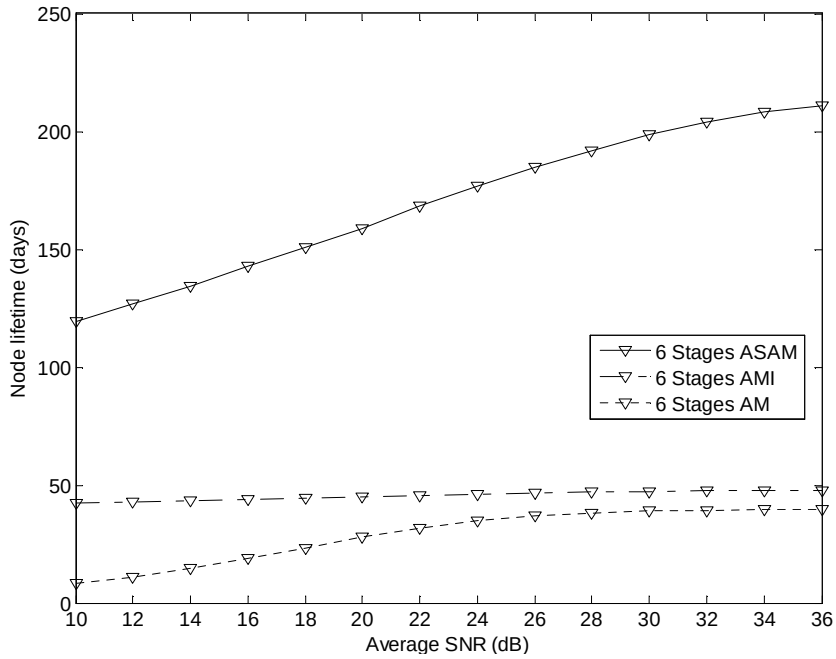

Figure 5.5: Node lifetime simulation: comparison of 6 stages ASAM, AMI, and AM when Lognormal shadowing σ = 8dB

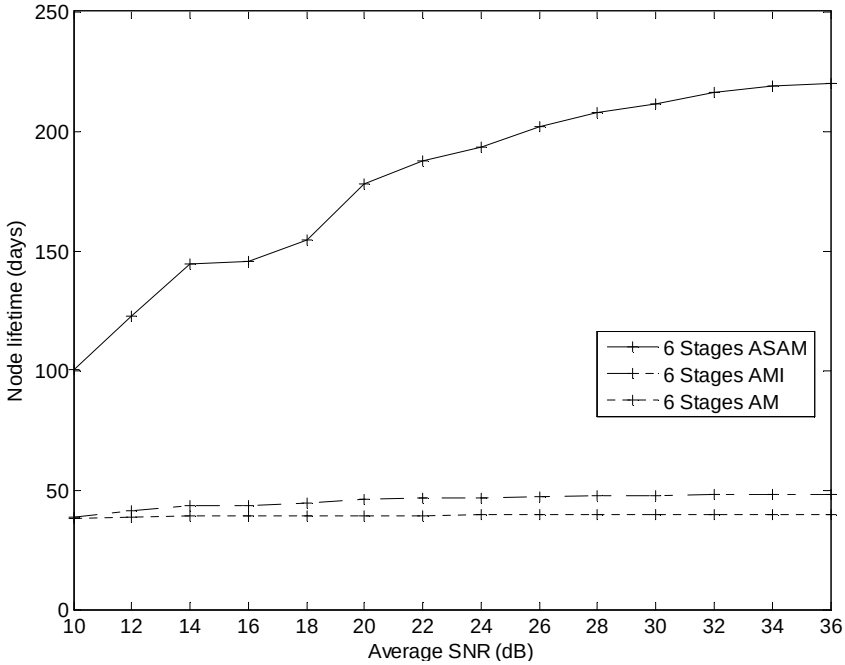

Figure 5.6: Node lifetime simulation: comparison of 6 stages ASAM, AMI, and AM when Rician fading K = 20dB

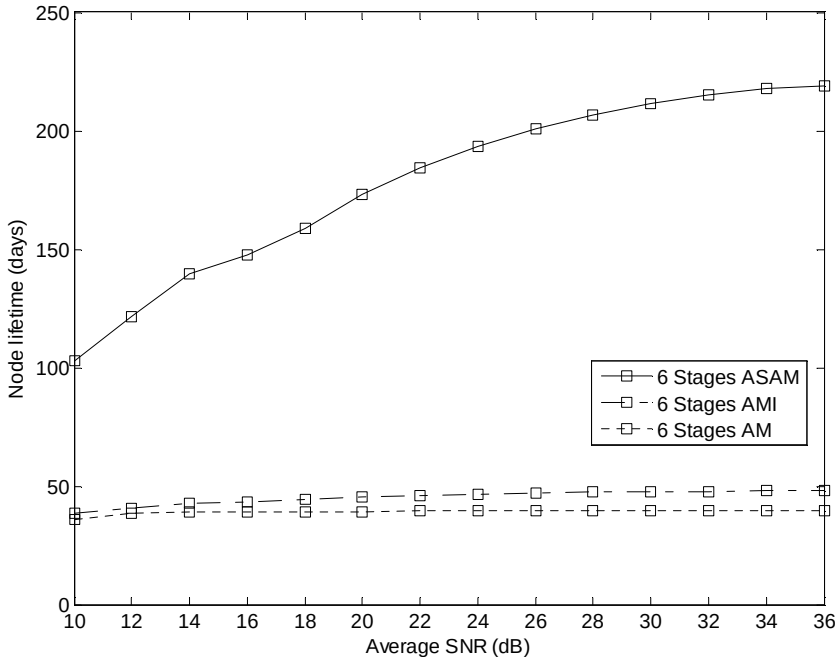

Figure 5.7: Node lifetime simulation: comparison of 6 stages ASAM, AMI, and AM when Rician fading K = 15dB

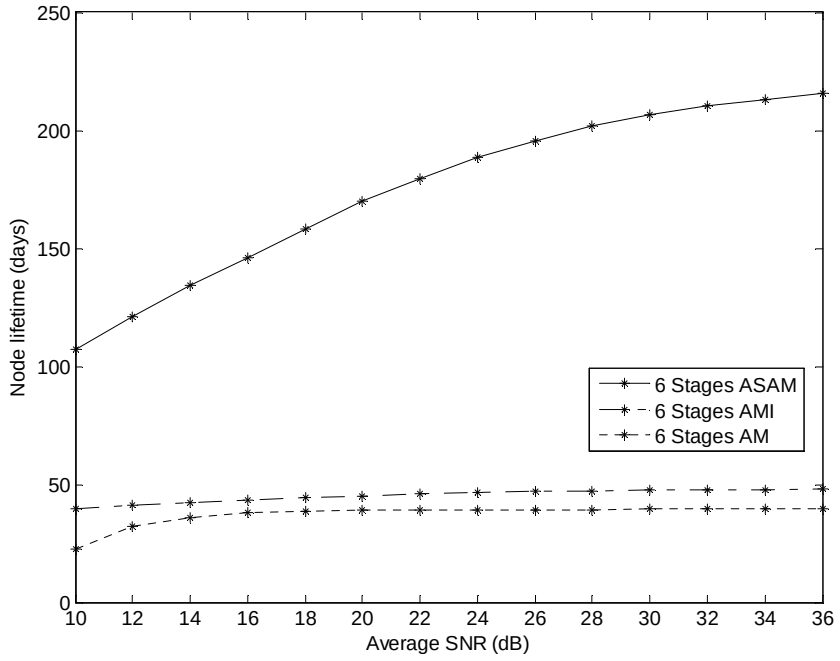

Figure 5.8: Node lifetime simulation: comparison of 6 stages ASAM, AMI, and AM when Rician fading K =10dB

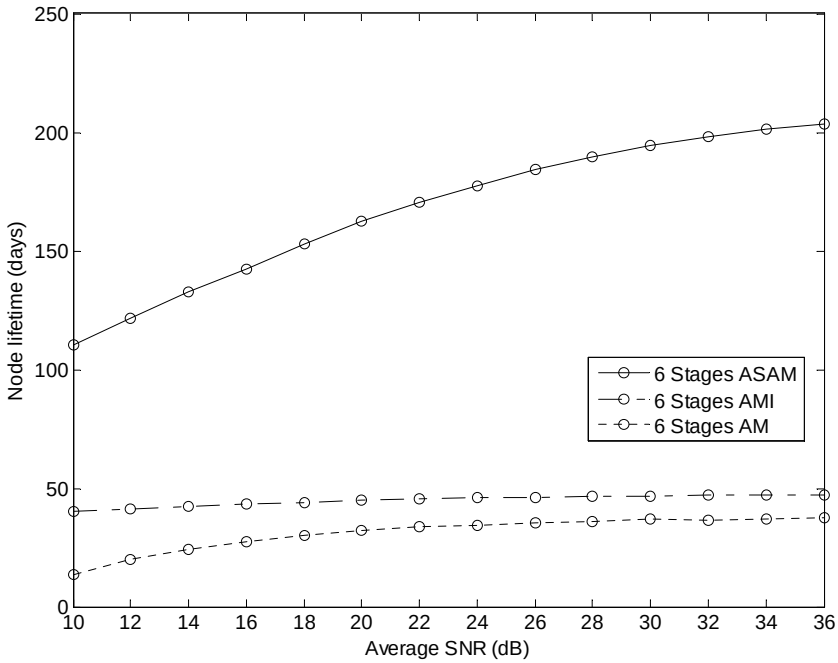

Figure 5.9: Node lifetime simulation: comparison of 6 stages ASAM, AMI, and AM when Rician fading K = 5dB

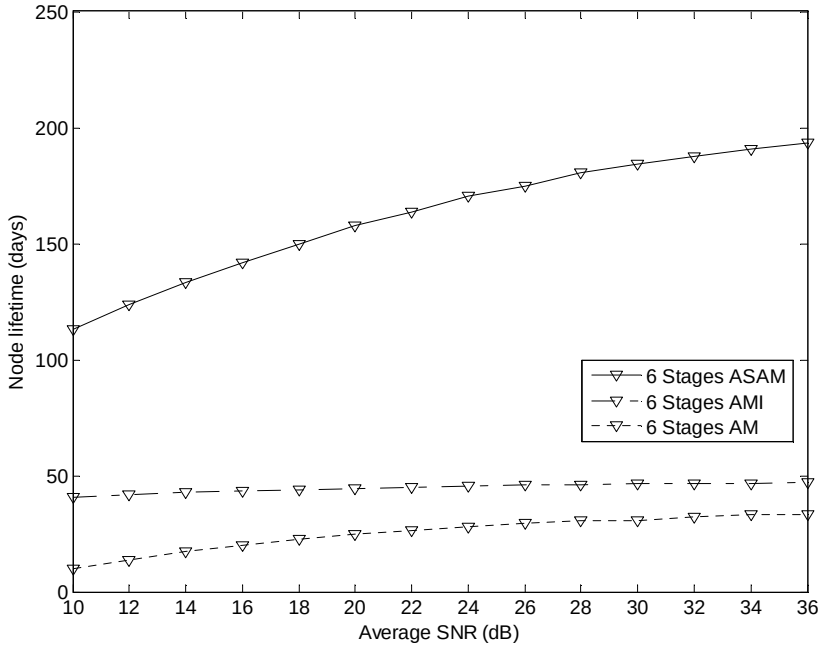

Figure 5.10: Node lifetime simulation: comparison of 6 stages ASAM, AMI, and AM when Rician fading K = 0

5.4.2 Channel Fading and Average SNR

Since sensor nodes are normally deployed to monitor and analyze complex phenomena over a large region, the wireless channels can be easily influenced by various fading conditions in WSNs.[56]. Different channel fading conditions exert different influences on per-node energy consumption, as examined in this section.

The transmission protocol allows the transmitter to have the freedom to choose between 6 modulation stages: no transmission, BPSK, 4QAM, 16QAM, 64QAM, and 256QAM. Here we consider a slowly-varying flat-fading channel. The channel changes much slower than the symbol data rate, so that it remains approximately constant over each transmission period. Lognormal propagation and Rician distribution are used to model the channel shadowing and fading effects, respectively (c.f. Sections 2.3 and 2.4 for details of the approximation). For Lognormal distribution, the standard derivation σ is chosen among $\{0, 2, 4, 6, 8\}$; for Rician distribution, the K-factor K is taken from $\{0, 5, 10, 15, 20\}$.

Figure 5.11 and Figure 5.12 display the node lifetime as a function of σ and K, for Lognormal shadowing and Rician fading effects, respectively. In Figure 5.11, it clearly shows that for each algorithm, under a given average SNR, stronger Lognormal shadowing (i.e., higher σ) yields a shorter node lifetime. In other words, the energy cost is reduced when the network operates in a good channel condition. The behavior is similar for Rician fading cases (see Figure 5.12). The node can operate longer when the fading in the wireless channel is minor (i.e., higher K). The Rician K-factor determines the communication line-of-sight (LOS) for the point-to-point communication. Hence, a smaller K-factor gives deeper fading in the channel and shorter operating time as a result. Moreover, the figures also demonstrate that the node lifetime is heavily dependent on the average SNRs in the network. For the same channel fading condition, increasing

the average SNR extends the node lifetime. For strong fading cases, a poor average SNR can substantially degrade node lifetime performance.

Although the figures indicate that for all the algorithms, the sensor nodes can operate longer with smaller channel fading and larger SNRs, the channel fading conditions and average SNRs show very distinct impacts on energy consumption for different algorithms. For AM, the channel condition has a bigger impact on the node lifetime at low SNRs than at high SNRs. As the average SNR increases, the lifetime gap between different fading conditions becomes smaller. For instance, in Figure 5.11, the node lifetime curves roughly overlap with each other for average SNR greater than 30dB. We can also conclude that the average SNR values become the dominant factor for the energy consumption when the node operates under deep channel fading. However, unlike in AM where good channel conditions considerably improve node lifetime, the channel fading conditions and average SNR values can only affect the energy consumption slightly in AMI.

Such behaviors are due to the fact that in AM, after the packet has been successfully transmitted, the channel still stays active for a certain period of time. For nodes operate in a poor channel condition, there are higher chances of resending the packet. This resending incurs more active power consumption of the node. On the other hand, AMI puts the node into the idle stage immediately after transmission. Even under poor channel conditions where a lot of retransmissions occur, the node only spends the idle power after the retransmission, which is normally much smaller than active power. The difference in energy consumption between various degrades of channel fading is thus not notable in AMI.

The channel fading conditions and average SNRs also have significant impacts on the node lifetime in ASAM. Compared to AM, the performance of the ASAM algorithm is more notably

influenced by the average SNR. The difference in node lifetime is approximately 120 days between the lowest and the highest SNRs for ASAM, while for AM, the difference is less than 30 days. In addition, it can also be found that the node lifetime is more susceptible to channel condition variations in low and high SNR regions, for AM and ASAM, respectively.

Interestingly, it can also be seen from Figure 5.11 and Figure 5.12 that for AMI and ASAM, in the low average SNR region, the node lifetime with larger σ turns out to be longer than smaller σ cases. Recall that σ represents the standard deviation of the instantaneous SNRs. Under low average SNR, a bigger σ indicates both a higher chance of retransmission and a higher chance of transmission with a larger data rate. Retransmission incurs additional energy consumption while a higher data rate reduces the energy cost by using less transmission time. For AMI and ASAM, the retransmission cost is essentially very small. It can be considered that the cost of retransmissions is approximately the same between large σ and small σ; hence the energy saving gained from higher-rate transmission outweighs the downside, i.e., the larger σ, the longer node lifetime, as shown in the plots. For AM cases, on the other hand, a smaller σ consistently yields better performance relative to a larger lifetime. Such phenomenon happens because the retransmission cost for AM is considerably higher than for AMI/ASAM due to the active power level used when retransmission occurs. The disadvantage of having larger σ outweighs the advantage in such cases.

Moreover, under a high average SNR, the node is already transmitting data with a high rate. Increasing σ, therefore, might contribute to a small degree to a better transmission speed, but would increase the likelihood of having low instantaneous SNR, i.e., a low transmission data rate and more energy consumption. As reflected in the figures, a smaller sigma always gives a longer node lifetime in the high average SNR region.

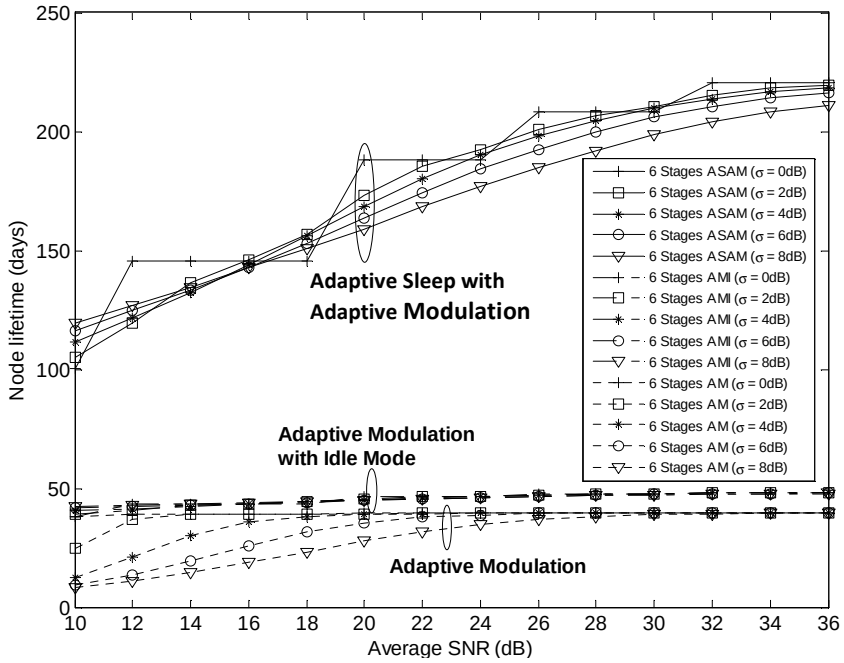

Figure 5.11: Node lifetime simulation: comparison of 6 stages ASAM, AMI, and AM under various Lognormal shadowing channel conditions

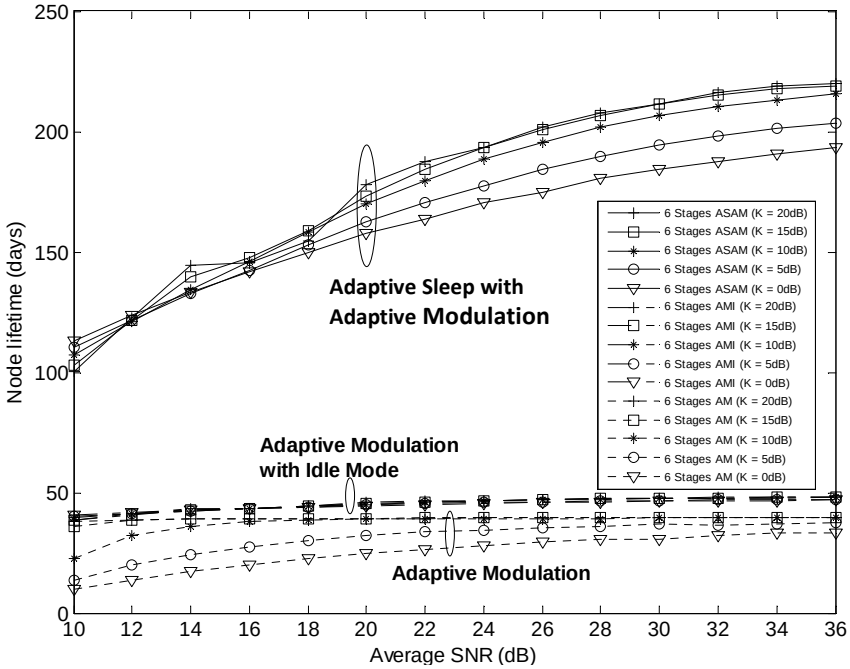

Figure 5.12: Node lifetime simulation: comparison of 6 stages ASAM, AMI, and AM under various Rician fading channel conditions

5.4.3 Traffic Intensity

Traffic intensity is a measure of the average occupancy of wireless resources during a period of time. It is normally used to estimate the number of packets in the network to be transmitted. In WSNs, the sensor node battery lifetime is heavily affected by the number of transmissions. In general, WSNs have low traffic intensity since the information can be stored in memory first and is only sent when necessary. Nodes can operate for a longer period of time if packets are not frequently sent. However, there are some occasions when the sensor nodes need to exchange information, report their statuses, and communicate with the relay nodes very often. During such situations, there can be a heavy traffic load in the communication network. Depending on the traffic intensity, the energy expenditure in the network can differ considerably.

In this section, we further investigate energy consumption using AM, AMI, and ASAM with different profiles of network traffic intensity, namely 1%, 10% and 100%. The network traffic is modeled using Poisson random distribution. A larger intensity indicates more packets that need to be transmitted in the same period of communication time.

Figure 5.13 and Figure 5.14 depict the node lifetime in AM under different traffic intensity profiles for Lognormal shadowing and Rician fading, respectively. It is evident from the figures that for low and moderate average SNRs, low traffic communications yield higher node lifetime. For a given traffic intensity, the node lifetime curves for different fading levels tend to converge as the average SNR increases. The converged node lifetime with 1% traffic intensity can be roughly 3-5 times as long as the 100% intensity case, depending on the fading type. Also, the convergence speed appears to be dependent on the traffic intensity. The heavier the traffic, the larger the average SNR that is required for the lifetime curves to reach convergence.

Similarly, the impact of traffic intensity on energy consumption is also studied for AMI. Figure 5.15 and Figure 5.16 illustrate how the AMI algorithm performs with respect to different traffic loads. As shown in the figures, a heavy traffic load in the channel reduces the sensor node lifetime in AMI, similar to the AM case. Nodes can operate up to approximately 49 days under 1% traffic intensity, while the time is reduced to 46 days and 38 days under 10% and 100% traffic intensity, respectively.

The results of ASAM algorithm cases are given in Figure 5.17 and Figure 5.18. As shown in the figures, the node lifetime can reach up to 439 days under a low traffic profile, which is almost 10 times longer than the node lifetime in AM and AMI. When the network traffic load gets heavier to 10% intensity, the node lifetime is reduced by nearly half to 220 days. Even under the full load (i.e. 100% traffic intensity), the node can still operate over 50 days, which is higher than AM and AMI.

For all the algorithms, it can be concluded that the node lifetime performance is highly dependent on the number of transmissions in the network. This results is expected as when the network has a heavier traffic load, it implies that more packets are in the queue waiting to be delivered. To complete the transmissions of all these packets, the node has to drain more energy from its battery, resulting in a shorter lifetime.

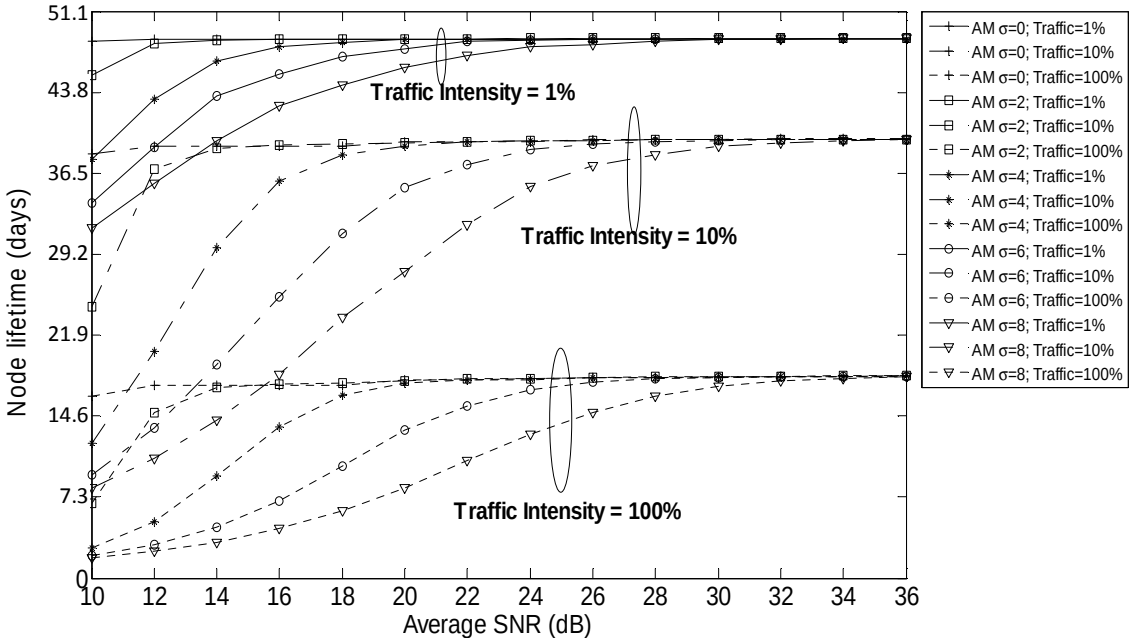

Figure 5.13: Impact of traffic intensity on node lifetime using AM under Lognormal shadowing. Traffic in the channel is 1%, 10% and 100% of the load

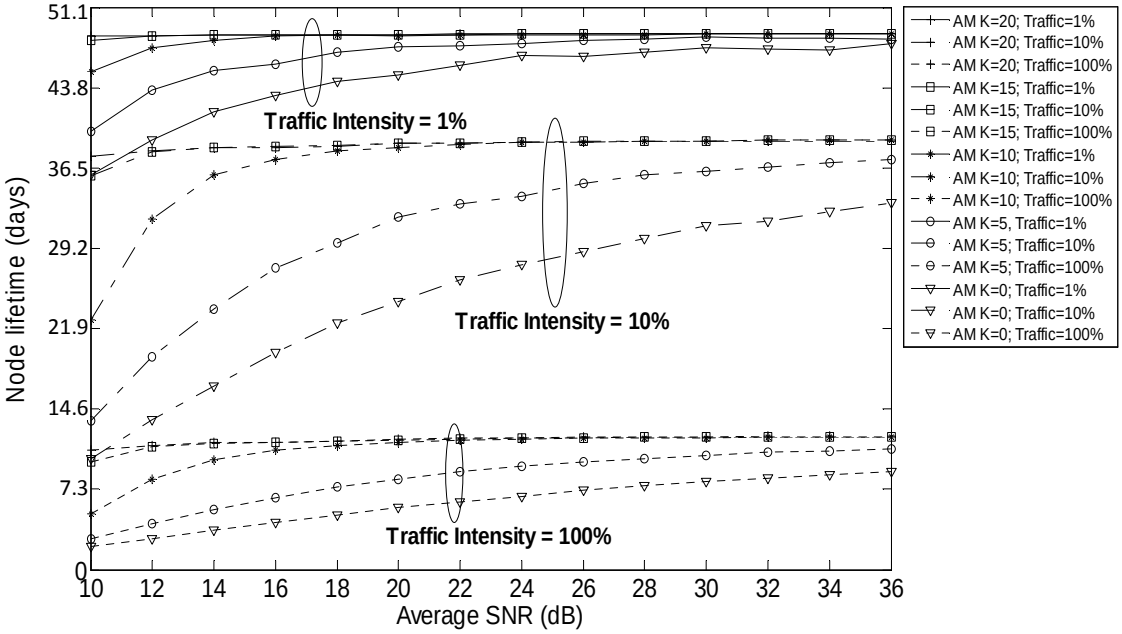

Figure 5.14: Impact of traffic intensity on node lifetime using AM under Rician fading. Traffic in the channel is 1%, 10% and 100% of the load

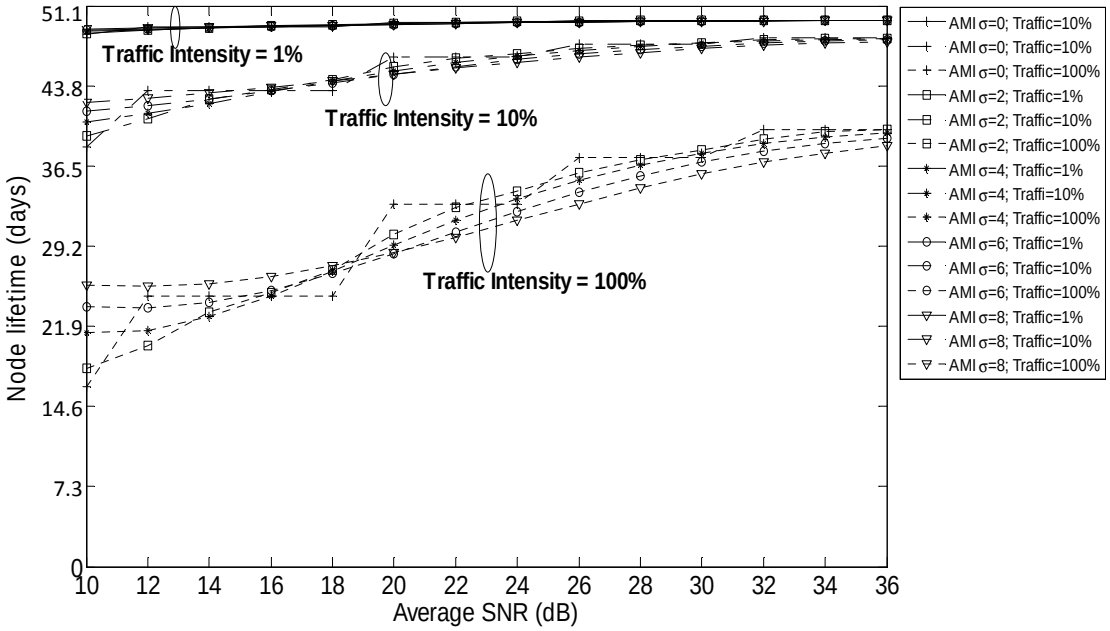

Figure 5.15: Impacts of traffic intensity on node lifetime using AMI under Lognormal shadowing. Traffic in the channel is 1%, 10% and 100% of the load

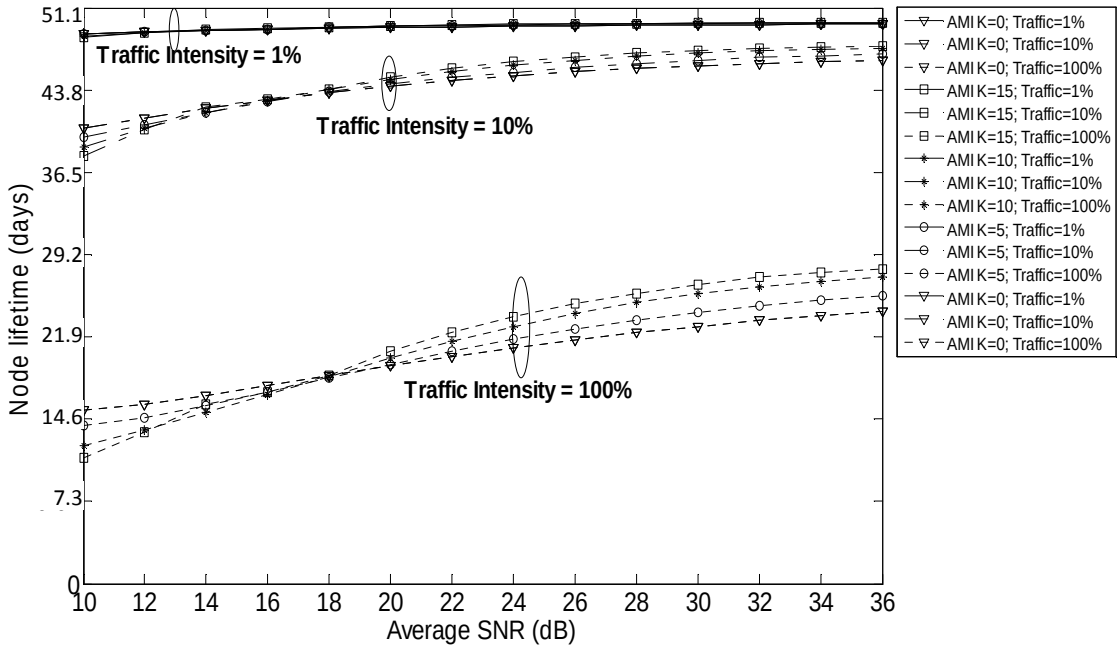

Figure 5.16: Impacts of traffic intensity on node lifetime using AMI under Rician fading. Traffic in the channel is 1%, 10% and 100% of the load

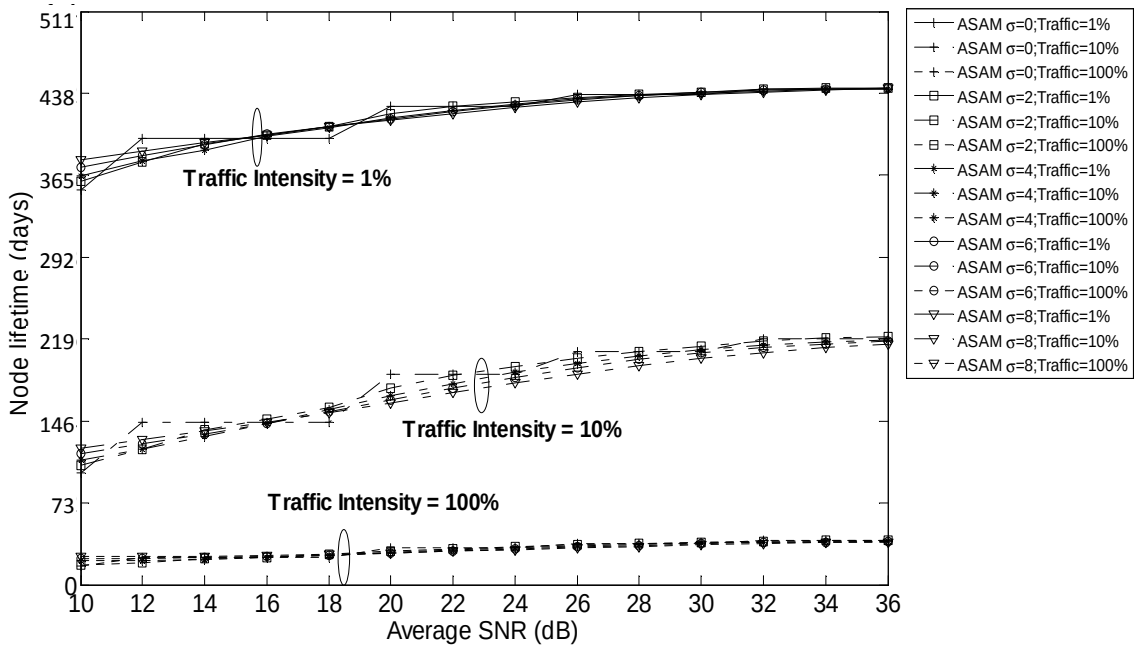

Figure 5.17: Impacts of traffic intensity on node lifetime using ASAM under Lognormal shadowing. Traffic in the channel is 1%, 10% and 100% of the load

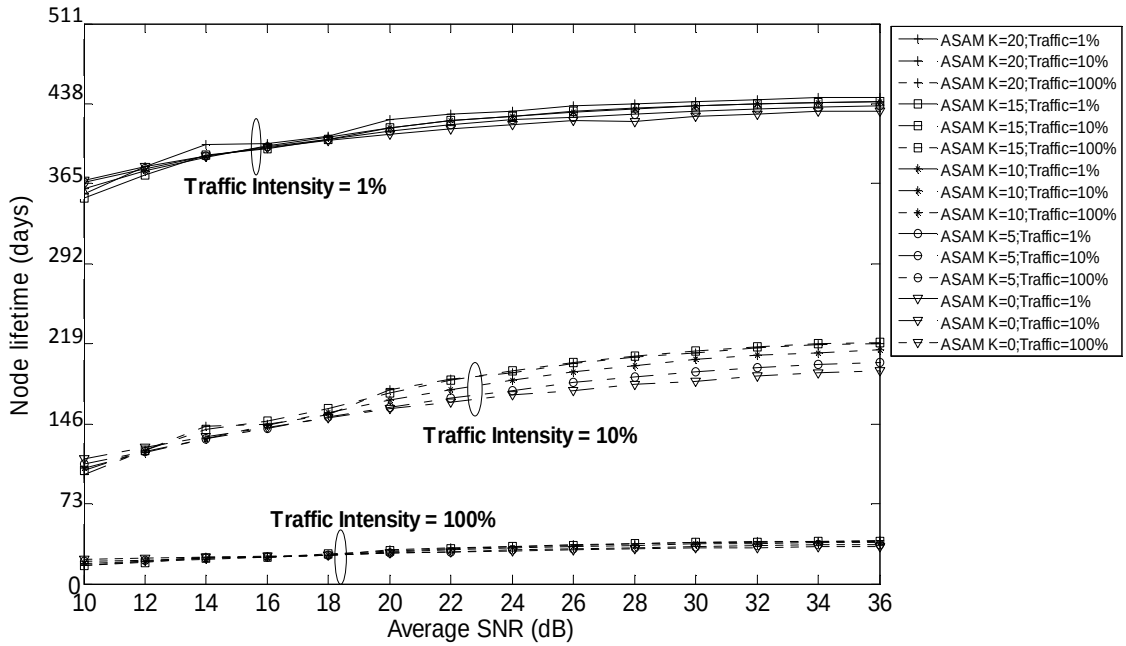

Figure 5.18: Impacts of traffic intensity on node lifetime using ASAM under Rician fading. Traffic in the channel is 1%, 10% and 100% of the load

5.4.4 Modulation stages

The link adaptation technique is designed to have multiple modulation schemes built in one transmitter. This technique offers the transmitter the freedom to switch to the most appropriate modulation scheme according to the CSI [8]. However, the number of stages used in AM varies from application to application and is also subject to the complexity of practical implementation.

In this experiment, we compare the energy efficiency using AM, AMI, and ASAM with different numbers of modulation stages. Four scenarios are compared: 1) 3 stages (no transmission, BPSK, QPSK), 2) 4 stages (no transmission, BPSK, QPSK, 16QAM), 3) 5 stages (no transmission, BPSK, QPSK, 16QAM, 64QAM), and 4) 6 stages (no transmission, BPSK, QPSK, 16QAM, 64QAM, 256QAM).

Node lifetime for the four scenarios is illustrated in Figure 5.19-Figure 5.28. As indicated by the figures, with more modulation stages built into the transmitter, the sensor node can operate for a longer period of time. This behavior is due to the fact that modulation levels restrict the transmission rate. Transmitters that can only choose from low-level modulation schemes have to use a smaller data rate even under very good channel conditions, hence increasing the transmission duration. On the other hand, when the transmitter is equipped with the possibility to choose from higher-level modulation schemes, transmissions benefit from a higher achievable data rate under good channel conditions and thus become less energy-expensive. Moreover, it can also be observed that transmitters with more modulation stages exhibit an advantage after certain SNR thresholds (see Figure 5.19 for example). These threshold values are calculated by the discrete rate continuous power link adaptation policy.

Comparing AM, AMI, and ASAM, it is clearly indicated in the figures that the number of modulation stages has the most significant impact on the node lifetime in ASAM, followed by

AMI, and has the least important effects in AM. In general, a transmitter equipped with more modulation stages has a longer operating lifetime. The most significant improvement is achieved by ASAM, as the node lifetime is increased by more than 70 days from 3 stages to 6 stages. The node lifetime in AMI also shows a slight improvement when using more modulation stages. More stages can increase the node lifetime up to 7 days under good channel conditions. However, the number of modulation stages barely affects the node lifetime when AM is used, with less than one day improvement gained under the same condition.

Such behaviors can be interpreted as follows. The major benefit of using more modulation stages lies in the increased capability of taking advantage of the good channel conditions to reduce transmission time. During the saved amount of time, the node can switch from the most power-hungry transmission stage to some other stage, as determined by the specific algorithm. Between ASAM and AMI, the former adapts the duration of the sleep stage; while in the latter, the node still needs to operate in the idle stage, which consumes an extra portion of idle energy. Thus, because ASAM has more modulation schemes to choose from, it therefore can reduce more energy consumption by taking advantage of transmitting at a high data rate with a lower power level. For AM, however, the node operates in the active stage after the transmission, whose power level, although lower than transmission power, is still much higher than the sleep power and the idle power levels. As a result, even if the transmitter is able to choose modulation levels with higher data rates in AM, the energy saving is relatively insignificant compare to ASAM or AMI.

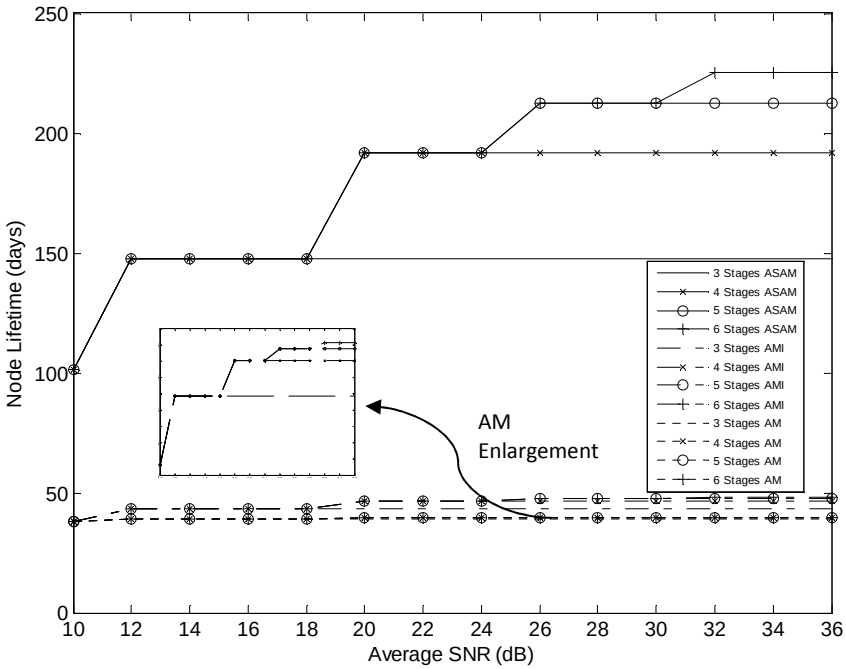

Figure 5.19: Impacts of modulation stages on node lifetime using ASAM, AMI, and AM under Lognormal shadowing when $\sigma = 0$

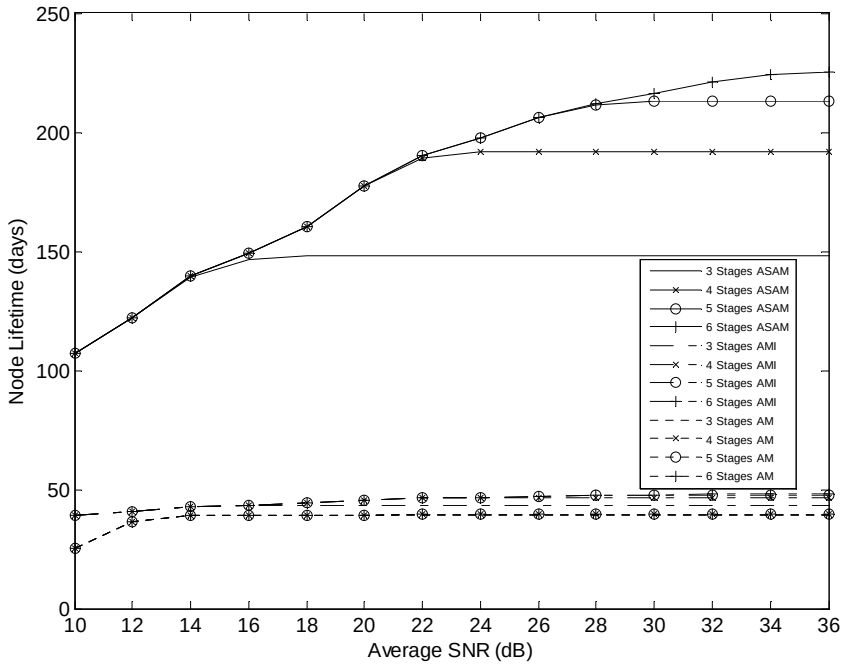

Figure 5.20: Impacts of modulation stages on node lifetime using ASAM, AMI, and AM under Lognormal shadowing when $\sigma = 2$dB

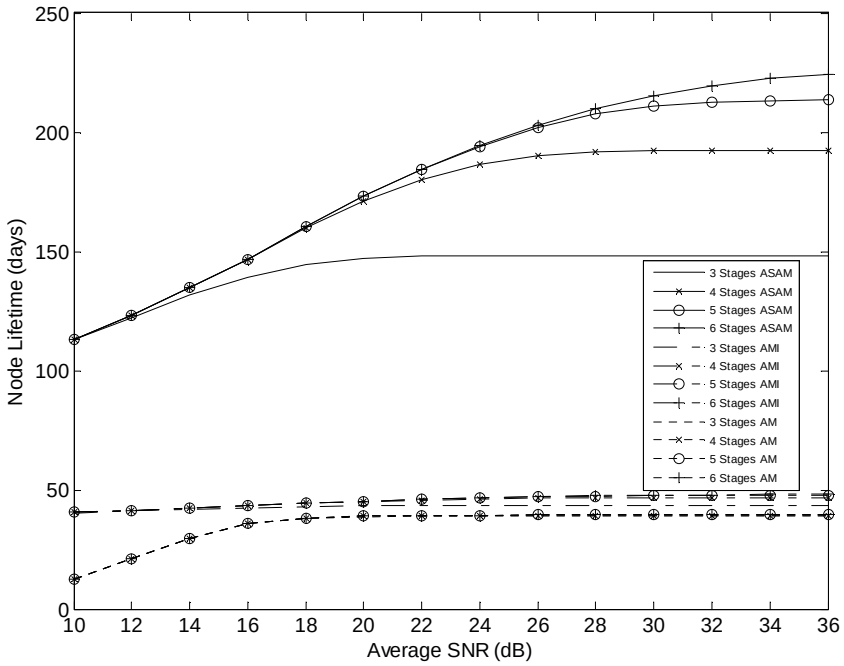

Figure 5.21: Impacts of modulation stages on node lifetime using ASAM, AMI, and AM under Lognormal shadowing when σ = 4dB

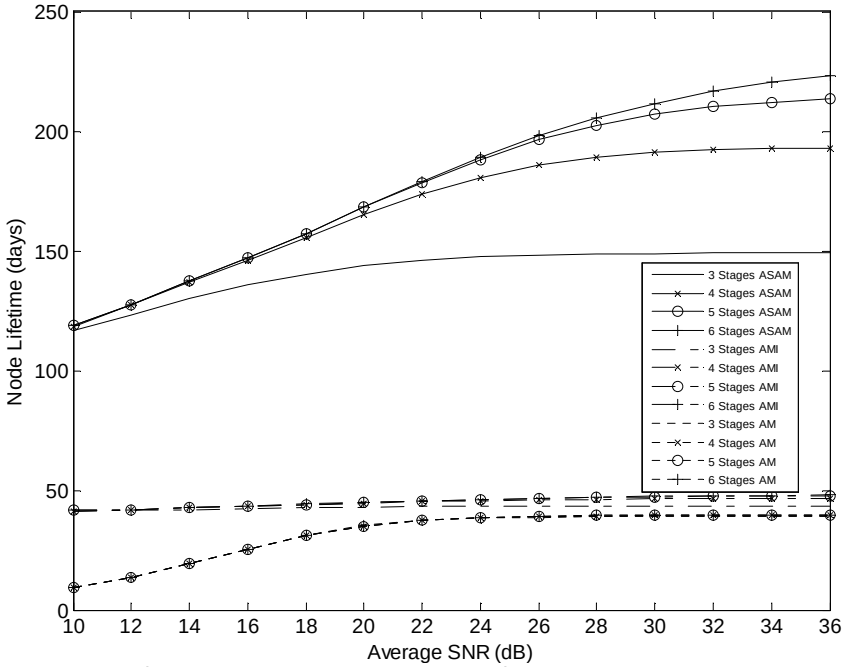

Figure 5.22: Impacts of modulation stages on node lifetime using ASAM, AMI, and AM under Lognormal shadowing when σ = 6dB

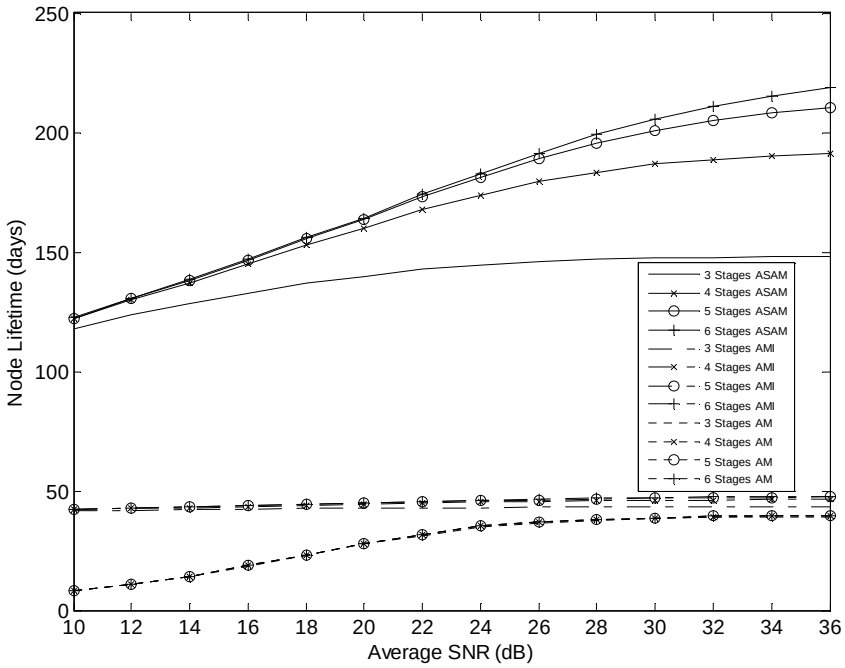

Figure 5.23: Impacts of modulation stages on node lifetime using ASAM, AMI, and AM under Lognormal shadowing when σ = 8dB

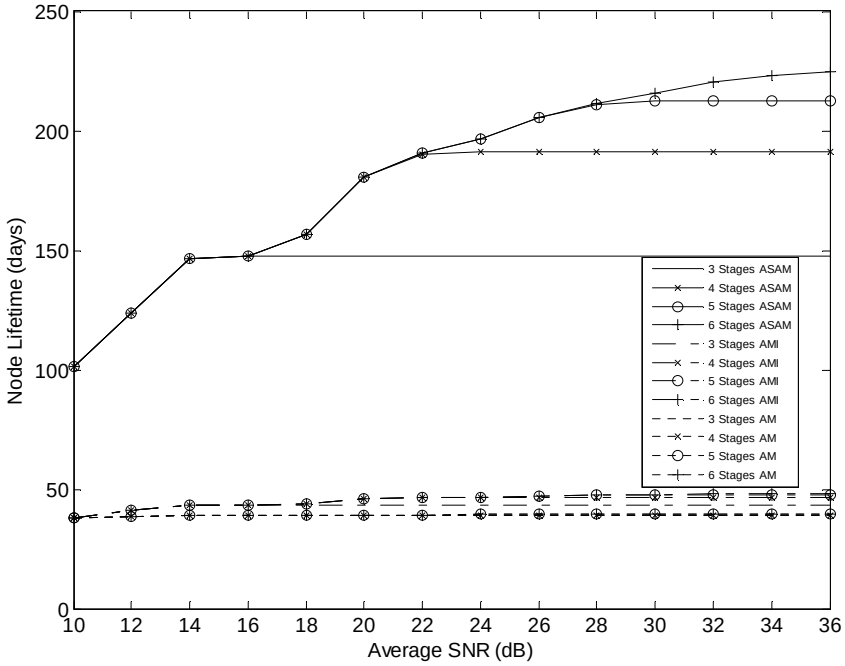

Figure 5.24: Impacts of modulation stages on node lifetime using ASAM, AMI, and AM under Rician fading when K = 20dB

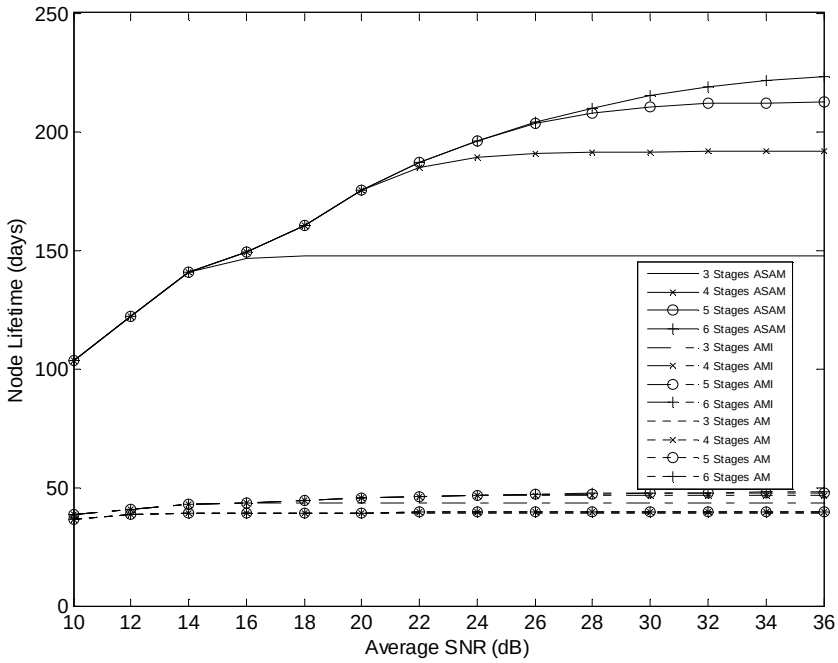

Figure 5.25: Impacts of modulation stages on node lifetime using ASAM, AMI, and AM under Rician fading when K = 15dB

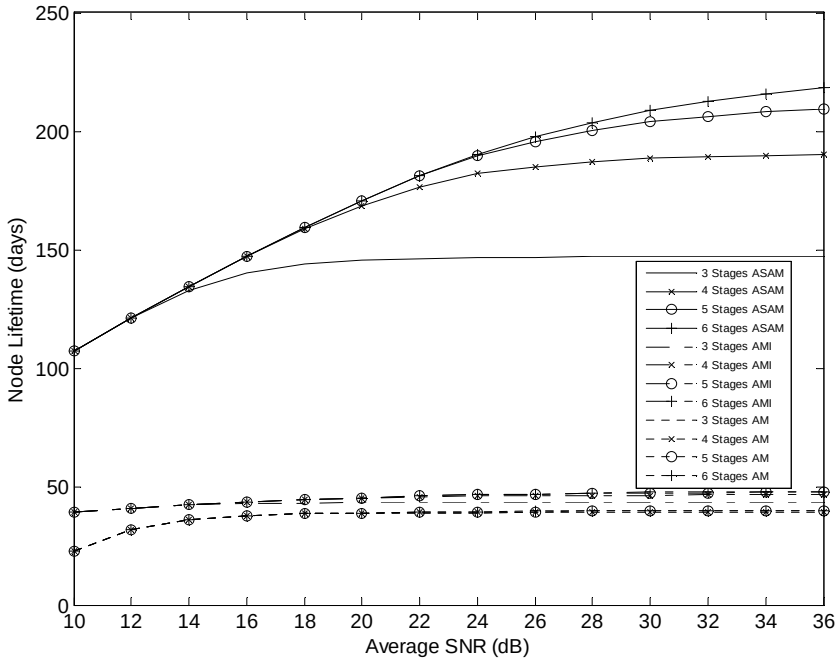

Figure 5.26: Impacts of modulation stages on node lifetime using ASAM, AMI, and AM under Rician fading when K = 10dB

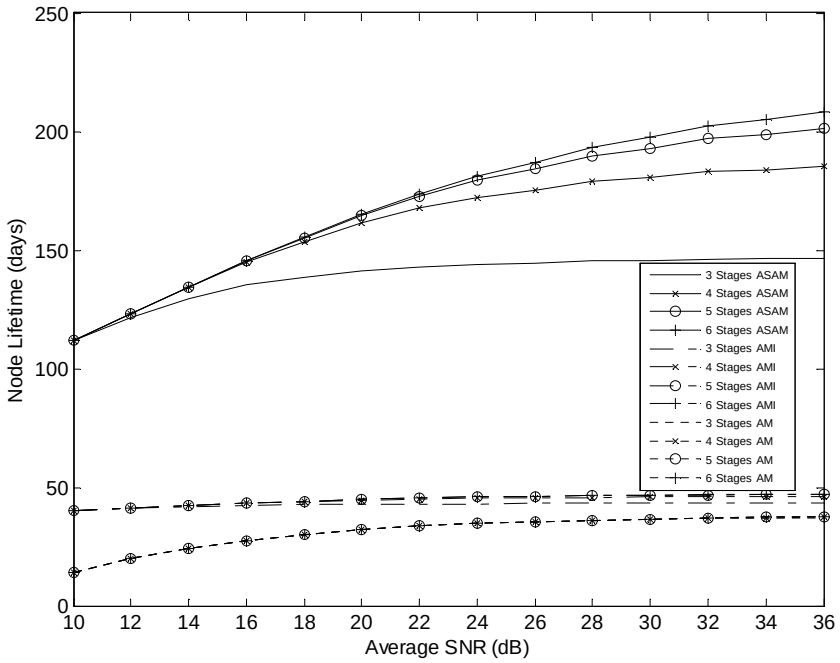

Figure 5.27: Impacts of modulation stages on node lifetime using ASAM, AMI, and AM under Rician fading when K = 5dB

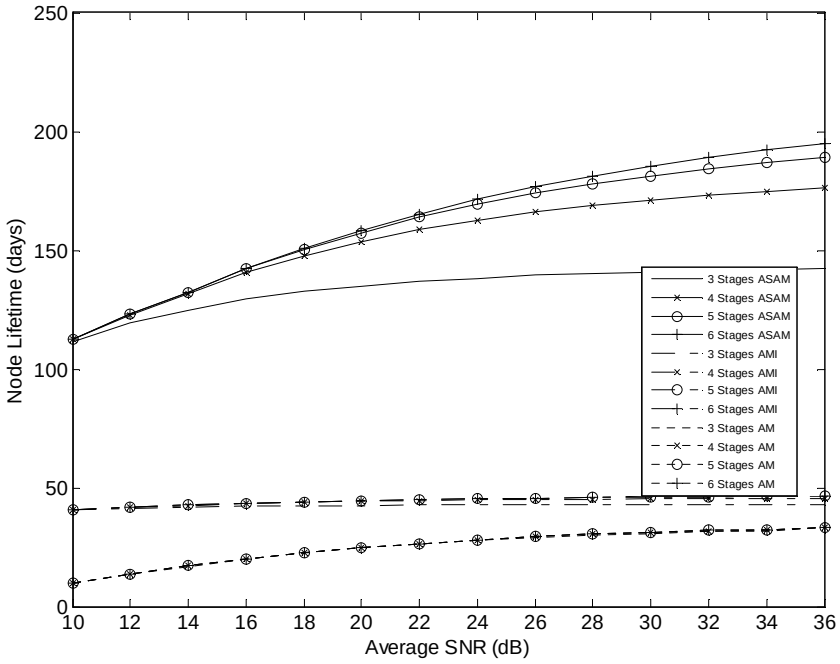

Figure 5.28: Impacts of modulation stages on node lifetime using ASAM, AMI, and AM under Rician fading when K = 0

5.4.5 Discussion of Energy Consumption

We have evaluated the node lifetime in WSNs using AM, AMI, and ASAM algorithms. Factors affecting the node lifetime were investigated, including channel fading, average SNRs, traffic intensity, and modulation stages. The impacts of the transmission parameters have been analyzed individually in previous sections (Section 5.4.2- Section 5.4.4).

The experimental results indicate the proposed ASAM algorithm outperforms the AM and AMI algorithms by more significantly reducing energy consumption. In general, the impacts of transmission parameters on the node lifetime are found to be similar for AM, AMI, and ASAM. For all the algorithms, Lognormal shadowing and Rician fading conditions show similar impacts on the node lifetime. The node can operate longer when the wireless link is located in a good channel condition with minor fading and high average SNRs. A lower traffic load for communication and more modulation stages in the transmitter also contribute to lifetime improvement.

However, there are still a few differences, as suggested by the results. Comparing the energy consumption under different degrees of fading effects, it can be found that the node lifetime can substantially benefit from good channel conditions in AM and ASAM. In AM, less fading in the channel can extend the node lifetime by approximately 30 days, compared to the case of deep fading, while for ASAM, the maximum increment of the node lifetime can reach up to 20 days. For AMI, on the other hand, the impact of channel conditions on the node lifetime is insignificant. In addition, for AM, variations in channel fading conditions affect the node lifetime considerably under low SNRs. For ASAM, however, the effect of channel fading is basically consistent when varying the average SNR; hence both the channel fading and average SNR play an important role in the energy consumption in the network.

Furthermore, the number of modulation stages is found to have considerable impact on the node lifetime for ASAM. The node lifetime can be improved by up to 70 days when switching from 3 stages modulation to 6 stages modulation. For AMI, using more modulation stages in the transmitter helps to improve the node lifetime by 7 days. However, the improvement attained in AM is trivial. Using more modulation stages slightly increases the operating time by one day under good channel conditions; the improvement is even smaller under poor channel conditions. Moreover, to build a large number of modulation schemes in one transmitter increases the hardware implementation complexity. When designing AM protocols, the tradeoff between the energy consumption reduction furnished by using more modulation stages and the practical implementation complexity and cost has to be considered.

Finally, the impacts of traffic intensity on node lifetime have also been studied. Results show that lower traffic in the channel gives a longer node lifetime, consistent among AM, AMI, and ASAM. In addition, node lifetime for a given traffic intensity tends to converge as the average SNR increases. The convergence speed, however, appears to be slower for a higher traffic load. Channel conditions are still found to be the dominant factor affecting the node lifetime in the same communication process.

5.5 Power Control Adaptation Policies

In this section, we investigate the adaptive power control policies in single-hop networks. Six modulation stages are available to the link adaptation: no transmission, BPSK, QPSK, 16QAM, 64QAM and 256QAM. The value of BER is set to 10^{-4}, and the average SNR is varied from 10dB to 36dB.

Since the power level increases rapidly only when the transmitter is switching to the next modulation stage (Section 3.6.3), the transmit power used in the communication processes does not necessarily remain as a constant at the highest level. A power control factor is introduced to adjust the value of transmit power within the same level of modulation. Based on equation (3.3), the optimal values of the power adaptation control factor are derived as shown in Figure 3.3.

In this analysis, power and rate are jointly adapted according to channel conditions. Link adaptation with an optimal discrete rate and an optimal power control is considered, in order to achieve maximal spectral efficiency under a given average BER constraint. The node lifetime is compared between the following six cases: 1) Adaptive Sleep combined with Adaptive modulation under Power Control (ASAM-PC), 2) Adaptive Sleep combined with Adaptive modulation NO Power Control (ASAM), 3) Adaptive Modulation with Idle mode under Power Control (AMI-PC), 4) Adaptive Modulation with Idle mode NO Power Control (AMI), 5) Adaptive Modulation under Power Control (AM-PC), and 6) Adaptive Modulation NO Power Control (AM). Different fading levels are still considered.

The power control factors for AM, AMI, and ASAM are calculated using optimal power adaptive polices. Table 5.2 lists the optimal power control factors obtained for different degrees of Lognormal shadowing. Under the same channel conditions, the power control factors for AM and AMI are fairly close, although values in AMI are slightly larger than in AM. However, the power control factors are considerably larger in ASAM, indicating that the power control adaptation policies perform better with ASAM.

This superior performance is due to the fact that ASAM has very good adaptation capability given the algorithm's ability to dynamically adjust the operating durations for both the transmission stage and the sleep stage. However, power control results in insignificant

improvements in AM and AMI cases, because nodes only adapt the duration of the transmission stage without taking the active and idle stages into consideration. Even though the power control algorithm is able to lower the power level of the transmission stage, the portion of active energy and idle energy still dominates the total energy consumption in the network. Therefore, in most of the cases, the effect of power control would be more noticeable for ASAM than for AM and AMI.

Furthermore, power control factors tend to be smaller under good channel conditions. In such conditions, all of the three algorithms can effectively adjust the transmission parameters to save energy. Power control adaptation policy in this case does not play an essential role, particularly for AM and AMI. However, when severe fading occurs, AM and AMI themselves can barely reduce the energy consumption to a satisfactory level. Further improvement can be achieved by power control algorithms. The values of the optimal power control factors thus become larger in these cases, implying that power control adaptation policy contributes to additional energy saving.

As shown in Table 5.2, for $\sigma = 0$, optimal power control factors are very small. Specifically, for low average SNRs, only 0.107% and 0.117% of the power can be controlled in the case of AM and AMI, respectively. For high SNRs, the effects of power control are negligible for both algorithms. However, when σ is increased to 8dB, power control adaptation policy reduces the transmit power by 4.55% in AMI, and 4.35% of the transmit power is controlled when using AM. The power control values in ASAM also become smaller under good channel conditions, but are still more significant compared to AM and AMI. The power control values for ASAM are 6.21% and 19.5% for the best (highest average SNR with the smallest σ) and the worst (lowest average SNR with the largest σ) channel conditions, respectively.

Table 5.2: Power Control Factors for Lognormal shadowing channel conditions

σ (dB)	Method	Power Control Factor (%)							
		SNR=10dB	14dB	18dB	22dB	26dB	30dB	34dB	38dB
0	ASAM-PC	14.6	13.1	11.9	11.2	10.3	8.79	7.43	6.21
	AMI-PC	0.117	3.57E-05	3.85E-09	1.70E-12	7.57E-16	7.82E-20	3.08E-23	3.25E-27
	AM-PC	0.107	3.21E-05	3.21E-09	1.60E-12	6.74E-16	6.74E-20	2.73E-23	2.73E-27
2	ASAM-PC	15.2	14.5	13.2	12.4	10.9	9.66	7.98	6.87
	AMI-PC	2.11	0.0173	4.41E-05	4.16E-06	7.41E-09	7.91E-10	4.58E-13	1.52E-12
	AM-PC	2.02	0.0138	2.25E-04	1.26E-06	2.28E-07	7.10E-11	5.06E-11	2.78E-14
4	ASAM-PC	16.7	15.5	14.7	12.9	11.2	9.97	8.76	7.11
	AMI-PC	3.64	1.81	0.666	0.146	0.0248	0.00365	2.44E-06	7.96E-10
	AM-PC	3.58	1.74	0.661	0.195	0.0264	0.00644	1.73E-07	1.70E-08
6	ASAM-PC	18.3	16.9	15.4	13.8	12.7	11.3	9.89	8.04
	AMI-PC	4.17	0.0495	1.39E-05	3.24E-09	1.35E-12	1.78E-16	4.75E-20	2.11E-23
	AM-PC	4.06	0.0522	2.96E-05	3.18E-09	1.33E-12	1.83E-16	7.49E-20	4.13E-23
8	ASAM-PC	19.5	17.6	16.3	15.7	13.9	12.4	12.1	11.8
	AMI-PC	4.55	1.24	0.138	0.00413	0.000125	2.09E-10	4.05E-14	1.03E-13
	AM-PC	4.35	1.17	0.111	0.00404	0.00438	6.11E-08	1.46E-12	2.42E-15

Node lifetime curves using power control adaptation policy with AM, AMI, and ASAM algorithms are shown in Figure 5.29-Figure 5.33 for Lognormal shadowing cases. As aforementioned, the power control algorithm is more effective in poor channel condition environments. Thus, the improvement of the node lifetime is also more obvious in such situations. Additionally, larger improvement is attained when combining power control with ASAM than with AM or AMI. Under the same channel condition, using the optimal power control in the ASAM algorithm can increase the node lifetime by more than 10 days, while power control barely benefits AM, especially under good channel conditions.

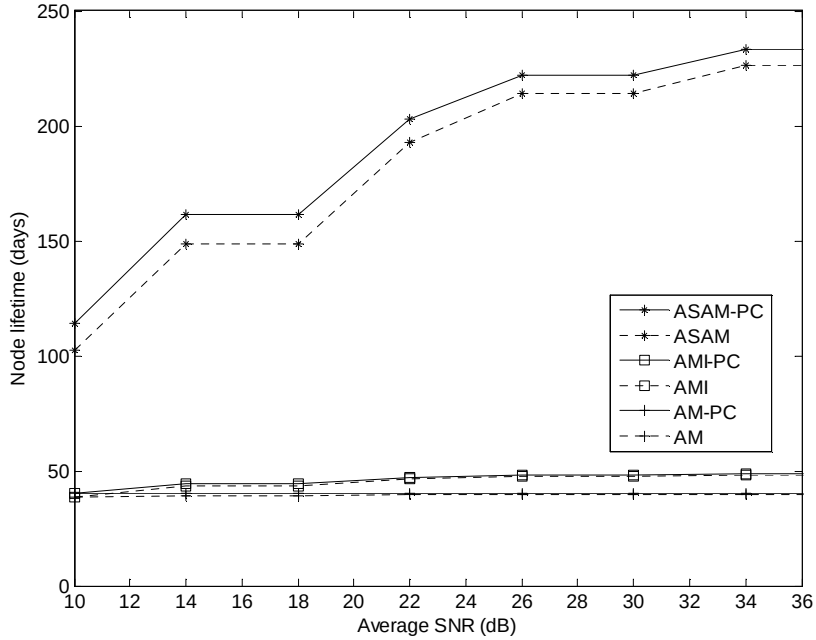

Figure 5.29: Power control impacts on node lifetime using 6 stages ASAM, AMI and AM under the Lognormal shadowing when $\sigma = 0$

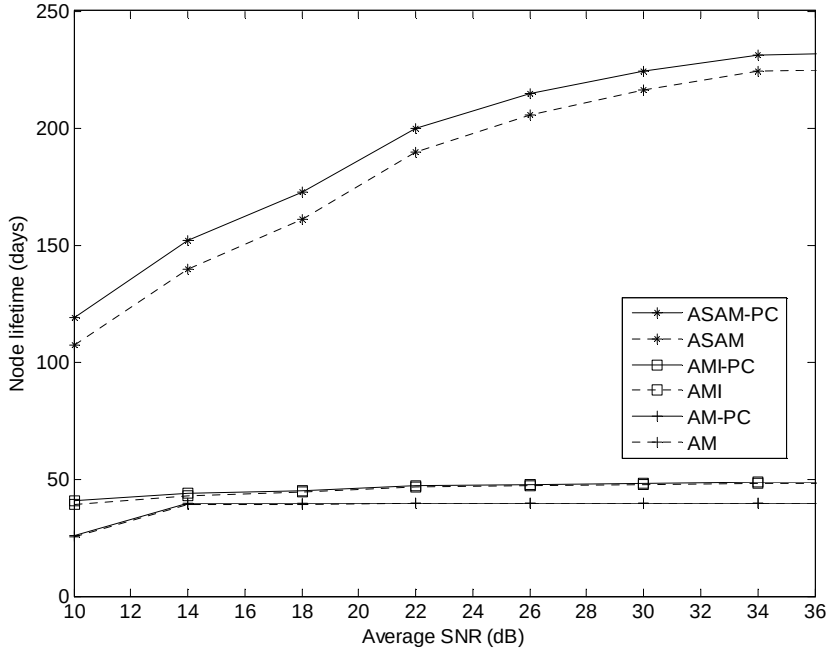

Figure 5.30: Power control impacts on node lifetime using 6 stages ASAM, AMI and AM under the Lognormal shadowing when $\sigma = 2$dB

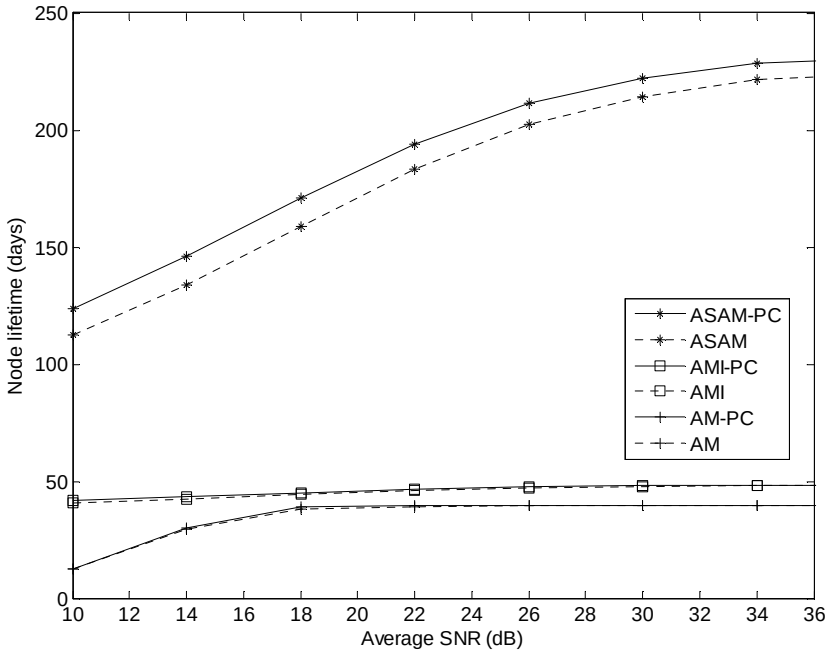

Figure 5.31: Power control impacts on node lifetime using 6 stages ASAM, AMI and AM under the Lognormal shadowing when σ = 4dB

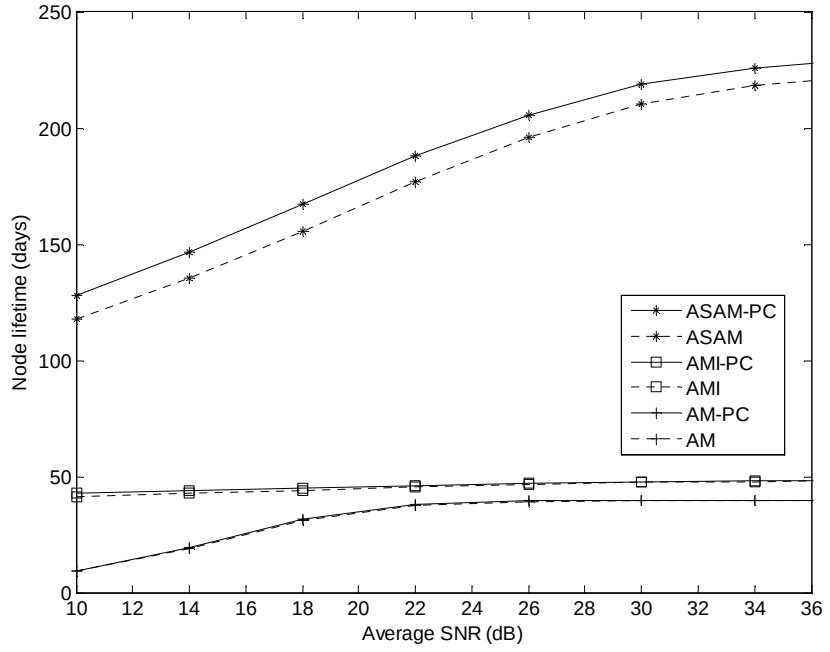

Figure 5.32: Power control impacts on node lifetime using 6 stages ASAM, AMI and AM under the Lognormal shadowing when σ = 6dB

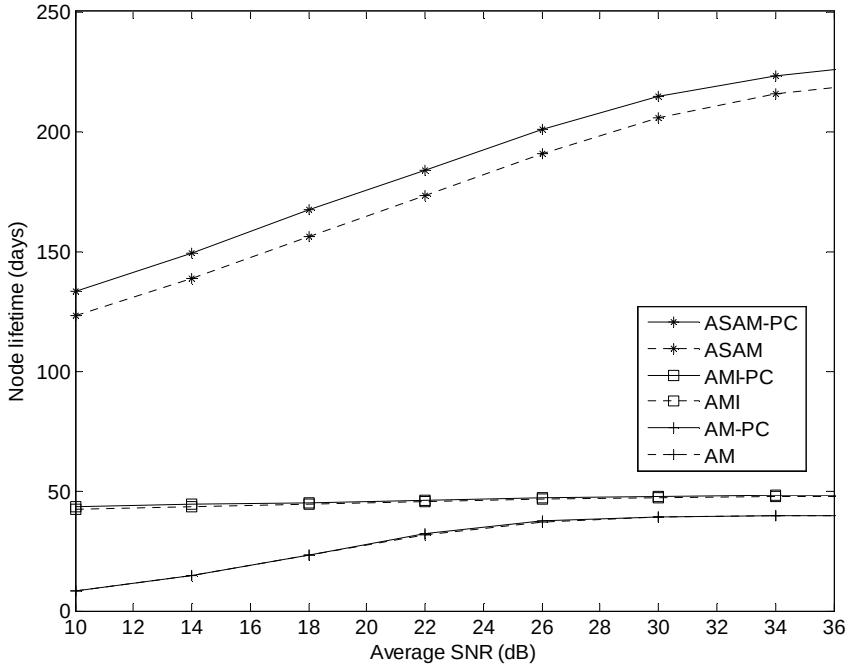

Figure 5.33: Power control impacts on node lifetime using 6 stages ASAM, AMI and AM under the Lognormal shadowing when σ = 8dB

Similarly, power control in Rician fading is also found to have comparable effects as in the Lognormal shadowing cases. Rician K-factors are varied among $\{0,5,10,15,20\}dB$. A higher K-factor indicates a larger LOS and hence a smaller fading effect. As listed in Table 5.3, the optimal power control factor values are larger in poor channel conditions than in good channel conditions. Node lifetime performance is shown in Figure 5.34-Figure 5.38. Similar to the Lognormal shadowing cases, nodes operate a slightly longer when combining power control policies with ASAM than with AM, indicating that the adaptation policy works better with ASAM.

Table 5.3: Power Control Factors for Rician fading channel conditions

K(dB)	Method	Power Control Factor (%)							
		SNR=10dB	14dB	18dB	22dB	26dB	30dB	34dB	38dB
20	ASAM-PC	14.8	13.6	12.9	12.1	11.4	10.6	9.86	9.03
	AMI-PC	0.417	0.00027	2.04E-07	2.14E-10	8.06E-13	2.12E-15	1.69E-18	9.24E-21
	AM-PC	0.396	0.000313	2.21E-07	1.75E-10	4.77E-13	7.00E-16	1.46E-18	8.45E-22
15	ASAM-PC	15.9	15.1	14.9	14.7	14.6	13.2	12.5	11.5
	AMI-PC	3.04	1.86	0.964	0.394	0.121	0.0291	0.000586	0.000299
	AM-PC	2.99	1.88	0.927	0.344	0.13	0.0373	0.0149	6.24E-05
10	ASAM-PC	18.7	17.9	16.6	15.7	15.2	14.6	13.8	12.5
	AMI-PC	4.37	0.663	0.106	0.0332	0.0109	0.00565	0.0119	0.00113
	AM-PC	4.15	0.588	0.0985	0.032	0.00633	0.00875	0.00921	0.000132
5	ASAM-PC	19.8	19.1	18.3	17.8	16.9	15.6	15.1	14.2
	AMI-PC	4.59	2.26	1.33	0.882	0.645	0.42	0.333	0.259
	AM-PC	4.48	2.21	1.33	0.882	0.673	0.486	0.324	0.298
0	ASAM-PC	20.9	19.4	18.7	18.1	17.7	16.4	16.1	15.4
	AMI-PC	4.75	1.62	0.718	0.389	0.257	0.142	0.138	0.103
	AM-PC	4.63	1.62	0.669	0.383	0.229	0.19	0.0857	0.0764

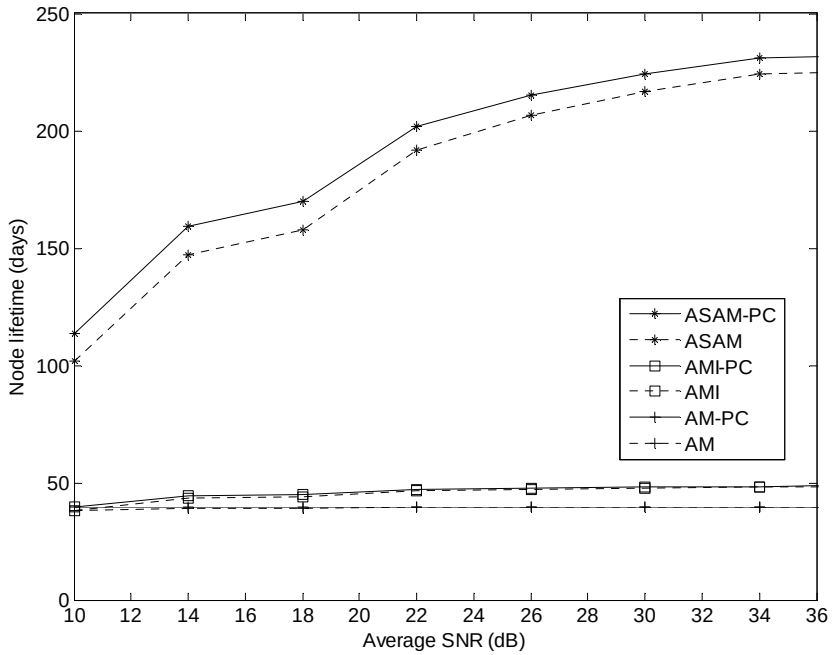

Figure 5.34: Power control impacts on node lifetime using 6 stages ASAM and AM under the Rician fading when K = 20dB

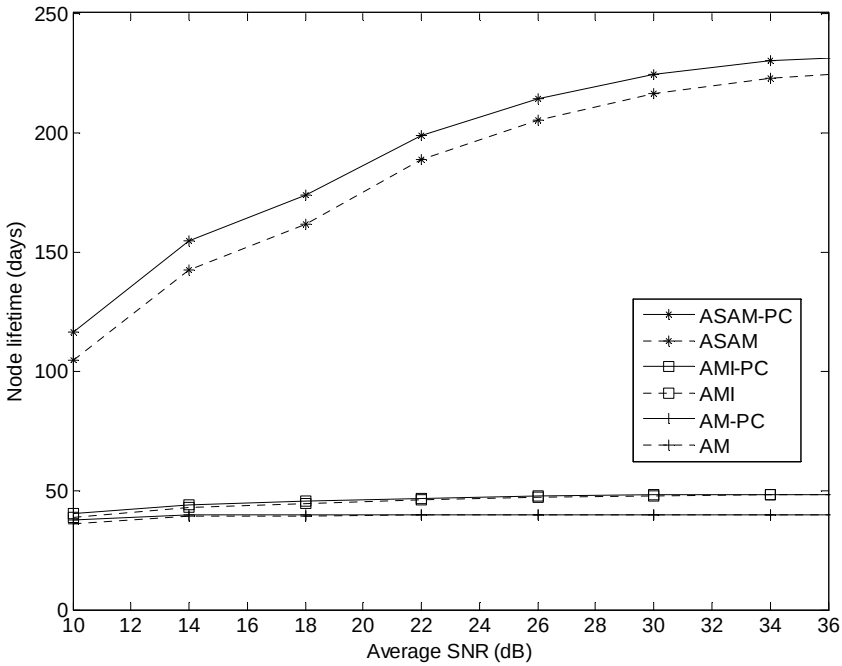

Figure 5.35: Power control impacts on node lifetime using 6 stages ASAM, AMI and AM under the Rician fading when K = 15dB

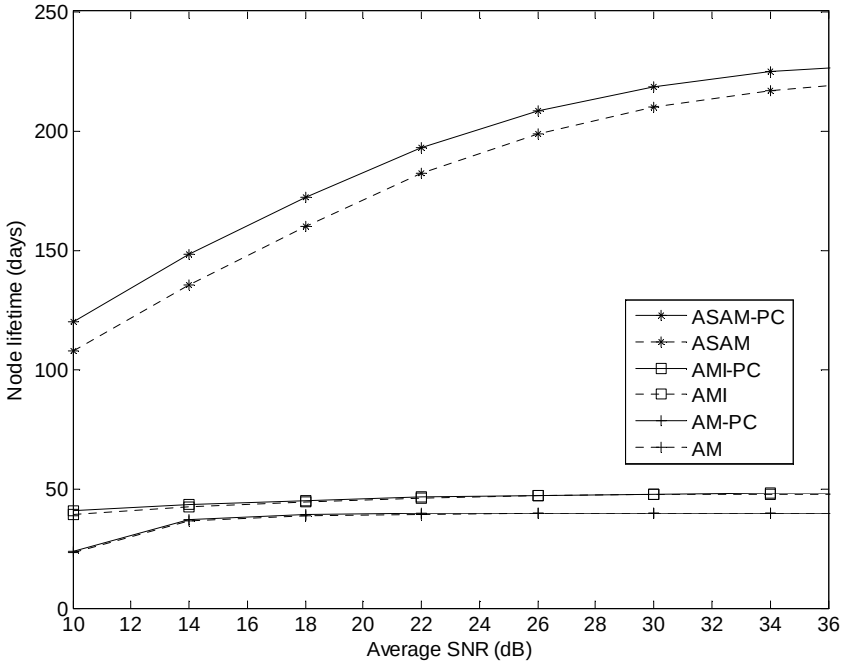

Figure 5.36: Power control impacts on node lifetime using 6 stages ASAM, AMI and AM under the Rician fading when K = 10dB

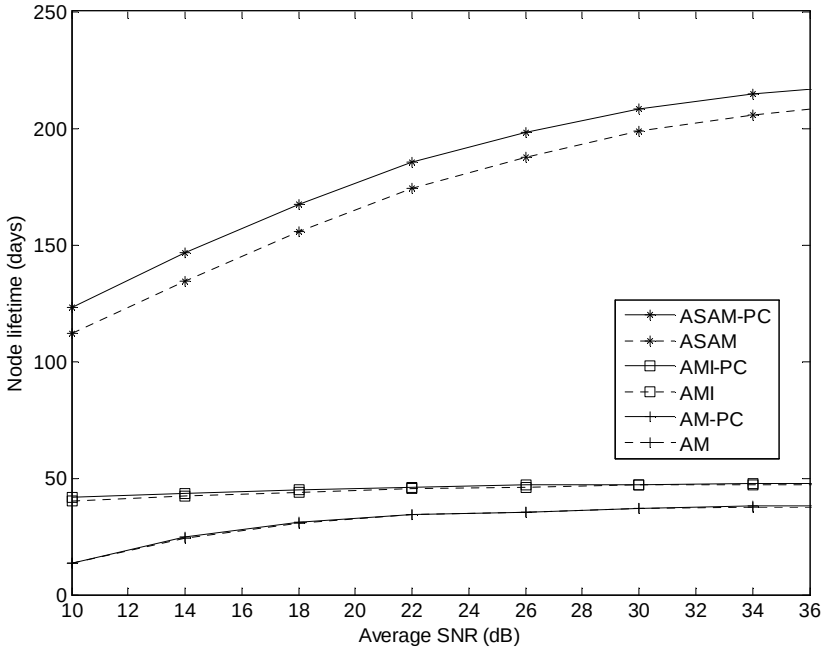

Figure 5.37: Power control impacts on node lifetime using 6 stages ASAM, AMI and AM under the Rician fading when K = 5dB

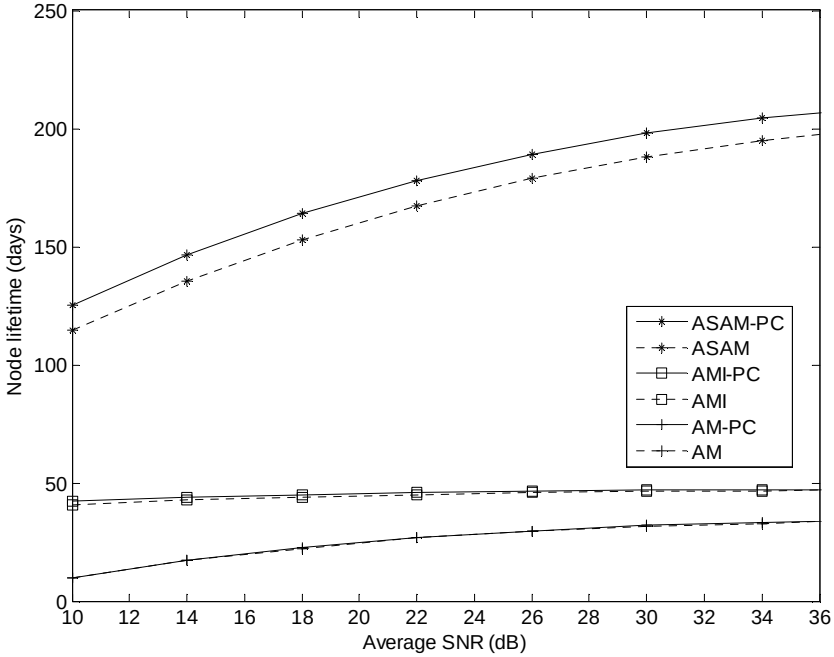

Figure 5.38: Power control impacts on node lifetime using 6 stages ASAM, AMI and AM under the Rician fading when K = 0

5.6 Two-Link Relay Network Adaptation

When there are multiple nodes in the network, the communication between nodes can be categorized into two types: (1) multi-hop relay networks that transmit the source data to the destination through relay nodes, and (2) multiple-link networks where multiple sources and destinations exist in the network and each source transmits data to its destination independently. Here, we investigate the energy consumption using link adaptation in two-link relay networks.

Recall the relay network link adaptation control explained in Section 4.4.1. The proposed adaptive power allocation policy is employed here. Network lifetime depends on the energy consumption of all wireless links along the communication path. Although the total available energy in the network is finite, the power allocated to each node can be adjusted to achieve optimal transmission quality with minimal energy consumption.

This simulation considers the simplest relay network with one relay node so that information will always be routed through the relay node to the destination. Hence, two links are created in the network: source to relay and relay to destination. Due to the wireless single multipath and scattering, the two wireless links can have different fading effects. The power allocation policy, therefore, is responsible for allotting the optimal power according to the instantaneous fading information of the links. The node lifetime is calculated under the following channel conditions: σ_1 = 2dB, σ_2 = {0, 4, 6, 8}dB for Lognormal shadowing and K_1 = 10dB, K_2 = {0, 5, 15, 20}dB for Rician fading. The comparative results of these channel conditions are displayed in Figure 5.39-Figure 5.46. Other results of the node lifetime are available in Appendix A. The optimal power allocation algorithm is compared to the case in which the total energy is evenly divided between the links.

It can be seen from the figures that for the two-link relay networks, improved node lifetime is obtained for all the algorithms with the optimal power allocation. The improvement is more notable for the combination of the power allocation algorithm and ASAM. As the node lifetime using ASAM is more subject to channel conditions than using AM, wisely allocating the energy to each link according to its channel fading is essential for enhancing the energy efficiency of the entire network in ASAM.

Moreover, the results also indicate that a more considerable increment can be achieved under more distinct fading conditions between the two links. Also, power allocation with the AM scheme is shown to perform better at low SNR regions than at high SNR region; with ASAM, the power allocation algorithm is found to improve the network lifetime more at high SNRs. As mentioned in Section 5.4.2, at high SNR regions, the node lifetime under different degrees of fading tends to converge in AM; hence, variations in channel fading conditions only exert minor influence on energy consumption. In the low SNR cases, however, node lifetime is much more sensitive to fading conditions; as a result, energy resources need to be more carefully allocated to improve energy efficiency. Conversely, for ASAM, the channel fading has more significant impacts on the node lifetime under high average SNRs. Therefore, adaptive power allocation is more demanding as SNR increases in this scenario.

The optimal power allocation factors of the two links are calculated and shown in Table 5.4 and Table 5.5 for cases of Lognormal shadowing and Rician fading, respectively. These values also corroborate the previous observations that ASAM benefits more from power allocation than AM. In general, the allocated power is biased to the link with inferior channel conditions. This is due to the fact that the energy resources must be allocated in such a way that operations of all links in the network are maintained simultaneously for the maximal period of time. Normally, the

node with the worst channel conditions has low energy efficiency and fails first. Recall equation (4.12). Since a network is considered functional only if both links are alive, the minimum of the lifetime of the two links needs to be maximized. Such phenomenon will naturally grant more energy to the link located in poorer channel conditions with higher energy expenditure so that by extending its lifetime, the lifetime of the entire network is extended.

Table 5.4: Optimal Power Allocation Factors for Two links: σ_1 = 2dB, σ_2 = {0, 4, 6, 8}dB

Optimal Allocation Factor	Method	SNR=10dB	14dB	18dB	22dB	26dB	30dB	34dB	38dB
		Two Links Channel Condition: σ_1 = 2dB, σ_2 = 0dB							
α_1	ASAM	0.56	0.56	0.55	0.54	0.53	0.51	0.51	0.5
α_2		0.44	0.44	0.45	0.46	0.47	0.49	0.49	0.5
α_1	AMI	0.51	0.51	0.51	0.5	0.5	0.5	0.5	0.5
α_2		0.49	0.49	0.49	0.5	0.5	0.5	0.5	0.5
α_1	AM	0.56	0.55	0.54	0.53	0.53	0.51	0.5	0.5
α_2		0.44	0.45	0.46	0.47	0.47	0.49	0.5	0.5
		Two Links Channel Condition: σ_1 = 2dB, σ_2 = 4dB							
α_1	ASAM	0.44	0.44	0.45	0.46	0.47	0.49	0.49	0.51
α_2		0.56	0.56	0.55	0.54	0.53	0.51	0.51	0.49
α_1	AMI	0.49	0.49	0.5	0.5	0.5	0.5	0.5	0.5
α_2		0.51	0.51	0.5	0.5	0.5	0.5	0.5	0.5
α_1	AM	0.33	0.45	0.49	0.49	0.5	0.5	0.5	0.5
α_2		0.57	0.55	0.51	0.51	0.5	0.5	0.5	0.5
		Two Links Channel Condition: σ_1 = 2dB, σ_2 = 6dB							
α_1	ASAM	0.45	0.41	0.39	0.38	0.35	0.32	0.3	0.29
α_2		0.55	0.59	0.61	0.62	0.65	0.68	0.7	0.71
α_1	AMI	0.49	0.49	0.49	0.5	0.5	0.5	0.5	0.5
α_2		0.51	0.51	0.51	0.5	0.5	0.5	0.5	0.5
α_1	AM	0.32	0.33	0.44	0.49	0.5	0.5	0.5	0.5
α_2		0.68	0.67	0.56	0.51	0.5	0.5	0.5	0.5
		Two Links Channel Condition: σ_1 = 2dB, σ_2 = 8dB							
α_1	ASAM	0.43	0.4	0.36	0.31	0.27	0.23	0.21	0.19
α_2		0.57	0.6	0.64	0.69	0.73	0.77	0.79	0.81
α_1	AMI	0.48	0.49	0.49	0.49	0.5	0.5	0.5	0.5
α_2		0.52	0.51	0.51	0.51	0.5	0.5	0.5	0.5
α_1	AM	0.27	0.28	0.38	0.45	0.48	0.5	0.5	0.5
α_2		0.73	0.72	0.62	0.55	0.52	0.5	0.5	0.5

Table 5.5: Optimal Power Allocation Factors for Two links: K_1 = 10dB, K_2 = {0, 5, 15, 20}dB

Optimal Allocation Factor	Method	SNR=10dB	14dB	18dB	22dB	26dB	30dB	34dB	38dB
		Two Links Channel Condition: K_1 = 10dB, K_2 = 0dB							
α_1	ASAM	0.43	0.4	0.36	0.31	0.27	0.23	0.21	0.19
α_2		0.57	0.6	0.64	0.69	0.73	0.77	0.79	0.81
α_1	AMI	0.47	0.48	0.48	0.48	0.49	0.49	0.5	0.5
α_2		0.53	0.52	0.52	0.52	0.51	0.51	0.5	0.5
α_1	AM	0.31	0.32	0.37	0.41	0.42	0.44	0.45	0.46
α_2		0.69	0.68	0.63	0.59	0.58	0.56	0.55	0.54
		Two Links Channel Condition: K_1 = 10dB, K_2 = 5dB							
α_1	ASAM	0.47	0.46	0.44	0.42	0.39	0.37	0.36	0.35
α_2		0.53	0.54	0.56	0.58	0.61	0.63	0.64	0.65
α_1	AMI	0.48	0.48	0.49	0.49	0.49	0.5	0.5	0.5
α_2		0.52	0.52	0.51	0.51	0.51	0.5	0.5	0.5
α_1	AM	0.37	0.4	0.44	0.47	0.47	0.48	0.49	0.49
α_2		0.63	0.6	0.56	0.53	0.53	0.52	0.51	0.51
		Two Links Channel Condition: K_1 = 10dB, K_2 = 15dB							
α_1	ASAM	0.52	0.55	0.56	0.58	0.59	0.6	0.62	0.64
α_2		0.48	0.45	0.44	0.42	0.41	0.4	0.38	0.36
α_1	AMI	0.52	0.52	0.52	0.51	0.51	0.51	0.5	0.5
α_2		0.48	0.48	0.48	0.49	0.49	0.49	0.5	0.5
α_1	AM	0.61	0.54	0.53	0.51	0.51	0.51	0.5	0.5
α_2		0.39	0.46	0.47	0.49	0.49	0.49	0.5	0.5
		Two Links Channel Condition: K_1 = 10dB, K_2 = 20dB							
α_1	ASAM	0.53	0.56	0.57	0.59	0.61	0.64	0.65	0.68
α_2		0.47	0.44	0.43	0.41	0.39	0.36	0.35	0.32
α_1	AMI	0.53	0.53	0.52	0.52	0.52	0.51	0.5	0.5
α_2		0.47	0.47	0.48	0.48	0.48	0.49	0.5	0.5
α_1	AM	0.67	0.63	0.59	0.54	0.52	0.51	0.51	0.51
α_2		0.33	0.37	0.41	0.46	0.48	0.49	0.49	0.49

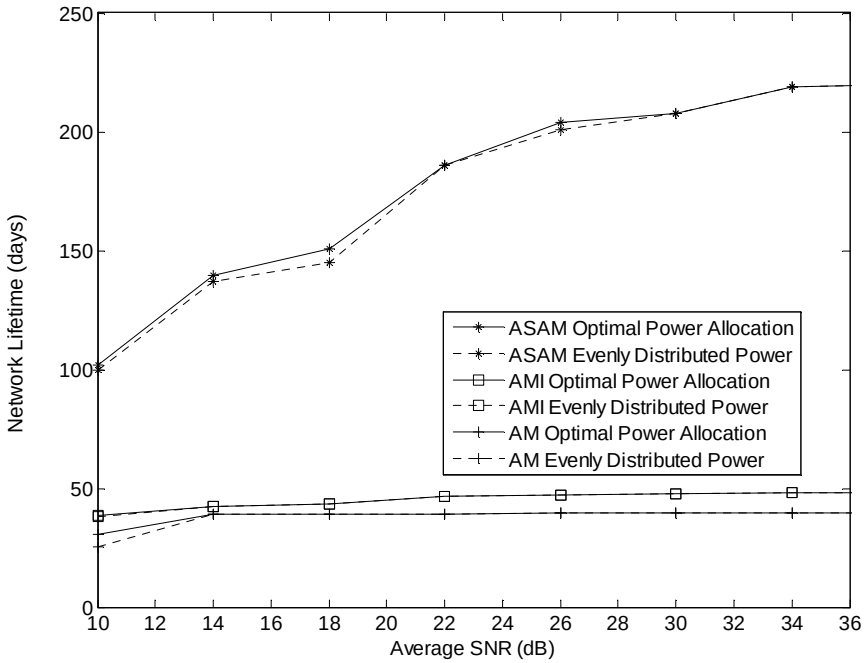

Figure 5.39: Power allocation under Lognormal shadowing. Two link channel conditions: σ_1 = 2dB, σ_2 = 0dB

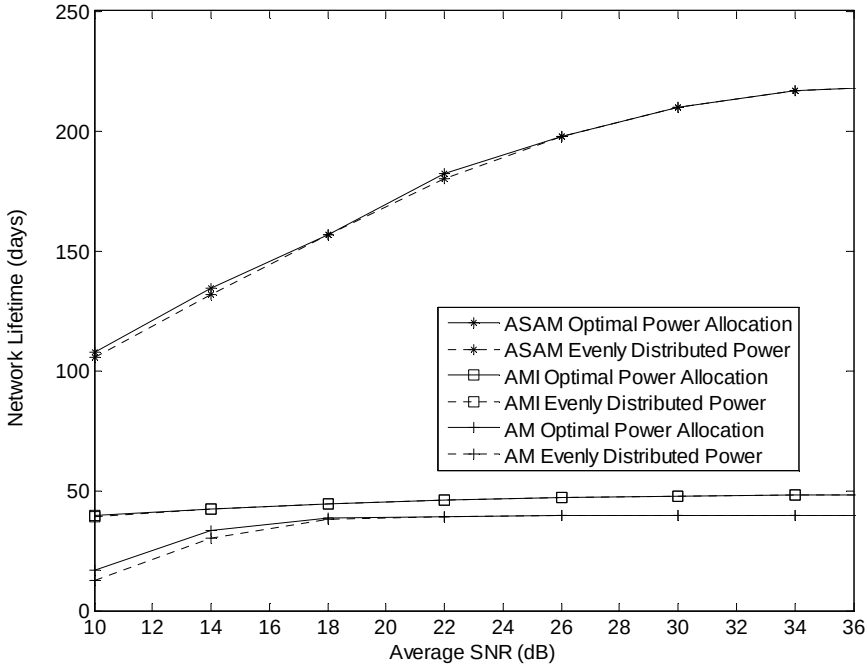

Figure 5.40: Power allocation under Lognormal shadowing. Two link channel conditions: σ_1 = 2dB, σ_2 = 4dB

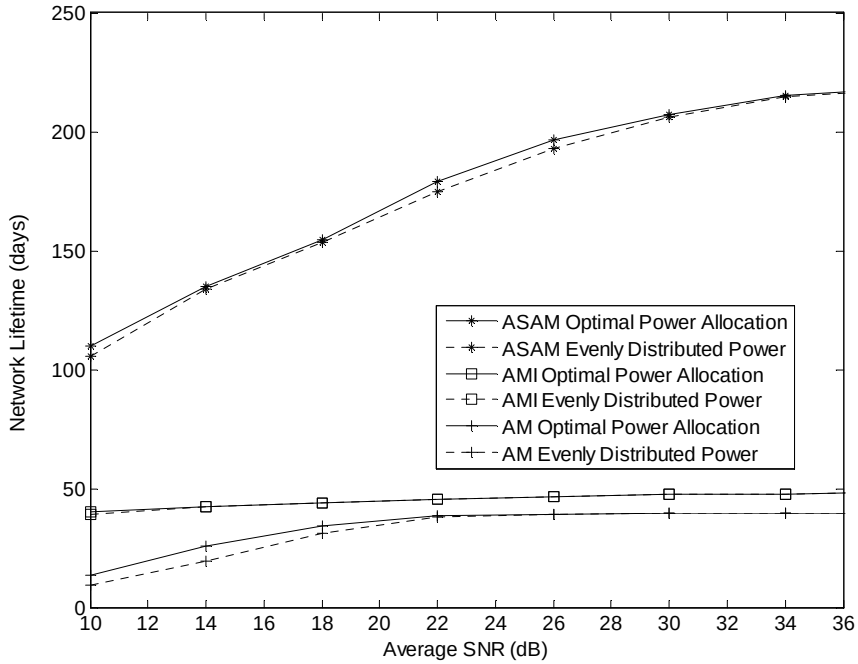

Figure 5.41: Power allocation under Lognormal shadowing. Two link channel conditions: σ_1 = 2dB, σ_2 = 6dB

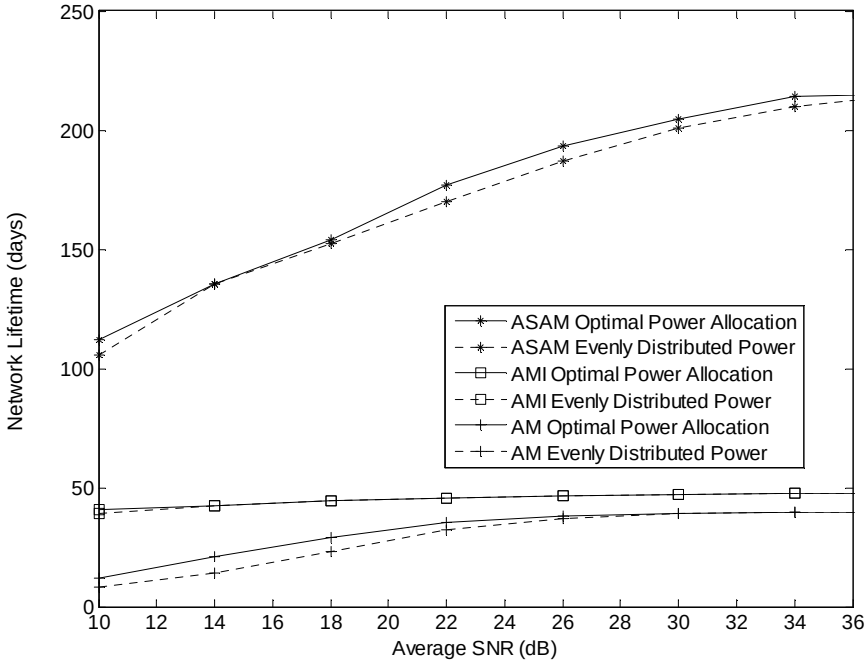

Figure 5.42: Power allocation under Lognormal shadowing. Two link channel conditions: σ_1 = 2dB, σ_2 = 8dB

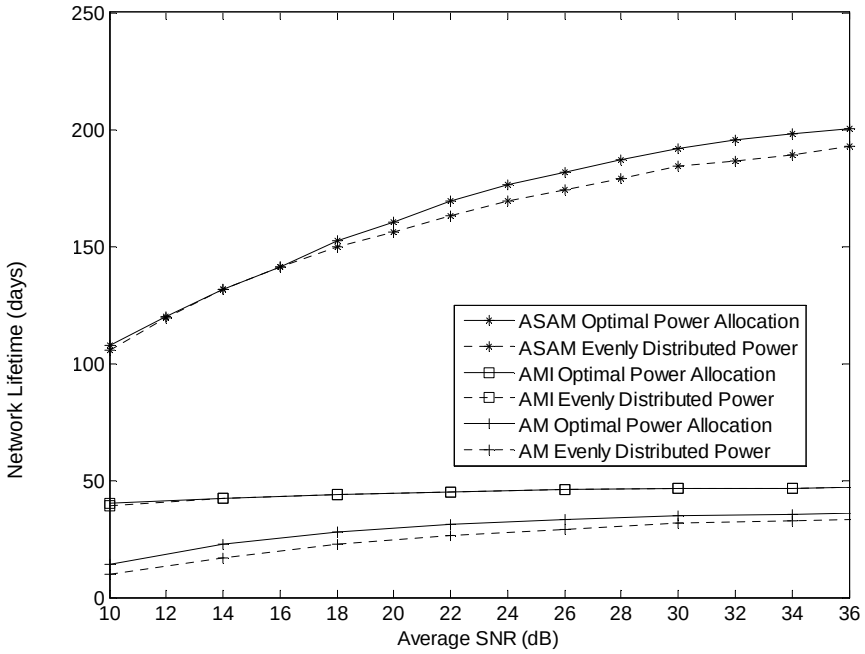

Figure 5.43: Power allocation under Rician fading. Two link channel conditions: K_1 = 10dB, K_2 = 0dB

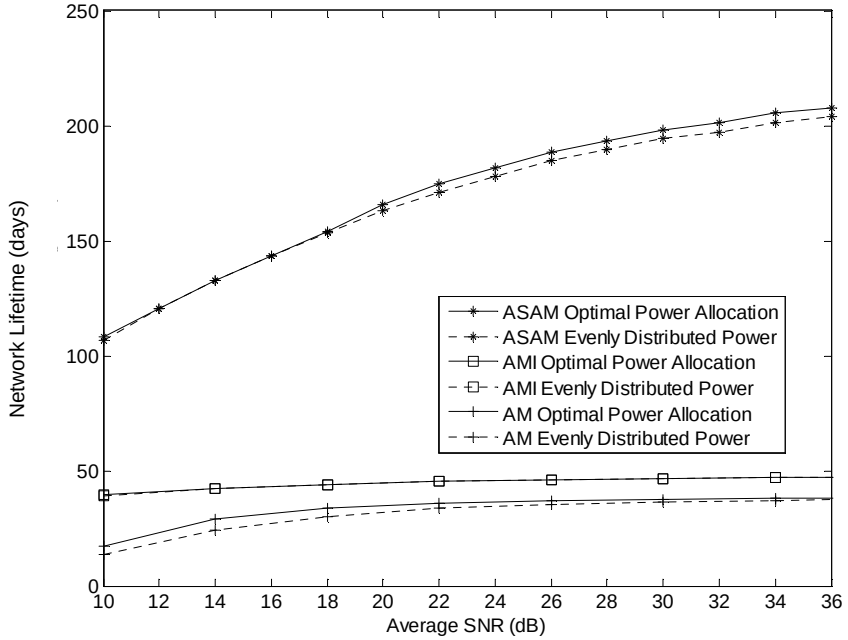

Figure 5.44: Power allocation under Rician fading. Two link channel conditions: K_1 = 10dB, K_2 = 5dB

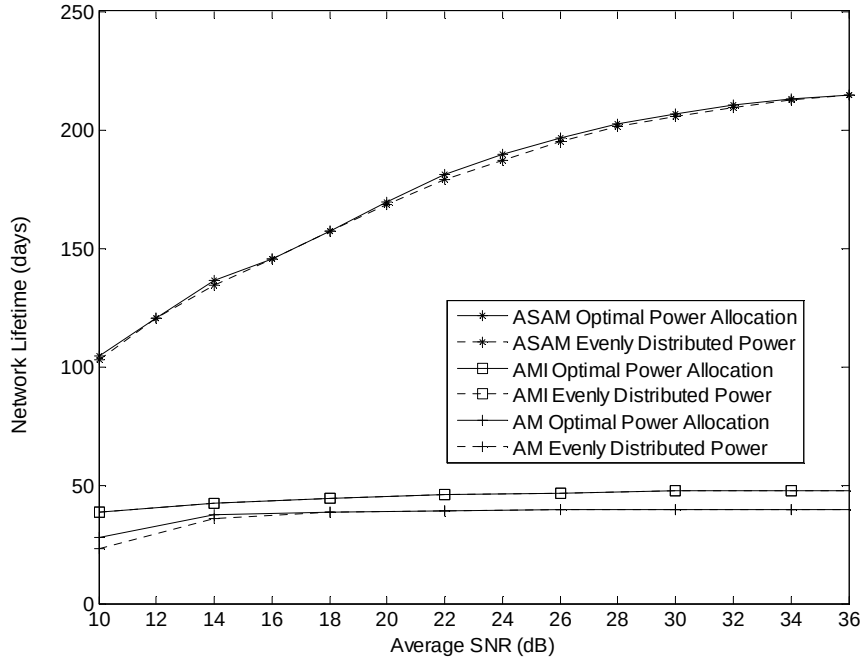

Figure 5.45: Power allocation under Rician fading. Two link channel conditions: K_1 = 10dB, K_2 = 15dB

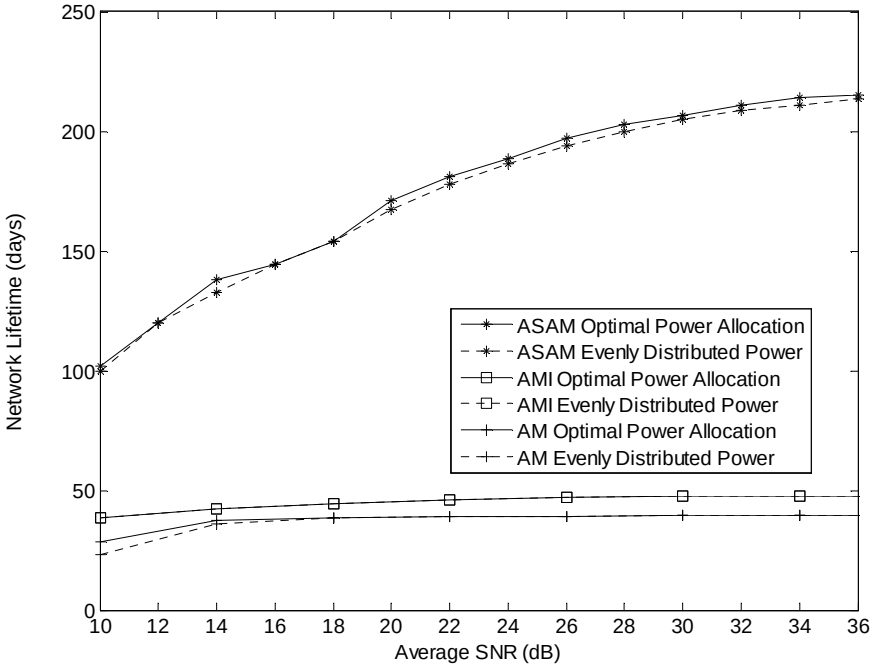

Figure 5.46: Power allocation under Rician fading. Two link channel conditions: K_1 = 10dB, K_2 = 20dB

5.7 Commercial Wireless Sensor Model Performance

The experiments on energy consumption prove that the proposed ASAM algorithm substantially increases the node lifetime relative to AM. Here, we further investigate the performance of this algorithm when applied to commercial wireless sensor nodes with different transmitter conditions.

Recent research focuses on examining the performance of the IEEE 802.15.4 transceivers and measuring the current values drained from the power source for different operating modes [61], [62], [63]. Based on these empirical characteristics of battery consumption, the node lifetime is calculated as a function of the operating current of the sensor nodes. Three commercial wireless transceivers are evaluated here, namely CC2430, CC2520 and MC1322. For the purpose of energy saving, the commercial IEEE 802.15.4 transceivers are able to switch between operating modes with different current consumptions. Here, we are specifically interested in the current consumption of the transmission, active and sleep modes. The functionalities of these operating modes have been explained in Section 4.2.

Table 5.6 displays the current consumption for the three operating modes as provided by the datasheets of the transceivers, which is based on the experimental results. Total available battery capacity for each node is assumed to be 1200mAhr, and packets are sent every 10 seconds. We still consider different degrees of shadowing and fading. For Lognormal shadowing σ takes value in $\{0, 2, 4, 6, 8\}dB$, and for Rician fading K-factor K is chosen from $\{0, 5, 10, 15, 20\}dB$.

Table 5.6: Current Consumption of CC2480, CC2520 and MC1322 transceivers

Transceivers	Operating Voltage (V)	Transmission Stage (mA)	Active Stage (mA)	Idle Stage (mA)	Sleep Stage (uA)
CC2430	2.0-3.6	27	12.3	0.19	0.3
CC2520	1.8–3.6	25.8	10	0.175	0.03
MC1322	2.0–3.6	32	15	0.9	0.3

Results are presented in Figure 5.47-Figure 5.56. It can be seen from the plots that ASAM consistently yields the longest operating time among the three link adaptation techniques. Comparing AMI and AM, although the former slightly improves the node lifetime, the performances of the both AMI and AM are in general very close. The trends of the node lifetime performance using commercial transceivers are very similar to the previous simulated transmitter model. This indicates that the proposed ASAM algorithm is a promising technique for improving the nodes operating lifetime for commercial IEEE 802.15.4-compliant transceivers. In addition, good channel conditions also improve the node lifetime since smaller fading effects hardly cause any retransmissions.

Furthermore, since the transmitters have different current consumptions for the transmission, active, idle and sleep stages, these values influence the power levels and, therefore, affect the total energy consumption of the nodes. Thus, it is also worthwhile to analyze the node lifetime variations which are caused by different current consumption. It is observed that all the commercial transmitters have much lower current consumption values than the simulated transmitter model (see Table 5.1 for the parameters' values). As listed in Table 5.6, CC2520 has the lowest overall current consumption for all operating modes, while MC1322 has the highest consumption.

As illustrated in Figure 5.47-Figure 5.56, the node lifetime of all commercial transceivers is overall longer than the simulated transmitter model, given the smaller current consumptions in these commercial products. The CC2520 transceiver has the longest node lifetime since it operates at the lowest overall current consumption. Under good channel conditions, it can operate for over 625 days using the ASAM algorithm, while it can still last nearly 200 days and 250 days using the AM and AMI, respectively. CC2430 has moderate node lifetime, relatively close to the node lifetime of CC2520. For the same channel conditions, CC2430 operates for up to 615 days using the ASAM algorithm, almost 245 and 181 days using the AMI and AM techniques, respectively. The MC1322 transceiver gives the shortest node lifetime: 510 days, 198 days and 146 days, using the ASAM, AMI, and AM, respectively. This is expected because both CC2520 and CC2430 transceivers consume low current in the idle stage. Compared to MC1322, the idle mode current consumption can be reduced to nearly 1/5 of the current in CC2520 and CC2430. Although CC2520 and CC2430 have very close idle mode current, their current consumption in the transmission and active modes is still different. The higher current consumption in CC2430 leads to a shorter node lifetime relative to CC2520.

Among current values of all operating modes, the consumption during the idle mode is the most significant factor determining node lifetime. However, the current drained for transmission and active modes also shows a small impact. Moreover, the current consumption during the sleep stage as well has considerable impact on the node lifetime, particularly for the ASAM algorithm. Since it adaptively adjusts the duration of the sleep stage, reduced sleep current consumption can further improve the node lifetime in ASAM.

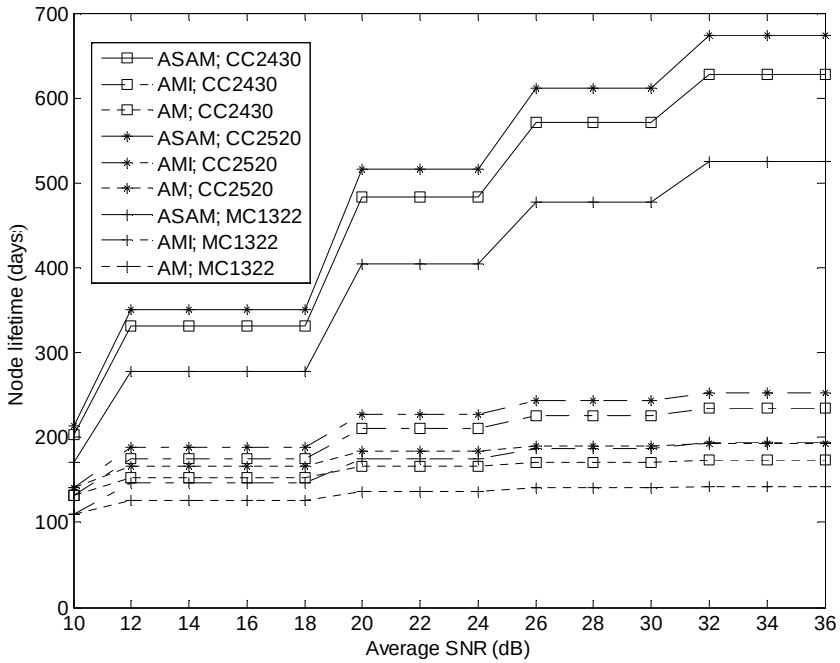

Figure 5.47: Comparison of the node lifetime of commercial IEEE 802.15.4-compliant transceivers using 6 stages ASAM, AMI, and AM under Lognormal shadowing when $\sigma = 0$

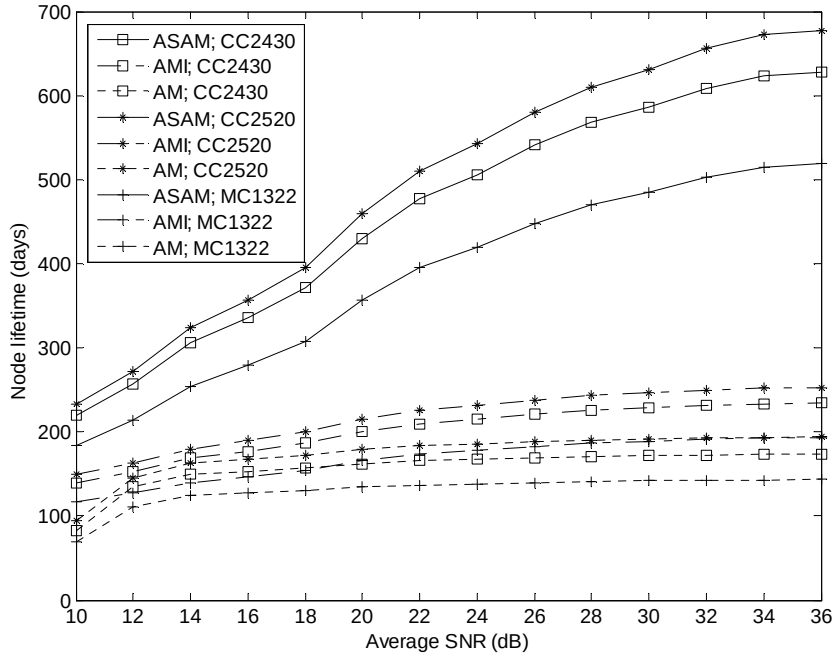

Figure 5.48: Comparison of the node lifetime of commercial IEEE 802.15.4-compliant transceivers using 6 stages ASAM, AMI, and AM under Lognormal shadowing when $\sigma = 2$dB

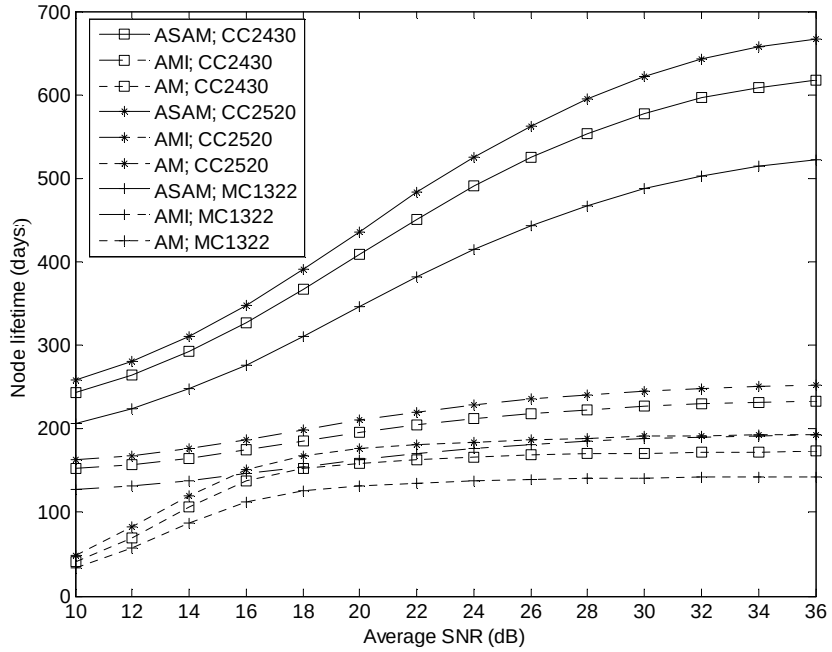

Figure 5.49: Comparison of the node lifetime of commercial IEEE 802.15.4-compliant transceivers using 6 stages ASAM, AMI, and AM under Lognormal shadowing when σ = 4dB

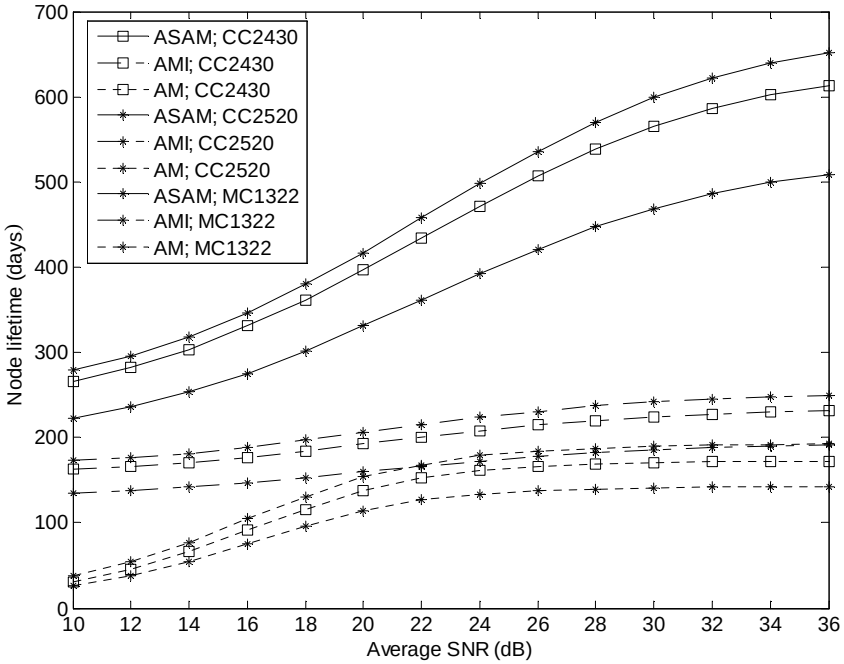

Figure 5.50: Comparison of the node lifetime of commercial IEEE 802.15.4-compliant transceivers using 6 stages ASAM, AMI, and AM under Lognormal shadowing when σ = 6dB

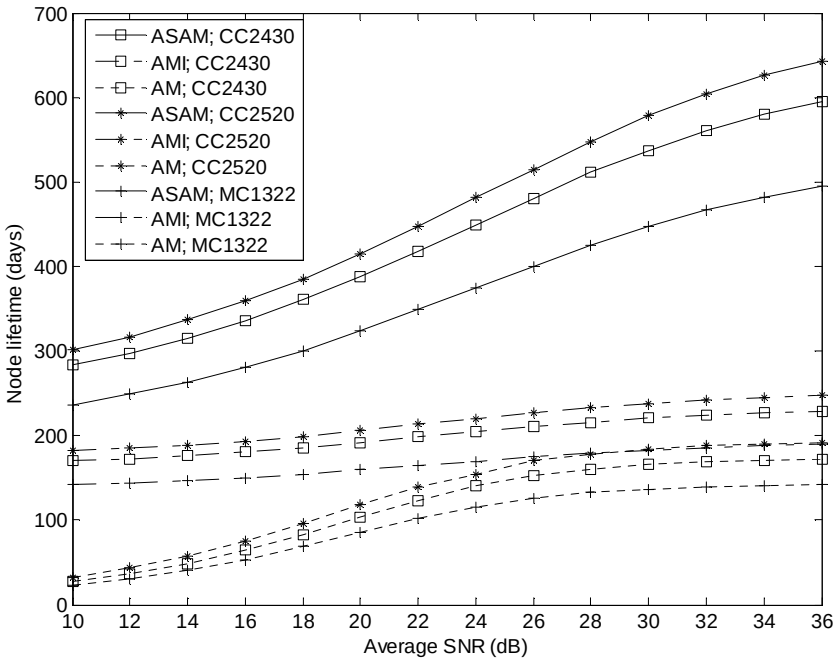

Figure 5.51: Comparison of the node lifetime of commercial IEEE 802.15.4-compliant transceivers using 6 stages ASAM, AMI, and AM under Lognormal shadowing when σ = 8dB

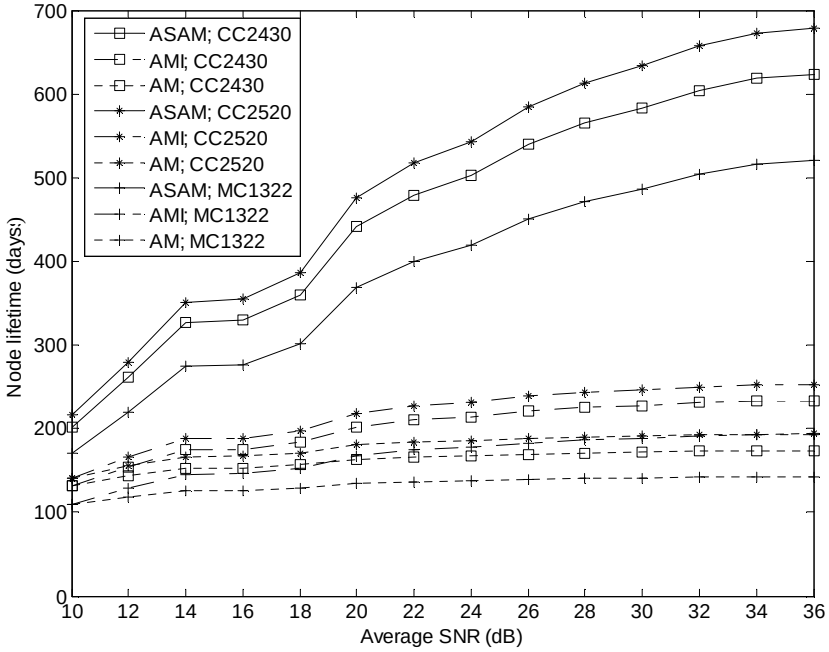

Figure 5.52: Comparison of the node lifetime of commercial IEEE 802.15.4-compliant transceivers using 6 stages ASAM, AMI, and AM under Rician fading when K = 20dB

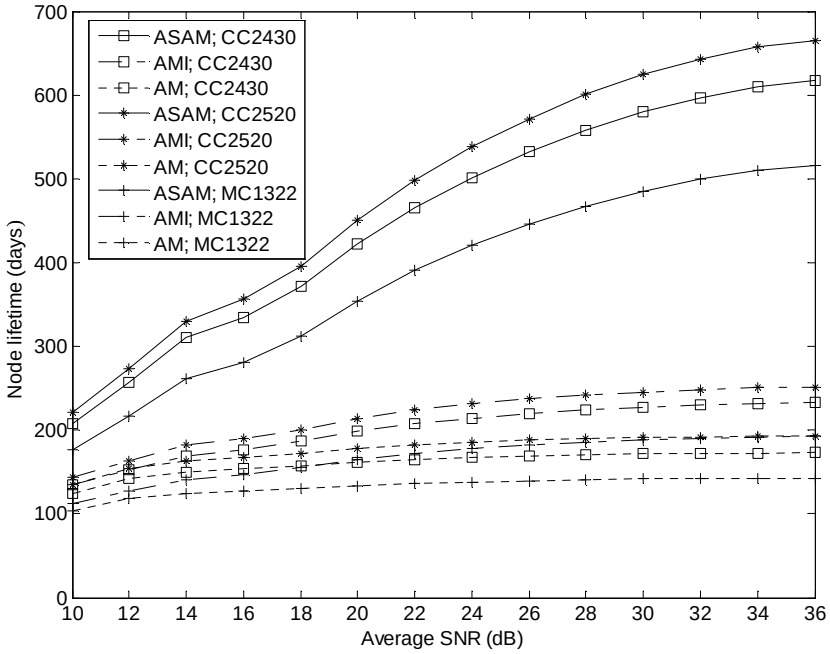

Figure 5.53: Comparison of the node lifetime of commercial IEEE 802.15.4-compliant transceivers using 6 stages ASAM, AMI, and AM under Rician fading when K = 15dB

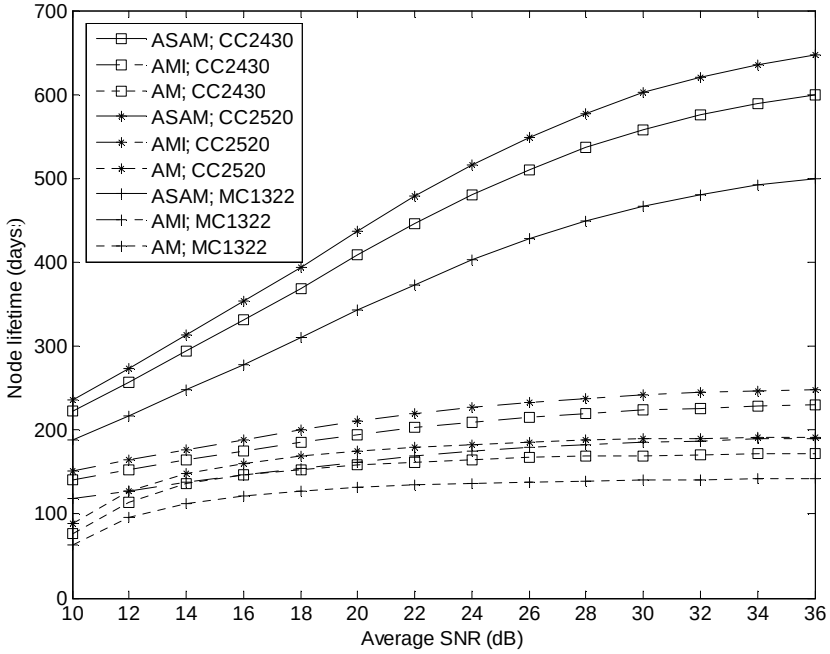

Figure 5.54: Comparison of the node lifetime of commercial IEEE 802.15.4-compliant transceivers using 6 stages ASAM, AMI, and AM under Rician fading when K = 10dB

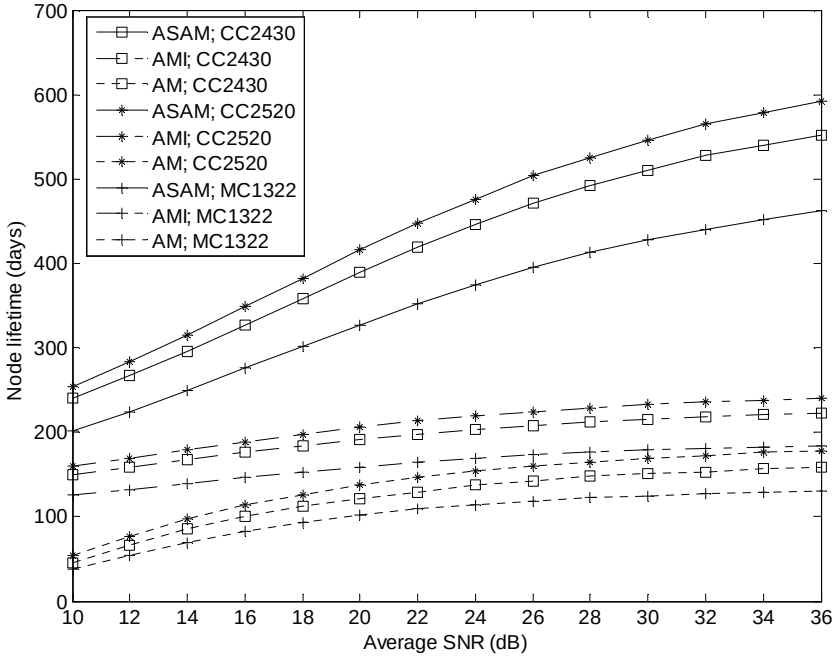

Figure 5.55: Comparison of the node lifetime of commercial IEEE 802.15.4-compliant transceivers using 6 stages ASAM, AMI, and AM under Rician fading when K = 5dB

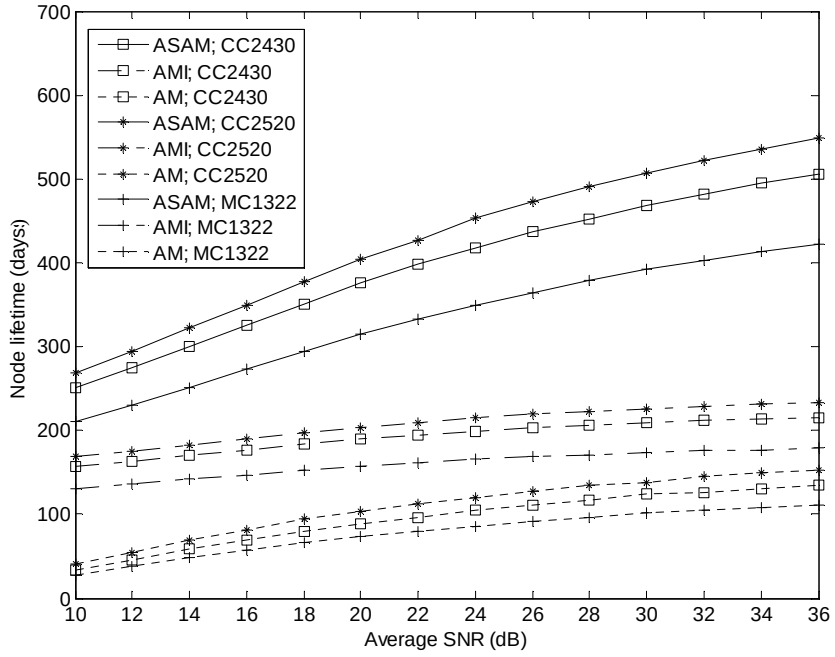

Figure 5.56: Comparison of the node lifetime of commercial IEEE 802.15.4-compliant transceivers using 6 stages ASAM, AMI, and AM under Rician fading when K = 0

5.8 Summary

In this chapter, we have evaluated the link adaptive policies explained in Chapter 3 and Chapter 4. The proposed ASAM technique is compared with AM and AMI schemes in terms of energy consumption behaviors. Transmission parameters are investigated for their impact on node lifetime using different adaptation techniques. The results show that the channel fading condition plays an important role in the node lifetime for AM protocols at the low SNR region, while both the channel fading and average SNRs are the dominant factor in ASAM for the energy consumption. The number of modulation stages also exhibits a significant impact on the node lifetime in ASAM but not for AMI or AM. In addition, the traffic intensity has a comparable impact on the three algorithms; lower traffic reduces the energy consumption in the network.

Optimal power control and power allocation factors are calculated for single-hop networks and multi-hop relay networks, respectively. The power control algorithm slightly improves the node lifetime in point-to-point communication. It performs better in poor channel conditions than in good channel conditions. Optimal power control factors are observed to improve the node lifetime more obviously in ASAM than in AM. In a multi-hop relay network, the network lifetime improvement is also more considerable in ASAM when the optimal power allocation algorithm is applied to ASAM and AM.

Finally, ASAM is proved to be able to introduce more effective energy saving than AM when evaluated on commercial IEEE 802.15.4-compliant transceivers using the current consumption values in their datasheets. In general, idle stage current consumption is the key factor affecting the node lifetime, while transmission and active current levels are found to have a slight impact as well.

Chapter 6

Conclusions and Future Work

6.1 Conclusions

This thesis investigated the PHY layer characteristics and implementation issues of AM and ASAM for energy constrained wireless communication networks. We have explained in detail the main components of the link adaptation feedback system model and discussed several AM techniques. We extended the work done by Goldsmith [8] and investigated the energy consumption using link adaptations. The switching level thresholds for the modulation schemes and the variable-rate variable-power adaptation polices for the MAC layer protocols were computed. The energy consumption of the adaptive protocols in various networks was evaluated. An ASAM algorithm was developed and was incorporated into the link adaptation policies. The proposed algorithm was compared with the AM scheme. In addition, the optimal power allocation values for multi-hop relay networks were computed and the maximum network lifetime was compared between several link adaptive protocols.

The simulation results indicate that discrete rate continuous power adaptation protocol can effectively control the energy consumption in the energy constrained network where all nodes share a finite amount of energy available to the system. It is shown that AM is a promising technique increasing the data rate while AS notably enhances the power efficiency. The combination of the two can achieve optimal energy consumption in the network, thereby improving the system's operating lifetime. The performance of point-to-point communication and multi-hop networks was investigated. The proposed the power allocation algorithm was compared to other link adaptive protocols for multi-hop relay networks, and promising results are obtained.

Furthermore, it has been shown that various transmission parameters had different impacts on energy consumption for AM, AMI, and ASAM. Channel fading conditions have a large impact on the energy consumption for AM, especially at low SNR regions. However, for ASAM, both the channel fading conditions and average SNR values show significant impacts on the node lifetime variation. Additionally, a high modulation stage improves the node lifetime more in ASAM than in AMI and AM. Traffic intensity in the wireless communication path plays a considerable role in node lifetime for AM, AMI, and ASAM; however, its impact on the three schemes are similar. We further investigated the two-link multi-hop relay network model and explored the relation between power allocation and energy consumption. By employing the optimal power allocation algorithm, the network operating lifetime could be substantially improved in the multi-hop relay networks. This algorithm performs better when the communication paths have more distinct channel fading; and these impacts are more obvious in the ASAM case.

6.2 Future Work

The analysis in this thesis opens several paths for future investigation and research. While the studies tried to be as comprehensive as possible, there are still a few issues that can be investigated which are outside the scope of this work. Possible future research includes the following:

1. Explore a verity of codes to improve the capacity of the fading channel with transmitter adaptation. Due to the simulation and implementation complexity, this analysis has only considered uncoded rectangular MQAM constellations. Future research on the network performance that combines coding theory with link adaptation is necessary. The coding rate

and scheme can be considered as additional parameters and contributed to the energy optimization formula. Other transmission parameter such as the error probability, channel capacity and bandwidth could be jointly considered. Such joint optimization of the allocation factor for these parameters is an interesting research topic that may yield valuable results.

2. To achieve accurate simulations with less complexity, this study assumes the perfect receiver estimation and error-free feedback links with no delay in the current channel conditions. One of the interesting extensions of this work could be to investigate the effect of the overall system performance when there is error and mismatch in the system model components. The error model can be implemented using MATLAB as a function of the estimation errors and the feedback delay. Moreover, the perfect routing protocol is also assumed in the network. All sensor nodes have full acknowledgements of their neighbors; therefore, the best relay nodes are selected. Future research could work on developing real-time and energy-efficient routing protocols. This investigation can be evaluated using OPNET and implemented in micro-controllers for realistic network testing.
3. We have considered a finite total available energy in the network, so the nodes will stop operating after the battery limits is reached. A possible future research could be to build a renewable energy model for some of the inner-nodes communications. Instead of constantly being dead when energy is used up, the node can generate new energy after a certain period of time. These regenerative nodes allow the battery to be recharged so that the total available energy is not fixed in the network. The renewable energy model can be proposed in addition to contribute to the total energy consumption. The study can investigate network performance with different number of regenerative nodes.

4. In this analysis, we considered a simple relay network where the nodes form a two-link communication system. Future investigation can extend the work to more links. In addition, WSNs are newly developed in 3D grid deployment [64]. A future direction would be to test the link adaptation techniques in multiple layer environments. Moreover, we analyzed the multiple sources and destinations in the network with all the communication paths having the same distance and independent transmission. An interesting extension of the work would be to study how the system performs in a multiple-links network where the correlated shadowing effect exists.
5. Another possible extension of this thesis would be to implement the power allocation and link adaptation policies in actual networks. As ASAM algorithm is confirmed to reduce energy consumptions in commercial IEEE 802.15.4-compliant transceivers, it can be implemented in microprocessors using C++ programming language, and then the actual product can be investigated and evaluated in the realistic sensing environments.

Bibliography

[1] S. Phoha, *et al.*, *Sensor network operations*. Hoboken, N.J. and Piscataway, Wiley; IEEE Press, 2006.

[2] S. G. Cui, *et al.*, "Energy-constrained modulation optimization," *IEEE Transactions on Wireless Communications*, vol. 4, pp. 2349-2360, Sep 2005.

[3] T. He, *et al.*, "Achieving real-time target tracking using wireless sensor networks," *Proceedings of the 12th IEEE Real-Time and Embedded Technology and Applications Symposium*, pp. 37-48, 2006.

[4] H. Karl, *et al.*, *Wireless sensor networks : first European workshop, EWSN 2004, Berlin, Germany, January 19-21, 2004, proceedings*. New York: Springer-Verlag, 2004.

[5] T. Yan, *et al.*, "Design and optimization of distributed sensing coverage in wireless sensor networks," *Acm Transactions on Embedded Computing Systems*, vol. 7, 2008.

[6] I. F. Akyildiz, *et al.*, "Wireless multimedia sensor networks: A survey," *IEEE Wireless Communications*, vol. 14, pp. 32-39, Dec 2007.

[7] V. Rajaravivarma, *et al.*, "An overview of Wireless Sensor Network and applications," *Proceedings of the 35th Southeastern Symposium on System Theory*, pp. 432-436, 2003.

[8] A. Goldsmith, *Wireless communications*. Cambridge ; New York: Cambridge University Press, 2005.

[9] T. S. Rappaport, *Wireless communications : principles and practice*, 2nd ed. Upper Saddle River, Prentice Hall PTR, 2002.

[10] J. G. Proakis and M. Salehi, *Digital communications*, 5th ed. Boston: McGraw-Hill, 2008.

[11] M. K. Simon and M.-S. Alouini, *Digital communication over fading channels*, 2nd ed. Hoboken, Wiley-Interscience, 2005.

[12] M. S. Alouini and A. J. Goldsmith, "Adaptive modulation over Nakagami fading channels," *Wireless Personal Communications*, vol. 13, pp. 119-143, May 2000.

[13] H. Matsuoka, *et al.*, "Adaptive modulation system with variable coding rate concatenated code for high quality multi-media communication systems," *1996 IEEE 46th Vehicular Technology Conference, Proceedings, Vols 1-3*, pp. 487-491, 1996.

[14] H. Alasady and M. Ibnkahla, "Adaptive modulation over nonlinear time-varying channels," *European Transactions on Telecommunications*, vol. 18, pp. 685-692, Nov 2007.

[15] A. J. Goldsmith and P. P. Varaiya, "Capacity of fading channels with channel side information," *IEEE Transactions on Information Theory*, vol. 43, pp. 1986-1992, Nov 1997.

[16] J. K. Cavers, "Variable-Rate Transmission for Rayleigh Fading Channels," *IEEE Transactions on Communications*, vol. Co20, pp. 15, 1972.

[17] J. F. Hayes, "Adaptive Feedback Communications," *IEEE Transactions on Communication Technology*, vol. Co16, pp. 29, 1968.

[18] S. T. Chung and A. J. Goldsmith, "Degrees of freedom in adaptive modulation: A unified view," *IEEE Transactions on Communications*, vol. 49, pp. 1561-1571, Sep 2001.

[19] W. T. Webb and R. Steele, "Variable-Rate Qam for Mobile Radio," *IEEE Transactions on Communications*, vol. 43, pp. 2223-2230, Jul 1995.

[20] A. J. Goldsmith and S. G. Chua, "Variable-rate variable-power MQAM for fading channels," *IEEE Transactions on Communications,* vol. 45, pp. 1218-1230, Oct 1997.
[21] D. L. Goeckel, "Adaptive coding for time-varying channels using outdated fading estimates," *IEEE Transactions on Communications,* vol. 47, pp. 844-855, Jun 1999.
[22] J. Hagenauer, "Rate-Compatible Punctured Convolutional-Codes (Rcpc Codes) and Their Applications," *IEEE Transactions on Communications,* vol. 36, pp. 389-400, Apr 1988.
[23] M. Rice and S. B. Wicker, "Adaptive Error Control for Slowly Varying Channels," *IEEE Transactions on Communications,* vol. 42, pp. 917-926, Feb-Apr 1994.
[24] B. Vucetic, "An Adaptive Coding Scheme for Time-Varying Channels," *IEEE Transactions on Communications,* vol. 39, pp. 653-663, May 1991.
[25] T. Ue, *et al.*, "Symbol rate and modulation level-controlled adaptive modulation TDMA TDD system for high-bit-rate wireless data transmission," *IEEE Transactions on Vehicular Technology,* vol. 47, pp. 1134-1147, Nov 1998.
[26] A. Ghosh, *et al.*, "Broadband wireless access with WiMax/802.16: Current performance benchmarks and future potential," *IEEE Communications Magazine,* vol. 43, pp. 129-136, Feb 2005.
[27] Q. W. Liu, *et al.*, "Cross-layer combining of adaptive modulation and coding with truncated ARQ over wireless links," *IEEE Transactions on Wireless Communications,* vol. 3, pp. 1746-1755, Sep 2004.
[28] F. Peng, *et al.*, "Adaptive modulation and coding for IEEE 802.11n," *2007 IEEE Wireless Communications & Networking Conference, Vols 1-9,* pp. 657-662, 2007.
[29] J. L. C. Wu, *et al.*, "An adaptive multirate IEEE 802.11 wireless LAN," *15th International Conference on Information Networking, Proceedings,* pp. 411-418, 2001.
[30] T. H. Chan, M. Hamdi, C.Y. Cheung, and M. Ma, "A Link Adaptation Algorithm in MIMO-Based WiMAX Systems," *Journal of Communications,* vol. 2, pp. 16-24, Aug 2007.
[31] B. Classon, *et al.*, "Channel coding for 4G systems with adaptive modulation and coding," *IEEE Wireless Communications,* vol. 9, pp. 8-13, Apr 2002.
[32] A. Furuskar, *et al.*, "EDGE: Enhanced data rates for GSM and TDMA/136 evolution," *IEEE Personal Communications,* vol. 6, pp. 56-66, Jun 1999.
[33] S. Nanda, *et al.*, "Adaptation techniques in wireless packet data services," *IEEE Communications Magazine,* vol. 38, pp. 54-64, Jan 2000.
[34] S. Otsuki, *et al.*, "Square-QAM Adaptive Modulation/Tdma/Tdd Systems Using Modulation Level Estimation with Walsh-Function," *Electronics Letters,* vol. 31, pp. 169-171, Feb 2 1995.
[35] A. Y. Alemdar, "Link Adaptation For Energy Constrained Networks," Master of Science (Engineering), Department of Electrical and Computer Engineering, Queen's University, Kingston, 2008.
[36] A. Chandrakasan, *et al.*, "Design considerations for distributed microsensor systems," *Proceedings of the IEEE 1999 Custom Integrated Circuits Conference,* pp. 279-286, 1999.
[37] J. M. Rabaey, *et al.*, "PicoRadio supports ad hoc ultra-low power wireless networking," *Computer,* vol. 33, pp. 42, Jul 2000.
[38] B. M. Sadler, "Fundamentals of energy-constrained sensor network systems," *IEEE Aerospace and Electronic Systems Magazine,* vol. 20, pp. 17-35, Aug 2005.

[39] Y. W. Hong, *et al.*, "Cooperative communications in resource-constrained wireless networks," *IEEE Signal Processing Magazine*, vol. 24, pp. 47-57, May 2007.
[40] Y. T. Hou, *et al.*, "On energy provisioning and relay node placement for wireless sensor networks," *IEEE Transactions on Wireless Communications*, vol. 4, pp. 2579-2590, Sep 2005.
[41] R. Min, *et al.*, "Energy-centric enabling technologies for wireless sensor networks," *IEEE Wireless Communications*, vol. 9, pp. 28-39, Aug 2002.
[42] S. C. Cripps, *Advanced techniques in RF power amplifier design*. Boston: Artech House, 2002.
[43] K. Akkaya and M. F. Younis, "survey on routing protocols for wireless sensor networks," *Ad Hoc Networks*, vol. 3, pp. 325–349, 2005.
[44] K. Sohrabi, *et al.*, "Protocols for self-organization of a wireless sensor network," *IEEE Personal Communications*, vol. 7, pp. 16-27, Oct 2000.
[45] C. Intanagonwiwat, *et al.*, "Directed diffusion for wireless sensor networking," *IEEE Transactions on Networking*, vol. 11, pp. 2-16, Feb 2003.
[46] J. Van Greunen, *et al.*, "Adaptive Sleep Discipline for Energy Conservation and Robustness in Dense Sensor Networks," presented at the 2004 IEEE International Conference on Communications, 2004.
[47] D. P. Van Greunen J., A. Bonivento, J. Rabaey, K. Ramchandran, A.S. Vincentelli, A.S. , "Adaptive Sleep Discipline for Energy Conservation and Robustness in Dense Sensor Networks," presented at the IEEE International Conference on Communications, 2004.
[48] J. M. Rabaey, *et al.*, "PicoRadio supports ad hoc ultra-low power wireless networking," *Computer*, vol. 33, p. 42, Jul 2000.
[49] J. M. Kahn, *et al.*, "Emerging challenges: Mobile networking for "Smart Dust"," *Journal of Communications and Networks*, vol. 2, pp. 188-196, Sep 2000.
[50] P. Agrawal and N. Patwari, "Correlated Link Shadow Fading in Multi-Hop Wireless Networks," *IEEE Transactions on Wireless Communications*, vol. 8, pp. 4024-4036, Aug 2009.
[51] N. Patwari and P. Agrawal, "Effects of correlated shadowing: Connectivity, localization, and RF tomography," *2008 International Conference on Information Processing in Sensor Networks, Proceedings*, pp. 82-93, 2008.
[52] M. Ilyas and I. Mahgoub, *Handbook of sensor networks : compact wireless and wired sensing systems*. Boca Raton: CRC Press, 2005.
[53] J. N. Al-Karaki and A. E. Kamal, "Routing techniques in wireless sensor networks: A survey," *IEEE Wireless Communications*, vol. 11, pp. 6-28, Dec 2004.
[54] A. S. Tanenbaum, *Computer networks*, 4th ed. Upper Saddle River, NJ: Prentice Hall PTR, 2003.
[55] V. K. N. Lau and Y.-K. R. Kwok, *Channel-adaptive technologies and cross-layer designs for wireless systems with multiple antennas : theory and applications*. Hoboken, John Wiley, 2006.
[56] D. Wagner and R. Wattenhofer, *Algorithms for sensor and ad hoc networks : advanced lectures*. Berlin ; New York: Springer, 2007.
[57] W. Ye, *et al.*, "An energy-efficient MAC protocol for wireless sensor networks," *IEEE Infocom 2002: The Conference on Computer Communications, Vols 1-3, Proceedings*, pp. 1567-1576, 2002.

[58] D. P. J. Van Greunen, A. Bonivento, J. Rabaey, K. Ramchandran, A.S. Vincentelli, A.S.; , "Adaptive Sleep Discipline for Energy Conservation and Robustness in Dense Sensor Networks," presented at the IEEE International Conference on Communications, 2004.

[59] R. Jurdak, *et al.*, "Radio Sleep Mode Optimization in Wireless Sensor Networks," *IEEE Transactions on Mobile Computing*, vol. 9, pp. 955-968, Jul 2010.

[60] C. Park, *et al.*, "Battery discharge characteristics of wireless sensor nodes: An experimental analysis," *2005 Second Annual IEEE Communications Society Conference on Sensor and Ad Hoc Communications and Networks*, pp. 430-440, 2005.

[61] E. Casilari, *et al.*, "Modeling of Current Consumption in 802.15.4/ZigBee Sensor Motes," *Sensors*, vol. 10, pp. 5443-5468, Jun 2010.

[62] M. Alnuaimi, *et al.*, "Performance evaluation of IEEE 802.15A physical layer using MatLab/Simulink," *2006 Innovations in Information Technology*, pp. 156-160, 2006.

[63] W. T. H. Woon and T. C. Wan, "Performance evaluation of IEEE 802.15.4 wireless multi-hop networks: simulation and testbed approach," *International Journal of Ad Hoc and Ubiquitous Computing*, vol. 3, pp. 57-66, 2008.

[64] F. M. Al-Turjman, *et al.*, "Connectivity Optimization for Wireless Sensor Networks Applied to Forest Monitoring," *2009 IEEE International Conference on Communications, Vols 1-8*, pp. 285-290, 2009.

Appendix A
Optimal Power Allocation

In Section 5.6, we discussed cases of the optimal power allocation for AM, AMI, and ASAM when the channel condition for the two links are σ_1 = 2dB, σ_2 = {0, 4, 6, 8}dB and K_1 = 10dB, K_2 = {0, 5, 15, 20}. Here, the results of optimal power allocation under other channel conditions are presented in Figure A.1-Figure A.8. We considered the following channel conditions for the two-link multi-hop relay network.

- Lognormal Shadowing: σ_1 = 0dB, σ_2 = {2, 4, 6, 8}dB
- Lognormal Shadowing: σ_1 = 4dB, σ_2 = {0, 2, 6, 8}dB
- Lognormal Shadowing: σ_1 = 6dB, σ_2 = {0, 2, 4, 8}dB
- Lognormal Shadowing: σ_1 = 8dB, σ_2 = {0, 2, 4, 6}dB
- Rician Fading: K_1 = 20dB, K_2 = {0, 5, 10, 15}
- Rician Fading: K_1 = 15dB, K_2 = {0, 5, 10, 20}
- Rician Fading: K_1 = 5dB, K_2 = {0, 10, 15, 20}
- Rician Fading: K_1 = 0dB, K_2 = {5, 10, 15, 20}

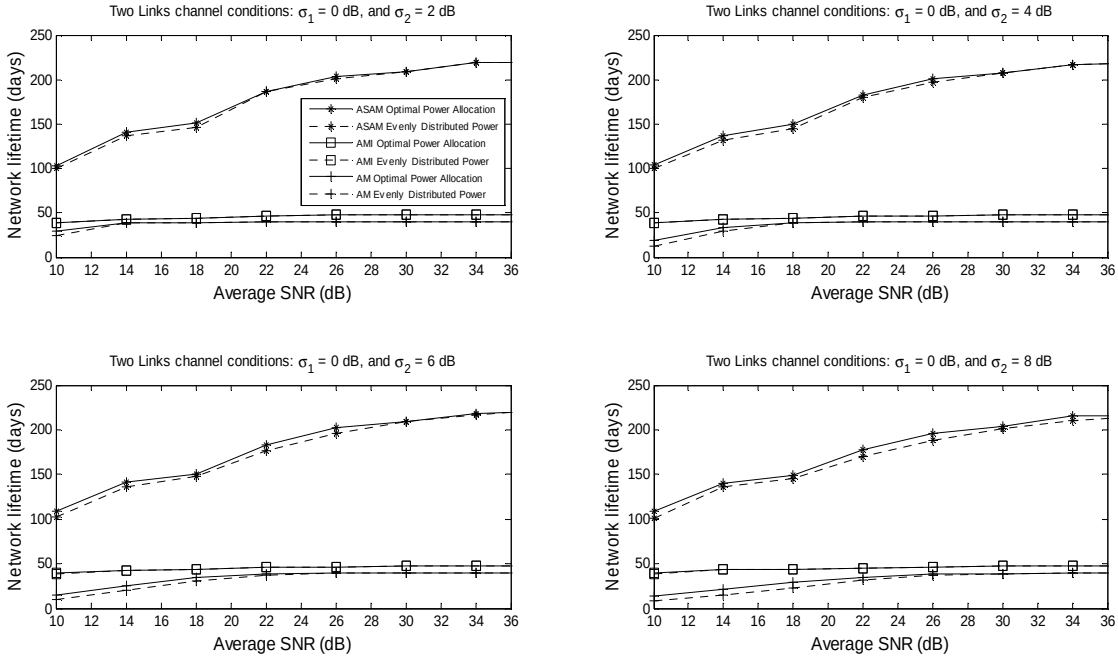

Figure A.1: Power allocation under Lognormal shadowing. Two link channel conditions: σ_1 = 0dB, σ_2 = {2, 4, 6, 8}dB

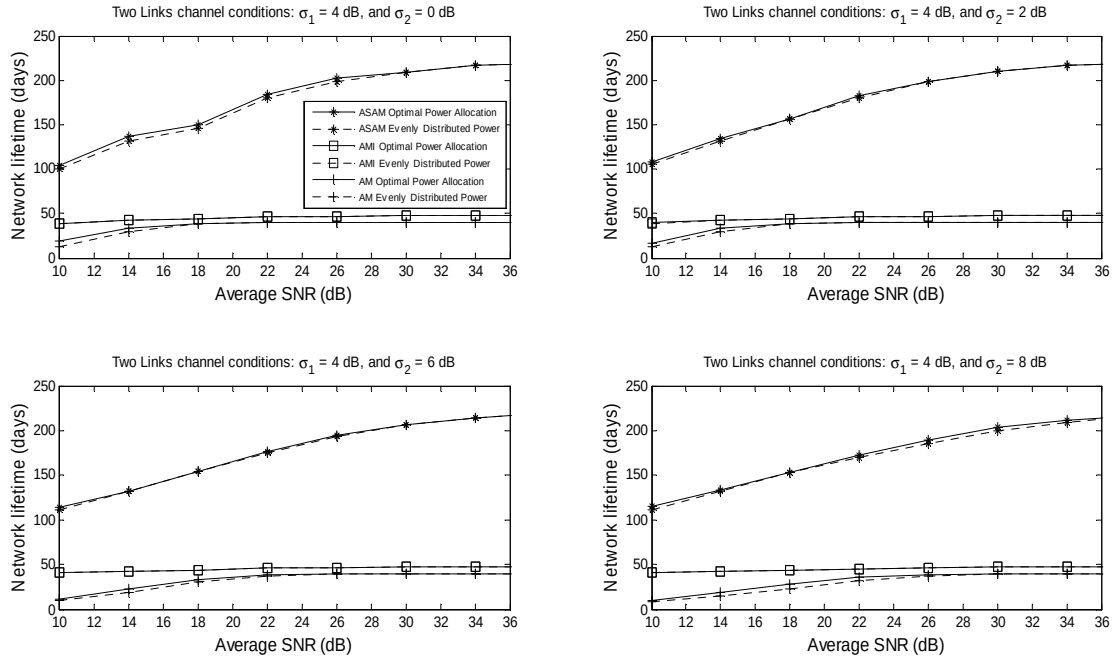

Figure A.2: Power allocation under Lognormal shadowing. Two link channel conditions: σ_1 = 4dB, σ_2 = {0, 2, 6, 8}dB

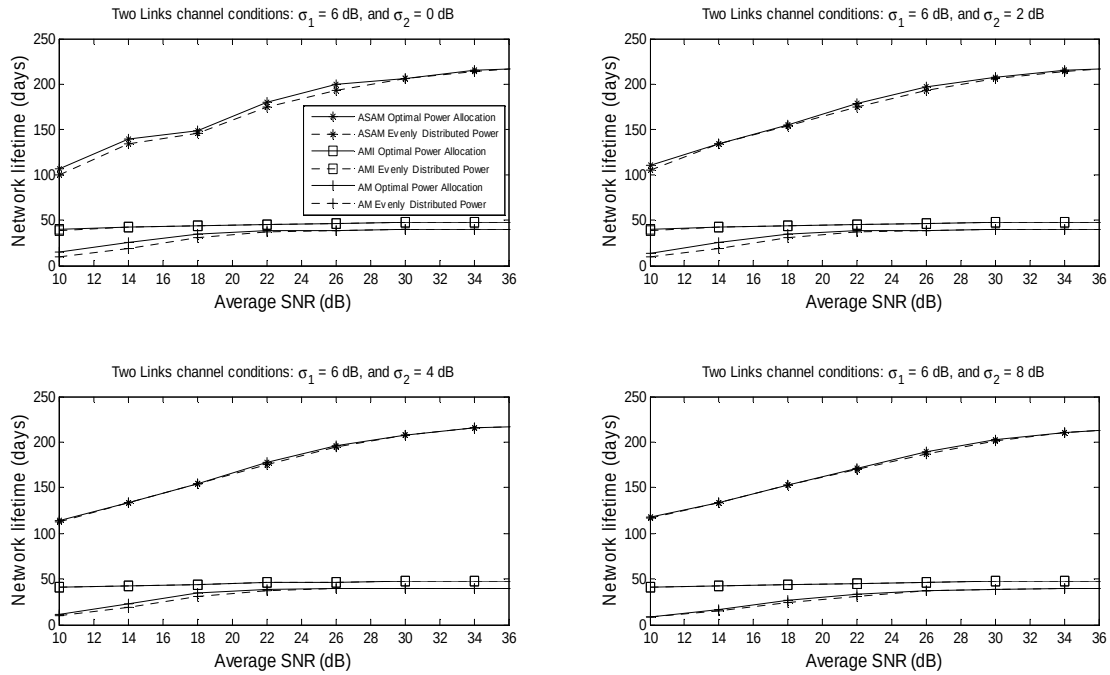

Figure A.3: Power allocation under Lognormal shadowing. Two link channel conditions: σ_1 = 6dB, σ_2 = {0, 2, 4, 8}dB

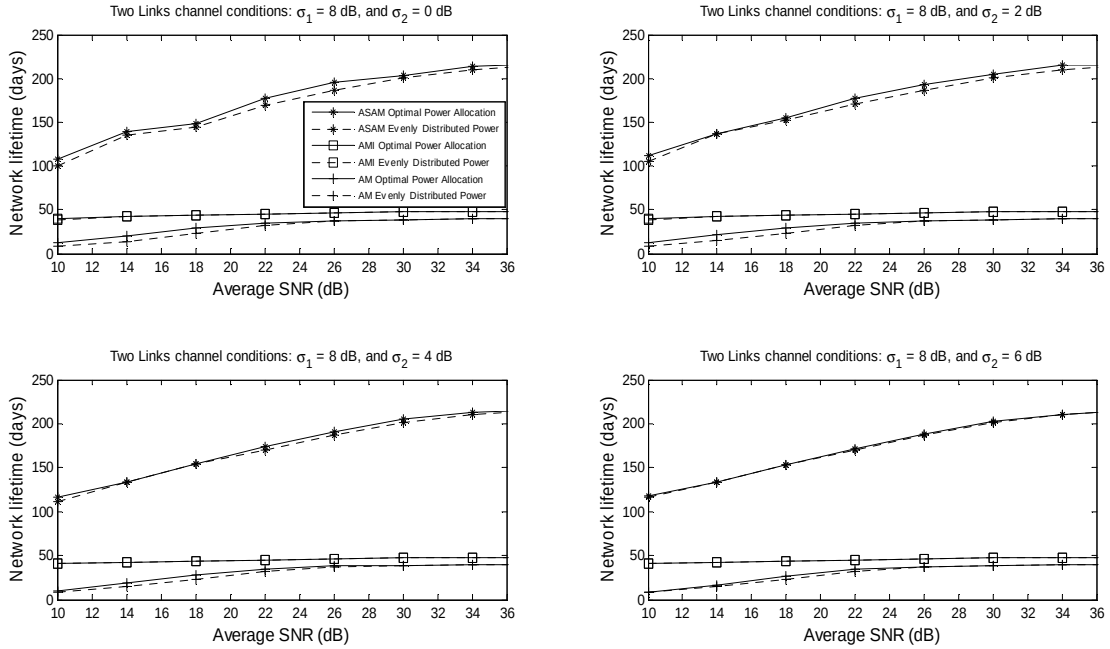

Figure A.4: Power allocation under Lognormal shadowing. Two link channel conditions: σ_1 = 8dB, σ_2 = {0, 2, 4, 6}dB

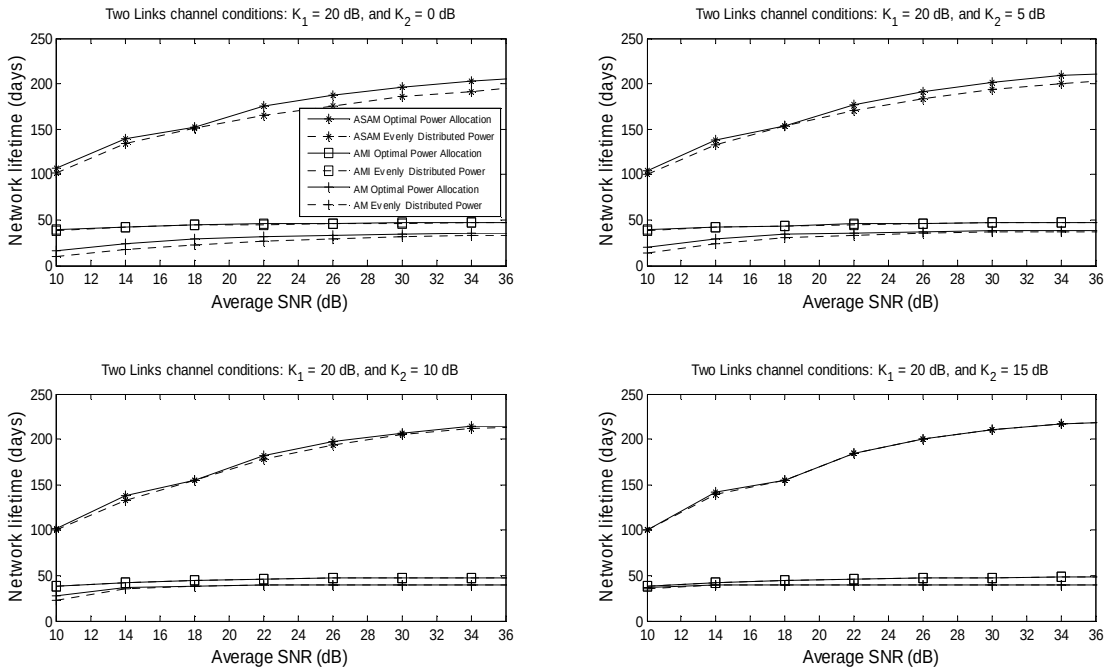

Figure A.5: Power allocation under Rician Fading. Two link channel conditions: K_1 = 20dB, K_2 = {0, 5, 10, 15}

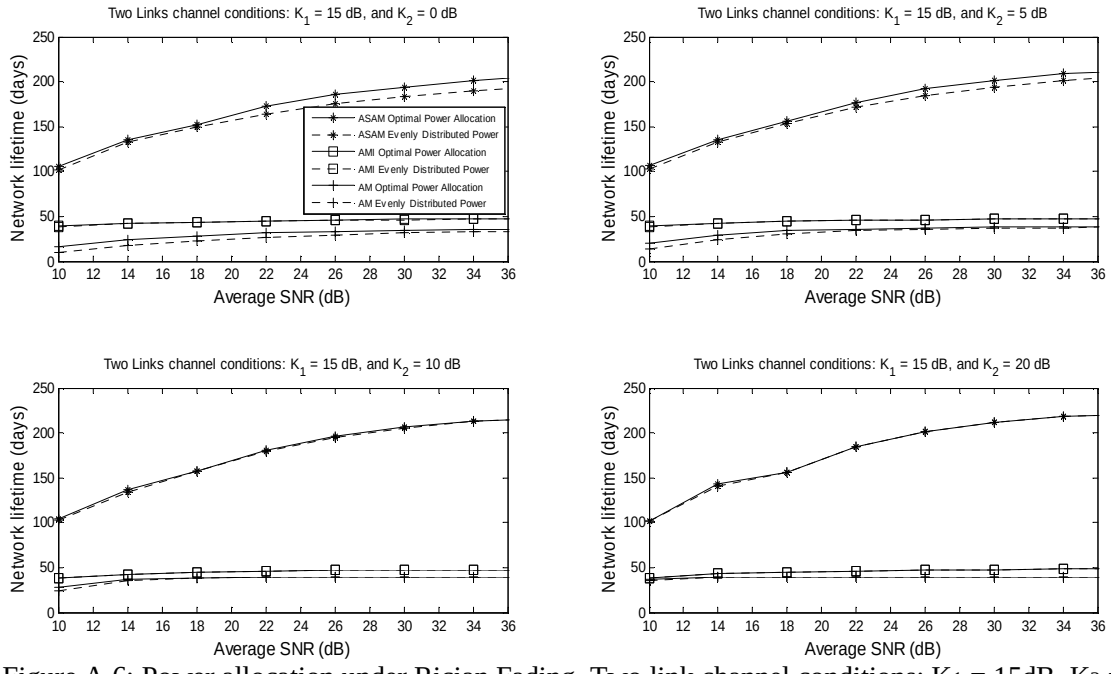

Figure A.6: Power allocation under Rician Fading. Two link channel conditions: K_1 = 15dB, K_2 = {0, 5, 10, 20}

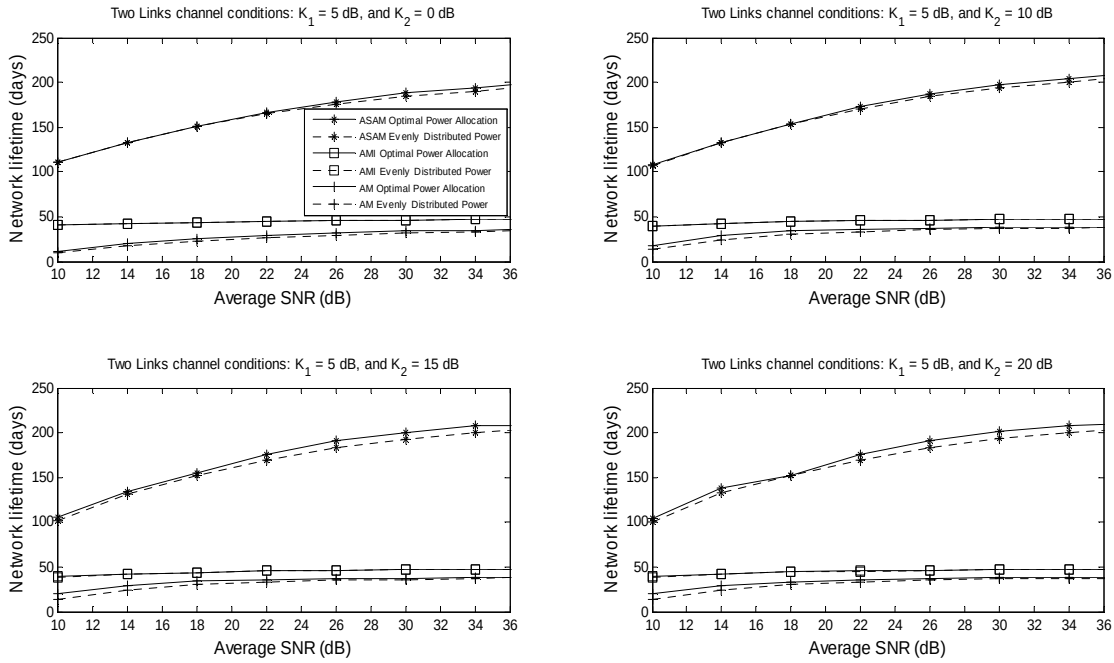

Figure A.7: Power allocation under Rician Fading. Two link channel conditions: K_1 = 5dB, K_2 = {0, 10, 15, 20}

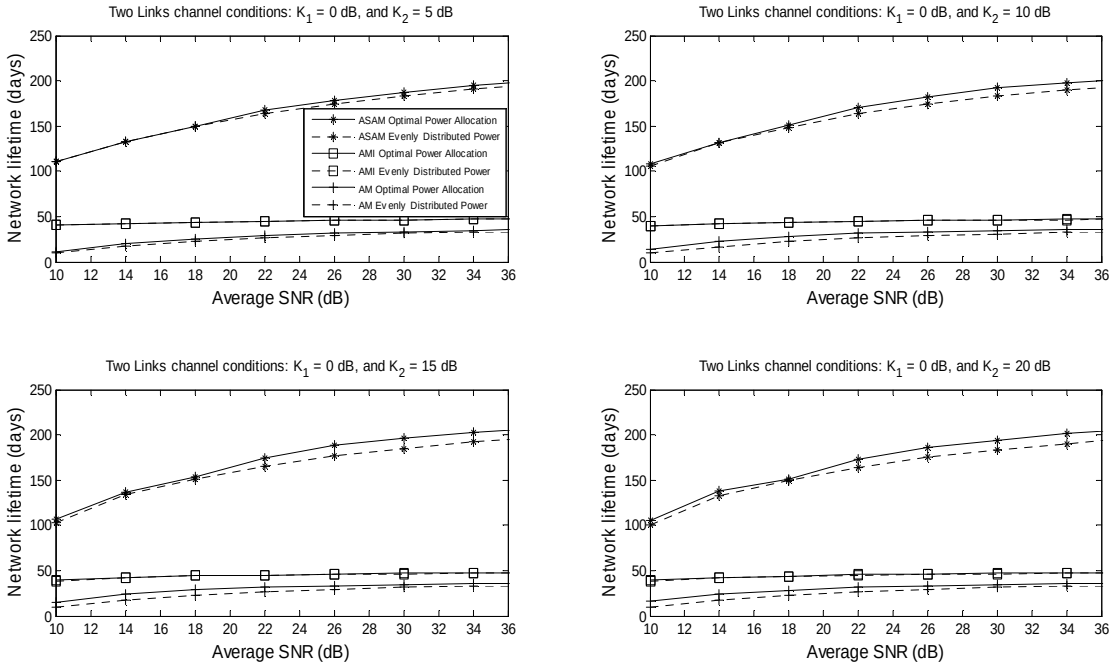

Figure A.8: Power allocation under Rician Fading. Two link channel conditions: K_1 = 0dB, K_2 = {5, 10, 15, 20}